Charles University in Prague

First Faculty of Medicine

Academic program: Biochemistry and Pathobiochemistry

Mgr. Jana Cesnekova

Functional characterization of LACE1 ATPase and mitochondrial AAA proteases YME1L and AFG3L2 in mitochondrial protein homeostasis

Funkční charakterizace LACE1 ATPázy a mitochondriálních AAA proteáz YME1L a AFG3L2 v mitochondriální proteinové homeostáze

PhD thesis

Supervisor: RNDr. Lukas Stiburek, Ph.D.

Prague, 2018

Prohlášení:

Prohlašuji, že jsem závěrečnou práci zpracovala samostatně a že jsem řádně uvedla a citovala všechny použité prameny a literaturu. Současně prohlašuji, že práce nebyla využita k získání jiného nebo stejného titulu.

Souhlasím s trvalým uložením elektronické verze mé práce v databázi systému meziuniverzitního projektu Theses.cz za účelem soustavné kontroly podobnosti kvalifikačních prací.

V Praze, 3.10.2018

Mgr. Jana Česneková

Podpis: …….

Identifikační záznam

Česneková, Jana. Funkční charakterizace LACE1 ATPázy a mitochondriálních AAA proteáz YME1L a AFG3L2 v mitochondriální proteinové homeostáze. [Functional characterization of LACE1 ATPase and mitochondrial AAA proteases YME1L and AFG3L2 in mitochondrial protein homeostasis]. Praha, 2018. 132 stran. Disertační práce. Univerzita Karlova v Praze, 1. lékařská fakulta, Klinika dětského a dorostového lékařství. Vedoucí práce RNDr. Lukáš Stibůrek, Ph.D.

Identification record

Cesnekova, Jana. Functional characterization of LACE1 ATPase and mitochondrial AAA proteases YME1L and AFG3L2 in mitochondrial protein homeostasis. [Funkční charakterizace LACE1 ATPázy a mitochondriálních AAA proteáz YME1L a AFG3L2 v mitochondriální proteinové homeostáze]. Prague, 2018. 132 pages. PhD thesis. Charles University in Prague, First Faculty of Medicine, Department of Pediatrics and Adolescent Medicine. Supervisor RNDr. Lukas Stiburek, Ph.D.

ABSTRAKT

Udržení mitochondriální proteinové homeostázy je nezbytnou podmínkou pro průběh klíčových buněčných procesů a udržení buněčné integrity. Je zajištěna mnoha specifickými mitochondriálními proteázami s možnými chaperonovými funkcemi aktivních v různých mitochondriálních subkompartmentech.

V první části této disertační práce jsme se zaměřili na charakterizaci funkčního překrývání a spolupráce proteolytických podjednotek AFG3L2 a YME1L mitochondriálních komplexů m-a i-AAA lokalizovaných ve vnitřní mitochondriální membráně. Dvojitě utišená buněčná linie AFG3L2/YME1L vykazovala výraznou změnu ve zpracování isoforem OPA1, výrazné zvýšení proteázy OMA1 a snížení proteinu SPG7. Naše výsledky ukazují spolupráci a částečně i nadbytečné funkční překrývání proteáz AFG3L2 a YME1L v udržení mitochondriální proteinové homeostázy, a dále podtrhují jejich důležitost pro mitochondriální a buněčné funkce a integritu.

Cílem druhé části bylo charakterizovat buněčnou funkci proteinu LACE1 v mitochondriální proteinové homeostáze. Protein LACE1 je lidský homolog kvasinkové ATPázy Afg1. Z našich výsledků vyplývá, že LACE1 je mitochondriální integrální membránový protein, který existuje jako součást tří komplexů o přibližné molekulové hmotnosti 140, 400 a 500 kDa a zprostředkovává degradaci jaderně kódovaných podjednotek COX4, COX5A a COX6A komplexu IV. Použitím afinitní purifikace proteinu LACE1-FLAG jsme zjistili, že protein přímo interaguje s podjednotkami COX4 a COX5A komplexu IV, proteázou YME1L a proteinem p53. Pomocí ektopické exprese mutantních variant K142A v oblasti Walker A a E214Q v oblasti Walker B jsme prokázali, že intaktní ATPázová doména je nezbytná pro degradaci jaderně kódovaných podjednotek komplexu IV. Dále jsme zjistili, že protein LACE1 vykazuje významnou proapoptotickou aktivitu, která je závislá na proteinu p53 a je nezbytná pro jeho translokaci do mitochondrií indukovanou mitomycinem c. Naše výsledky ukazují, že protein LACE1 má nezastupitelnou úlohu v proteolýze proteinů podjednotek oxidativního fosforylačního systému, zprostředkovává mitochondriální translokaci p53 a jím indukovanou apoptózu nezávislou na jeho transkripci.

Klíčová slova: apoptóza, dýchací řetězec, komplex IV, mitochondrie, oxidativní fosforylace, proteáza AFG3L2, proteáza YME1L, protein LACE1, tumor-supresorový protein p53, translokace

ABSTRACT

Mitochondrial protein homeostasis is crucial for cellular function and integrity. It is ensured by many specific mitochondrial proteases with possible chaperone functions located across the various mitochondrial subcompartments.

In the first part, we have focused on characterization of functional overlap and cooperativity of proteolytic subunits AFG3L2 and YME1L of the mitochondrial inner membrane complexes m- and i-AAA in HEK293 cells. The double AFG3L2/YME1L knockdown cells showed severe alteration in OPA1 protein processing, marked elevation in OMA1 protease and severe reduction in SPG7. Our results reveal cooperative and partly redundant involvement of AFG3L2 and YME1L in the maintenance of mitochondrial protein homeostasis and further emphasize their importance for mitochondrial and cellular function and integrity.

The aim of the second part was to characterize the cellular function of LACE1 (lactation elevated 1) in mitochondrial protein homeostasis. LACE1 protein is a human homologue of yeast Afg1 (ATPase family gene 1) ATPase. We show that LACE1 is a mitochondrial integral membrane protein that exists as a part of three complexes of approximately 140, 400 and 500 kDa. We demonstrate that LACE1 mediates degradation of nuclear-encoded complex IV subunits COX4, COX5A and COX6A. Using affinity purification of LACE1-FLAG expressed in LACE1-knockdown background, we show that the protein interacts physically with COX4 and COX5A subunits, YME1L protease, and p53 protein. We demonstrate by ectopic expression of both K142A Walker A and E214Q Walker B mutants that an intact ATPase domain is essential for LACE-mediated degradation of nuclear-encoded complex IV subunits. We further show that LACE1 exhibits significant pro-apoptotic activity, which is dependent on p53, and is necessary for mitomycin c-induced translocation of p53 into mitochondria. Our work have identified that LACE1 has a role in protein turnover of subunits of the oxidative phosphorylation system and mediates mitochondrial translocation of p53 and its transcription-independent apoptosis.

Key words: AFG3L2 protease, apoptosis, complex IV, LACE1 protein, mitochondria, oxidative phosphorylation, p53 tumor suppressor protein, respiratory chain, translocation, YME1L protease

ACKNOWLEDGEMENTS

I would like to thank my supervisor RNDr. Lukas Stiburek, Ph.D. for the opportunity to participate in the mitochondrial research and for his feedback throughout the duration of this project.

I would like to thank also to RNDr. Hana Hansíková, CSc. for her valuable comments, helping hand and support.

My thanks belong to fellow PhD students and to all staff of the Laboratory for Study of Mitochondrial Disorders at First Faculty of Medicine, Charles University and General University Hospital. It has been a pleasure to work with enthusiastic and dedicated colleagues

Above all, my thanks go to my family and friends for their support and endless patience.

This work was supported by Grant Agency of the Czech Republic Project GACR P305/10/P414, GACR 13-07223S, GACR GB14-36804G, and GGAS-1401-00-5-216 (MITOCENTRUM), by Grant Agency of the Charles University Project GAUK 277511 and 870214, and by institutional projects MSM 0021620806, 1M6837805002, UNCE 204011, RVOVFN64165, and PRVOUK P24/LF1/3.

Obsah

ABBREVIATIONS

A.T.C.C.	American type culture collection
AA(s)	amino acid(s)
AAA protease	ATPases associated with diverse cellular activities
ADP	adenosine diphosphate
AFG3L1	ATPase family gene 3 like 1
AFG3L2	ATPase family gene 3-like 2
AIF	apoptosis-inducing factor
Ala	alanine
ALAS	δ-aminolevulinate synthase
AMP	adenosine monophosphate
AMPK	(AMP)-activated protein kinase
Arg	arginine
Asn	asparagine
ATP	adenosine triphosphate
Bax	B-cell lymphoma -2-associated X protein
Bcl-2	B-cell lymphoma 2
BN PAGE	blue native polyacrylamide gel electrophoresis
BN/SDS PAGE	blue native/ sodium dodecylsulphate polyacrylamide gel electrophoresis
BSA	bovine serum albumine
Ccp1	cytochrome c peroxidase
cDNA	complementary DNA
CLPP	ATP-dependent caseinolytic protease - proteolytic subunit
CLPX	ATP-dependent caseinolytic protease – chaperone and sorting subunit
CLPXP	ATP-dependent caseinolytic protease
CoQ	coenzyme Q10
CRL-1573	human embryonic kidney cells 293
CYM1	cytosolic metalloprotease 1 (also known as MOP112)
Cys	cysteine
DBH2	reduced decylubiquinone
DDM	n-dodecyl β-D-maltoside
DHFR	dihydrofolate reductase
DMEM	Dulbecco's modified Eagle's medium
Drp1	dynamin related protein 1
DTT	dithiothreitol
EDTA	ethylenediaminetetraacetic acid
EMRE	mitochondrial Ca^{2+} uniporter (MCU) regulator
FAD/FADH2	flavin adenine dinucleotide oxidized/reduced form
FBS	fetal bovine serum
FCCP	carbonilcyanide p-triflouromethoxyphenylhydrazone
FtsH	Filamentous temperature sensitive H
Gln	glutamine

Glu	glutamic acid
Gly	glycine
HEK293	human embryonic kidney cells 293; ATCC® CRL-1573™
HEPES	4-(2-hydroxyethyl)-1-piperazineethanesulfonic acid
His	histidine
HtrA	high temperature requirement protein A
Icp55	intermediate cleaving peptidase
IgG2 Alpha	immunoglobulin G subclass 2
IMM	inner mitochondrial membrane
IMMP2L	inner mitochondrial membrane peptidase 2-like
IMP	inner membrane peptidase
Imp1	inner membrane peptidase subunit 1
Imp2	inner membrane peptidase subunit 2
IMS	inter membrane space
INF Gamma	interferon gamma
KCN	potassium cyanide
KD	knockdown
LACE1	lactation elevated 1
LB	Luria-Bertani medium
Leu	leucine
LON	long, undivided filaments upon UV irradiation, protease
Lys	lysine
MCU	mitochondrial Ca^{2+} uniporter
Mdm10	mitochondrial distribution and morphology protein 10
Mdm35	mitochondrial distribution and morphology protein 35
Met	methionine
$MgCl_2$	magnesium chloride
Mgr1	Mitochondrial genome-required protein 1
Mgr3	Mitochondrial genome-required protein 3
$MgSO_4$	magnesium sulfate
MIPEP	mitochondrial intermediate peptidase
MOP112	mitochondrial presequence protease (also known as CYM1)
MPP	mitochondrial processing peptidase
mRNA	messenger RNA
MRPL32	mitochondrial ribosomal protein L32
MRSA	methicillin resistant *Staphylococcus aureus*
mtDNA	mitochondrial DNA
mtHSP60	mitochondrial heat shock protein 60
mtHSP70	mitochondrial heat shock protein 70
mtUPR	mitochondrial unfolded protein response
MURE	mitochondrial unfolded protein response elements
NaCl	sodium chloride
NAD/NADH	nicotinamide adenine dinucleotide oxidized/reduced form
nDNA	nuclear DNA

Nsf1	cysteine desulfurase
OMA1	overlapping with the m-AAA protease
OMM	outer mitochondrial membrane
OPA1	optic atrophy 1
OXA1L	oxidase assembly 1-like protein
OXPHOS	oxidative phosphorylation system
p53	protein 53
PAMP	presenilin-associated metalloprotease
PARL	presenilins-associated rhomboid-like protease
PARP	poly (ADP-ribose) polymerase
PBS	phosphate buffer solution
Pcp1	processing of cytochrome c peroxidase protein 1
PEP	processing enhancing protein
PGAM5	mitochondrial serine/threonine-protein phosphatase
PGC-1 Alpha	proliferator-activated receptor gamma coactivator 1 alpha
PHB1	Prohibitin 1
PHB2	Prohibitin 2
Phe	Phenylalanine
PIC	protease inhibitor coctail
PINK1	phosphatase and tensin homologue (PTEN)-induced kinase
PMF	proton motive force
PMSF	phenylmethylsulfonyl fluoride
PNPase	polynucleotide phosphorylase
PNPEP3	Xaa-Proline aminopeptidase 3
Prep	presequence protease
Pro	proline
Psd1	phosphatidylserine decarboxylase
PUMA	p53 upregulated modulator of apoptosis
QCCR	coenzyme Q – cytochrome c reductase; complex III
RNAi	RNA interference
SCA	spinocerebellar ataxia
SDS PAGE	sodium dodecylsulphate polyacrylamide gel electrophoresis
Ser	serine
shRNA	short hairpin RNA
siRNA	small interfering RNA
SIRT3	NAD-dependent deacetylase sirtuin-3
Smac	second mitochondria-derived activator of caspases, also known as direct IAP binding protein with low pI, DIABLO)
Som1	sorting mitochondrial protein
Spg7	spastic paraplegia 7, paraplegin
SQR	complex II
SRH	second region of homology
StAR	steroidogenic acute regulatory protein
START	StAR-related lipid transfer protein

TBS	tris-buffered saline
TCA cycle	citric acid cycle
TCA	trichloroacetic acid
TFAM	mitochondrial transcription factor A
Thr	threonine
TIM	translocase of the inner membrane
TMPD	N,N,N`,N`-tetramethyl-1.4-phenylendiamine
tmRNA	transfer-messenger RNA
TNF Alpha	tumor necrosis factor alpha
TOM	translocase of the outer membrane
Tyr	tyrosine
wt	wild-type
YME1L	ATP-dependent metalloprotease yeast mitochondrial

1. INTRODUCTION

1.1. Mitochondria

1.1.1. Mitochondrial function and structure

Mitochondria (singular mitochondrion) were first described by Richard Altmann in 1890 who termed the mitochondria „bioblasts" (life germs). He proposed that these „bioblasts" were living inside the cells and were responsible for their „elementary functions" (Zhang, Lin et al. 2012). Mitochondria are double-membrane bound (Palade 1964) small oval organelles in the cytoplasm 0.5 - 2 μm in diameter and 10 μm in length (Lodish, Berk et al. 2000) showing striking interspecies and inter-tissue variations in shape, connectivity, and inner membrane morphology (Mannella 2008). They are found in most of the eukaryotic cells, however with few exceptions such as mature mammalian red blood cells (Lodish, Berk et al. 2000). Mitochondria not only produce the adenosine triphosphate (ATP), but also participate in many others cellular processes such as aging, apoptosis, calcium homeostasis, iron/sulfur cluster biogenesis, metabolism, respiration, ROS production, thermogenesis, tricarboxylic acid (Krebs cycle, TCA cycle), etc. More than 3300 proteins were classified in human mitochondria and mitochondria-associated fractions (Morgenstern, Stiller et al. 2017).

The mitochondria are structurally defined by their two membranes. A limiting outer mitochondrial membrane (OMM) that enwraps the energy-transducing inner mitochondrial membrane (IMM). The IMM encloses a dense, protein-rich matrix (Mannella 2006). Both mitochondrial membranes are phospholipid bilayers anchoring many other specific proteins (Alberts 2002). Due to such double-membraned organization, there are four distinct compartments to a mitochondrion. They are: i) the OMM, ii) the intermembrane space (IMS), iii) the IMM, iv) the cristae space and iv) the matrix (Lodish, Berk et al. 2000). The cristae space is formed by infoldings of IMM. This mitochondrial model is called the "Baffle" model. The electron tomography provided improved 3D visualizations of mitochondria *in situ.* This allowed creating a new model of membrane architecture. The latest model is called the "Crista junction" model. The large openings connect the intracristal and membrane spaces of the

"Baffle" model. In the "Crista junction" model, there are narrow tubular openings (crista junctions) that connect these spaces. Crista junctions were proposed to be a uniform structural component of all mitochondria (Perkins and Frey 2000, Logan 2006). The OMM is a 7 nm thick (Perkins, Renken et al. 1997) and encloses the entire organelle. They contain large number of integral membrane channel-forming proteins. These proteins are called porins (voltage-dependent anion channel, VDAC). The weight protein/phospholipid ratio is approximately 1:1. This ratio in the OMM is similar to the eukaryotic plasma membrane (Alberts 2002). Porins allow the unimpeded transport of molecules with molecular weight up to 5 kDa and thus ensure passage of small hydrophilic ions and metabolites (Campo, Peixoto et al. 2017). Larger preproteins can enter the mitochondria only if they possess a signaling sequence at their N-terminus. This is a typical important passage for small hydrophilic molecules and cationic metabolites. The translocases of the OMM bind the N-terminus of the preprotein and actively transfer it across the membrane (Herrmann and Neupert 2000). The translocases are large multisubunit proteins with a transmembrane β-barrel structure which forms a central hydrophilic pore. The translocase of the outer mitochondrial membrane 40 kDa (Tom40) is one of the essential OMM translocases. Tom40, together with other Tom22, Tom20, and Tom70 receptors are part of the TOM complex (Becker, Bannwarth et al. 2005, Yamano, Yatsukawa et al. 2008). The biogenesis of the TOM complex is mediated by mitochondrial distribution and morphology protein 10 (Mdm10). This protein creates the β-barrel channel (Ellenrieder, Opalinski et al. 2016). The mitochondrial import machinery protein 1 (Mim1) promotes the biogenesis of α-helical OMM proteins and constitutes the first OMM channel with a predicted α-helical structure (Kruger, Becker et al. 2017). Sorting and assembly machinery component 50 (Sam50) mediates import of β-barrel OMM proteins (Kutik, Stojanovski et al. 2008). In addition, several other channels have been identified in mitochondrial OMM vesicles (Kruger, Becker et al. 2017). The OMM also contains enzymes involved in diverse activities such as tryptophan degradation, fatty acids elongation, and the oxidation of epinephrine. These enzymes constitute fatty acid Co-A ligase, monoamine oxidase, and kynurenine hydroxylase, rotenone-insensitive NADH-cytochrome c-reductase et cetera (Alberts 2002). The IMS compartment is the space located between the OMM and the IMM. Mainly of the considerable permeability of OMM, the biochemical composition of IMS is similar to cytosol. The only difference is the absence of the large molecules. All proteins that are present within the IMS are encoded by nuclear genes and become synthesized in the cytosol. Most of the IMS proteins are anchored in OMM or IMM. On the contrary, cytochrome *c* is only loosely associated with IMM which permits its release to cytosol during

programmed cell death. IMM is the main barrier which separates protein-rich matrix from the IMS. The structure of the IMM is adapted to serve its function and thus IMM is extensively folded and compartmentalized. The numerous invaginations of the IMM are called cristae and are separated by cristae junctions. Cristae junctions delimit the intercristal space from the IMM juxtaposed to the OMM. The cristae are not random folds in the IMM but internal compartments formed by invaginations of the membrane. They significantly increase the total membrane surface area. Cristae are partially closed by transmembrane protein complexes and link the opposing crista membranes in a neck-like structure (Mannella, Marko et al. 1997, Mannella 2006). The number and the morphology of cristae junctions and the area of the intercristal space have been shown to change in accordance with the metabolic state of the mitochondria (Mannella, Marko et al. 1994). Cristae and crista junctions are two newly mitochondrial subcompartments revealed parts described in the "Crista junction" model. The complex of mitochondrial inner membrane organizing system (MINOS) is named after these two new parts. The same protein complex was identified independently in two other studies and named as mitochondrial contact site complex (MICOS) (Harner, Korner et al. 2011) or as the mitochondrial organizing structure (MitOS) (Hoppins, Collins et al. 2011). In contrast to OMM, the IMM consists of more than 76% of the mitochondrial proteins (Wallace 2005). One of the prominent constituents of the cristae junctions is the Mitofilin protein (Herrmann 2011). One of the typical IMM proteins is cardiolipin which stabilizes the electron transfer complexes (Scherer and Schmitz 2011). Owing to the evolutionar origin of mitochondria, the lipid composition of IMM shows similarity to the bacteria membrane. The IMM is freely permeable only to oxygen, carbon dioxide and water under the physiological conditions. The IMM is minimally permeable to ions and larger molecules. This feature of IMM is essential for the generation of transmembrane electrochemical proton gradient also known as the proton motive force (PMF). There are several specific ion transporters in the IMM such as adenine nucleotide transporter, P_i transporter, and many substrate transporters such as malate/succinate for HPO_4^{2-}, glutamate for aspartate, etc. Mitochondrial aqueous protein-rich matrix is the space within the IMM. The matrix contains approximately 66% of the total protein of the mitochondrion. Many biochemical reactions take place in the mitochondrial matrix such as TCA cycle (Krebs cycle), mitochondrial protein synthesis, part of the oxidative phosphorylation, transamination, urea cycle, etc.

Mitochondrial shape and size undergo dynamic changes in response to enviromental conditions. Mitochondria integrate into a complex reticulum to facilitate the substrate

transport. This reticulum interacts with other cell organelles such as the mitochondria-associated endoplasmic reticulum (ER) membranes (MAM). The MAM was first described on electron micrographs in the early 1950s (Bernhard and Rouiller 1956). ER and mitochondria are adjoined by tethers that are approximately 10 nm at the smooth ER and approximately 25 nm at the rough ER (Csordas, Renken et al. 2006). These relationships are currently being unrevealed (Simmen and Herrera-Cruz 2018). It is known that this interaction controls metabolic flow (Giordano 2018), production of reactive oxygen species (ROS) (Lee, Kam et al. 2018), calcium homeostasis as well as programme cell death (Szabadkai, Bianchi et al. 2006). Mitochondrial fusion and fission determine a final morphology of mitochondrial reticulum and thus turnover of the mitochondrial population and segregation of mitochondrial DNA (Berman, Pineda et al. 2008). The regulation of mitochondrial dynamics is ensured by the dynamine-like GTPase OPA1 (optic atrophy 1). OPA1 is a causal protein in human dominant optic atrophy (Ishihara, Fujita et al. 2006). It is synthesized with bipartite targeting sequence. OPA1 protein is located in the IMM folded cristae where it governs the delicate balance between fusion and fission of mitochondrial reticulum. Long, membrane-anchored forms of OPA1 (L-OPA1) are along with mitofusins (Mfn1 and Mfn2) required for mitochondrial fusion at the OMM. The proteolytic processing of L-OPA1 to short, soluble form S-OPA1 is located in the IMS. S-OPA1 limits fusion and can facilitate mitochondrial fission. Similarly, dynamin-like GTPase Mgm1(Sesaki, Dunn et al. 2006), the yeast homolgue of OPA1, has short (s-Mgm1) and long (l-Mgm1) isoforms and are one of the main components of mitochondrial fusion and their mutual balance is essential for the mitochondrial morphology and thus maintenance of mtDNA (Zick, Duvezin-Caubet et al. 2009). Yeast mitochondrial escape 1 like protease (YME1L) cleaves OPA1 constitutively. On the contrary, OPA1 cleavage by the IMM protease OMA1 (activities overlapping with the m-AAA protease) is stress-induced (Baker, Lampe et al. 2014). Therefore, under stress conditions, the stress-activated protease OMA1 promotes mitochondrial fragmentation and can triggers cell death. On the other hand, mitochondrial fission involves the recruitment and oligomerization of cytosolic dynamin-related protein 1 (Drp1). It is facilitated by OMM adapter proteins mitochondrial fission factor (MFF), as well as MID49 and MID51 and cleaved S-OPA1 forms might also play a role in this process (MacVicar and Langer 2016).

1.1.2. Mitochondrial DNA

The endosymbiotic theory of the mitochondrial origin is supported by phylogenetic analysis of conserved ribosomal RNAs (rRNA) (Sicheritz-Ponten, Kurland et al. 1998, Gray, Burger et al. 1999). Mitochondria represent prokaryotic cell related to α-proteobacteria which was incorporated to an eukaryotic ancestor cell 2.45 - 2.2 billionyears ago (Canfield, Kristensen et al. 2005, Passamonti and Ghiselli 2009, Desmond, Brochier-Armanet et al. 2011). They have their own mitochondrial DNA (mtDNA). Early eukaryotes acquired the ability to transform toxic oxygen into the fuel with higher efficiency. A process called aerobic respiration. The new ability allowed the early eukaryotes to colonize new and diverse ecological niches and set the possibility for the advent of complex multicellularity. Almost 90% of energetic demands of mammalian organisms are covered by ATP generated by the oxidative phosphorylation (OXPHOS) system in mitochondria. Moreover, mitochondria are involved in apoptosis, regulation of cellular Ca^{2+} homeostasis and generation of reactive oxygen species (ROS) etc. (Redza-Dutordoir and Averill-Bates 2016). A comparison of non-ribosomal proteomes of α-proteobacteria and eukaryotes revealed that protomitochondrial metabolism was based on aerobic catabolism of amino acids (AAs), glycerol and lipids provided by the host. Over the time, considerable endosymbiotic gene transfer from the protomitochondrion to the host nucleus occurred. However, many genes were lost due to redundancy. As a result, the nuclear genome has become larger and more complex and the mitochondrial genome has diminished. A comparison of proteomes suggests that only 22% of human mitochondrial proteins are of protomitochondrial descent (Gabaldon and Huynen 2003). Mammalian mtDNA, first described in 1963, is a multi-copy DNA located within the mitochondrial matrix (Nass and Nass 1963). Mammalian cells contain between 1000 and 10 000 copies of mtDNA based on cellular energy demand. High energy-dependent consuming tissues such as myocardium has proportionally higher amounts of mtDNA. For example mature mammalian oocytes contain around 100 000 copies of mtDNA. MtDNA does not undergo replication through the early stages of embryogeneses (Bratic, Hench et al. 2009). MtDNA heteroplasmy described a condition in which mutated and normal mtDNA molecules coexist within one cell. The proportion of mutant mtDNA molecules to those wild-type determines both the penetrance and severity of expression of mtDNA diseases. A uniform collection of mtDNA in cell is called homoplasmy. In this case, the mtDNA is either entirely normal or entirely mutant. The proportion of mutant variant has important consequences in understanding of mitochondrial disease (Payne, Wilson et al. 2013). Human mtDNA is

circular double-stranded molecule that consists of 15 569 base pairs. It encods a total of 37 genes, of which encoder for 13 essential polypeptides (proteins) of catalytic or regulatory subunits of OXPHOS, 22 for mitochondrial transfer RNA (tRNA), and 2 for mitochondrial ribosomal RNAs (rRNA). The nucleotide strands are categorized in heavy (H-strand) and light strand (L-strand) according to their nucleotide composition. H-strand is guanine rich in comparison with the cytosine-rich L-strand. The heavy strand encodes 28 genes and the light strand encodes 9 genes (Anderson, Bankier et al. 1981) (Fig. 1.1.).

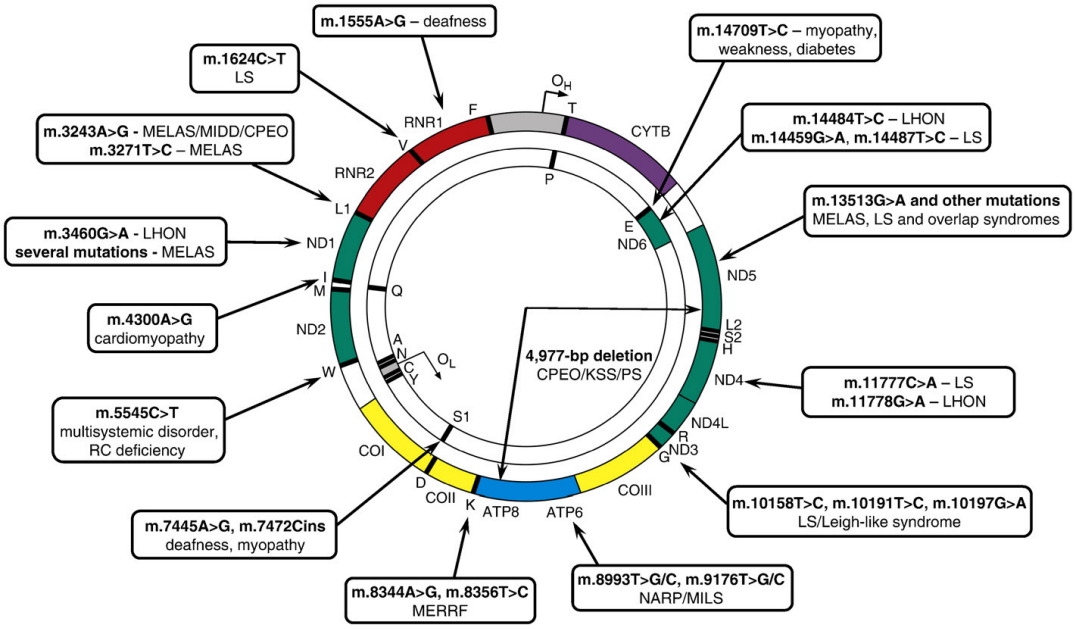

Fig. 1.1. Mitochondrial DNA mutations and human diseases. Genotype:phenotype correlations in human mitochondrial disease. The circular, double-stranded human mitochondrial genome is depicted with sites of common mtDNA mutations highlighted. Associated clinical presentations are also highlighted. CPEO, chronic progressive external ophthalmoplegia; LHON, Leber hereditary optic neuropathy; LS, Leigh syndrome; MELAS, mitochondrial myopathy, encephalopathy, lactic acidosis, and stroke-like episodes; MERRF, myoclonic epilepsy and ragged red fibres; MILS, maternally inherited Leigh syndrome; NARP, neurogenic weakness, ataxia, and retinitis pigmentosa; PS, Pearson syndrome. (Tuppen, Blakely et al. 2010).

In many unicellular organisms such as *Tetrahymena*, green alga *Chlamydomonas reinhardtii*, and in some multicellular organisms such as in some *Cnidaria* species, the mtDNA is found as linearly organized DNA molecule. MtDNA is extremely efficient with ~93% representing a coding region. Unlike nuclear DNA (nDNA), mtDNA genes lack intronic regions, and overlapping genes, such as bovine and human ATP8 and ATP6 are present (Fearnley and Walker 1986, He, Ford et al. 2018). Four overlapping regions were described in ATP8/ATP6, ATP6/COX3, ND4L/ND4, and ND5/ND6 in *Rhynchocypris semotilus* (Yu, Kim et al. 2017).

Generally, this is a rare feature in animal genomes, as most genes are contiguous, separated by one or two non-coding base pairs. MtDNA contains only one significant non-coding region, the displacement loop (D-loop) (Andrews, Kubacka et al. 1999). The D-loop contains the site of mtDNA replication initiation (origin of heavy strand synthesis, OH) and also is the site of both H-strand transcription promoters (HSP1 and HSP2). The mitochondrial genetic code is different from nDNA. MtDNA uses only two stop codons "AGA" and "AGG". The last nuclear stop codon "UGA" encodes tryptophan (Temperley, Richter et al. 2010). In addition, "AUA" encodes for isoleucine in nDNA and methionine in mtDNA. It is generally assumed that mtDNA is exclusively maternally inherited. During mammalian zygote formation, sperm mtDNA is removed by ubiquitination. This occures already during the transport through the male reproductive tract (Sutovsky 2003). Consequently, the mtDNA content of zygote is determined exclusively by the previously unfertilized egg. On the other hand, transmission of a small amount of paternal mtDNA in mice (Kaneda, Hayashi et al. 1995) and humans has been described (Schwartz and Vissing 2002). However, paternal transmission of mtDNA in other animals may be both common and frequent. Theory suggests that the lack of paternal inheritance is either due to i) a dilution effect (sperm contain only 100 copies of mtDNA in comparison with 100 000 in the unfertilized egg), ii) selective ubiquitination of paternal mtDNA or iii) the "mtDNA bottleneck" that excludes the "minor" paternal alleles (Sutovsky 2003). Human mitochondrial DNA was the first significant part of human genome that have been sequenced. In most species, including humans, mtDNA shows predominantly maternal inheritance (Schon, DiMauro et al. 2012).

1.1.3. The oxidative phosphorylation system

Oxidative phosphorylation system (OXPHOS) is the major source of energy in most eukaryotic cells. OXPHOS is located in the cell membrane in prokaryotes and into the IMM in eukaryotes. This system mediates electron flow between four enzymes complex I (NADH-CoQ oxidoreductase), complex II (succinate-CoQ oxidoreductase), complex III (cytochrome bc1 complex), complex IV (cytochrome c oxidase), and two mobile electron carriers coenzyme Q (CoQ) and cytochrome *c* (cyt *c*). Each enzyme of the OXPHOS contains metal ions and prosthetic groups. Three of the complexes are proton pumps in the IMM in eukaryotes whereas in prokaryotes there are many different enzymes. The IMM allows compartmentalization of protons via their vectorial transport across the IMM by the action of

primary proton pumps. The OXPHOS enzymes from different tissues differ from each other in the proportion of the complexes as well as in the number of mobile electron transporters. The accumulated energy in the electrochemical proton gradient (also known as proton motive force, PMF) is composed of a dominant potential difference ($\Delta\Psi$) with contributing of ~15% proton gradient (ΔpH) (Voet 2010, Nicholls 2013). PMF is then utilized by ATP synthase for adenosine triphosphate (ATP) synthesis. These two sets of reactions are intertwined. During the oxidative phosphorylation, electrons are transferred from electron donors such as reduced NADH or $FADH_2$ to electron acceptors such as oxygen in redox reactions. NADH or $FADH_2$ are the coupled products of the oxidation of acetyl-CoA which is a central intermediate of various catabolic pathways such as oxidative breakdown of glucose, fatty acids, and lipids. The flow of electrons is an exergonic process so it releases energy. The synthesis of ATP is an endergonic process which requires an input of energy. Both the electron transport chain and the ATP synthase are embedded in the IMM. The energy is transferred from electron transport chain to the ATP synthase by movements of protons across this membrane, in a process called chemiosmosis (Mitchell and Moyle 1967, Mitchell 1970). Any proton leak across the IMM would cause a short-circuit and thus destroy the compartmentalization of protons and diminished the PMF. The energy-transducing membrane must, therefore, be essentially closed and have a high resistance to proton flux (Logan 2006). On the isolated mitochondria, it was observed a conserved molar ratio between the respiratory chain complexes and a variable stoichiometry for coenzyme Q and cytochrome *c*. The typical values are [1-1.5]:[30-135]:[3]:[9-35]:[6.5-7.5] for complex II:coenzyme Q:complex III:cytochrome c:complex IV in the different tissues. These tissue-specific qualitative differences manifest as different utilization of substrates (Benard, Faustin et al. 2006) or the lower ability of ATP production. This is typical for brown adipose tissue with selectively low content of functional ATP synthase in contrast to high levels of the transcripts of the β subunit of the F1 part of the ATPase and of the transcripts of the mitochondrial-encoded subunits (Houstek, Tvrdik et al. 1991). The otherway of PMF is in a form of heat via UCP1 uncoupling protein (Houstek, Andersson et al. 1995). Four of the OXPHOS protein complexes (complex I to complex IV) associate into stable entities called respiratory supercomplexes. Due to the bi-genomic origin of OXPHOS (except complex II), the synthesis of OXPHOS subunits by mitochondrial and cytosolic ribosomes and their biogenesis are logistically more complicated. It may be the cause of OXPHOS complex deficiency which can be encoded on either the mtDNA or nDNA (Rampelt and Pfanner 2016).

1.2. The proteolytic system of mitochondria

Cell survival and thus survival of the whole organism depends on essential processes in mitochondria such as OXPHOS. The OXPHOS is build up of both nuclear and mitochondrial encoded protein subunits. Due to the potential function-threatening defects, the quality of these protein subunits is continuously under tight control of specialized proteases. Various proteases within these organelles regulate mitochondrial biogenesis and ensure the complete degradation of redundant or damaged proteins. Many of these proteases are highly evolutionary conserved and ubiquitous in prokaryotic and eukaryotic cells. They can be sorted into four functional classes i) processing peptidases, ii) ATP dependent proteases, iii) oligopeptidases, and iv) other mitochondrial proteases. Processing peptidases cleave off mitochondrial targeting sequences of nuclearly encoded proteins and process mitochondrial proteins with regulatory functions. ATP dependent proteases either act as processing peptidases with regulatory functions or as quality-control enzymes degrading non-native polypeptides to peptides. Oligopeptidases degrade these peptides and mitochondrial targeting sequences to AA. Other mitochondrial proteases are the remaining proteases present in mitochondria that haven`t been functionaly classified yet (Koppen and Langer 2007). The degradation of the substrate proteins is under the N-end rule pathway. This rule governs the rate of the protein degradation through recognition of the N-terminal residue of proteins. The last N-terminal AA of the protein determines its half-life. The rule applies to both eukaryotic and prokaryotic organisms but with different strength, rules, and outcome. The proteolytic system of mitochondria produces peptides and free AAs and continuously release them from mitochondria (Kambacheld, Augustin et al. 2005).

1.2.1. Processing peptidases

The major function of mitochondrial processing peptidases is the removal of N-terminal sorting signals of nuclear-encoded subunits of the OXPHOS and other proteins imported to mitochondria (Gakh, Cavadini et al. 2002). The peptide sorting signals are the first 20–80 AA in preprotein (Burri and Keeling 2007). The N-terminal sequences are rich in hydrophobic and positively charged Arg residues and form hydroxylated amphipathic helixes. On the other hand, there are almost no negatively charged residues (Fukasawa, Tsuji et al. 2015). The signal sequences are both necessary and sufficient for import of the proteins that contain them.

This feature can be used for genetic engineering techniques because these signals can be linked to almost any cytosolic protein to direct the protein into the mitochondrial matrix.

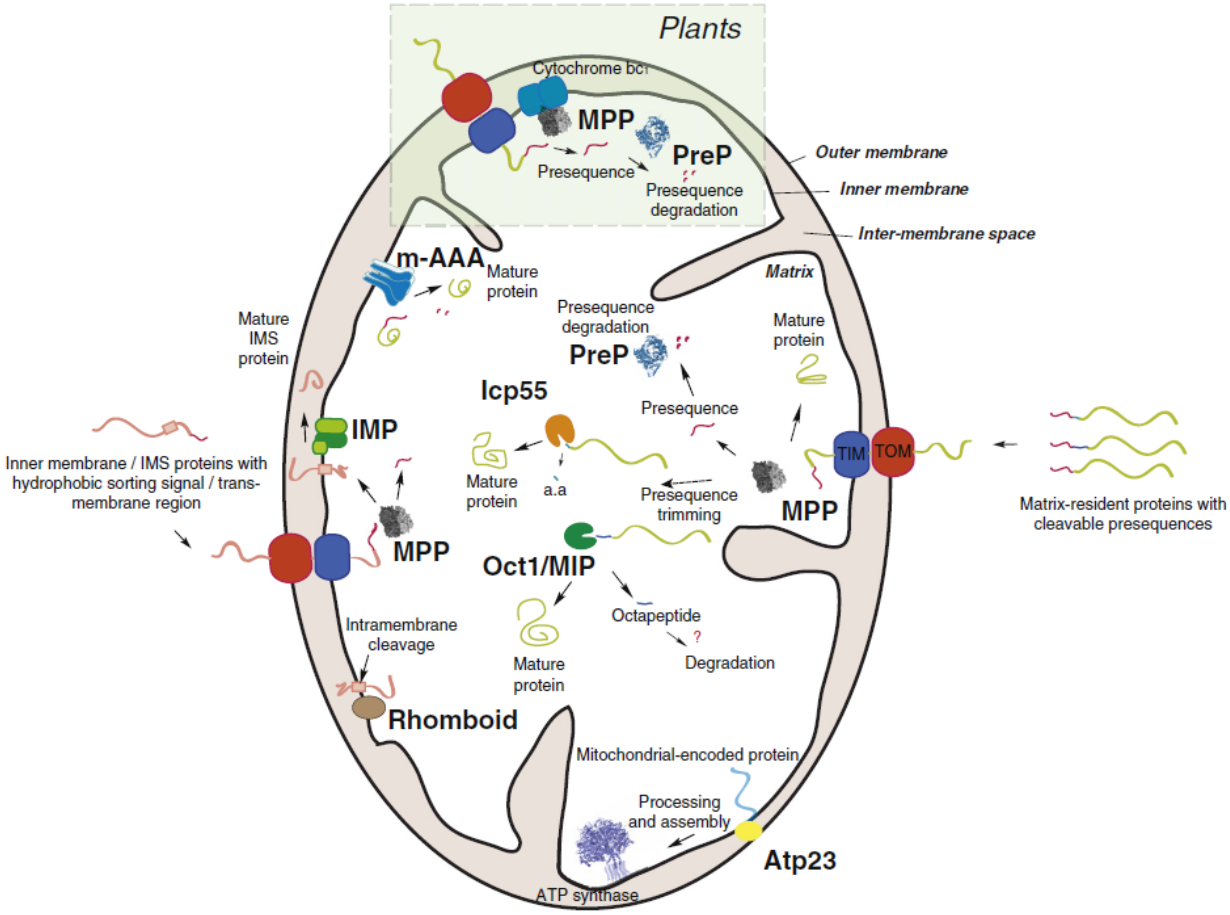

Fig 1.2. The overview of mitochondrial processing proteases. The preproteins are translocated across the OMM and the IMM via the TOM and the TIM complexes. Inside the mitochondrial matrix, the presequences are cut off by the MPP. In yeast and mammals, MPP is localized into the matrix. In plants, MPP is integrated into the complex III. Cleavage by MPP may be followed by additional cleavage of some precursors in the mitochondrial matrix by other mitochondrial proteases as MIP/Oct1 (also known as MIPEP) and/or Icp55. In case of proteins containing bipartite sorting signals, the targeting sequnces are processed subsequently i.e. by MPP followed by IMP. Obviously, another mitochondrial proteases are involved as well. The free peptides in the matrix are degraded by PreP protease. MPP – mitochondrial processing peptidase, Octl - mitochondrial intermediate peptidase, Icp55 - intermediate cleaving peptidase of 55 kDa, PreP - presequence protease, Atp23 - involved in processing of ATP6 subunit required for assembly of a functional ATPsynthase, m-AAA – mitochondrial ATPases associated with diverse cellular activities (Teixeira and Glaser 2013).

Preproteins are delivered to the mitochondria by cytosolic chaperones through the channel linked receptors in the OMM (Alberts 2002). They bind to receptors of translocases of the OMM (TOM) TOM 20, TOM22 and TOM70 and several other proteins. While TOM20 binds presequences, TOM22 binds both presequences and internal targeting peptides and on the other hand TOM70 binds to internal targeting peptides and acts as a docking point for

cytosolic chaperones (Stojanovski, Bohnert et al. 2012). The preproteins are translocated through TOM complex to the translocases of the IMM (TIM) TIM23 or TIM22. TIMs also act as chaperones. TIM23 binds precursor proteins at their N-terminus and transports some of these bound proteins into the mitochondrial matrix, and then facilitates insertion of their transmembrane domains into the IMM. The TIM22 mediates the insertion of a subclass of IMM proteins such as the ADP/ATP carrier protein. Proteins are targeted to submitochondrial compartments by multiple signals and pathways. The proteins targeted to the OMM, the IMS, and the IMM often require another signal sequence in addition to the matrix targeting sequence. After import of the preprotein, the first signal sequences are rapidly removed by the action of mitochondrial processing peptidases. In case of bipartite or multiple targeting sequence, proteases are able to act sequentially.

The mitochondrial processing peptidase (MPP; EC 3.4.24.- for MPP subunit Alpha) has molecular weight of approximately 100 kDa. It is heterodimeric zinc metallopeptidase localized into the mitochondrial matrix where its major function is to cut off the N-terminal mitochondrial targeting sequences. In more than 80% presequences cleavage sites have conserved motif containing an Arg at position –2 or -3 at the N-end from the scissile peptide bond. Schematically, it can be depicted Arg-X↓X and Arg-X-Phe/Tyr/Leu↓Ala/Ser-X where the arrow shows the cleavage site in addition to other distal basic residues and in some cases one aromatic residue at position +1 from N-end (Taylor, Smith et al. 2001, Zhang, Sjoling et al. 2001, Gakh, Cavadini et al. 2002). Processing by MPP depends on the surrounding residues in the mature protein downstream of the cleavage site and on the rest of protein structure such as flexible linkers (Waltner and Weiner 1995). The *Neurospora crassa* MPP consists of two proteins with molecular weight of 57 kDa and 52 kDa. The 57 kDa component exhibits a low but significant processing activity and so was termed MPP. The 52 kDa component does not show processing activity itself but greatly stimulates activity of MPP, and thus it is called processing enhancing protein (PEP) (Herrmann 2012). It is assumed that PEP facilitates the binding of substrate proteins to the MPP and the translocation of the preprotein through the TOM and TIM complexes (Hawlitschek, Schneider et al. 1988). The MPP component consists of two homologous subunits α and β and both are required for the processing activity (Schneider, Arretz et al. 1990). The α-MPP subunit has a highly conserved glycine-rich loop required for the recognition of N-terminal targeting sequence of preproteins (Dvorakova-Hola, Matuskova et al. 2010). The β-MPP has His-X-X-Glu-His-X-X-Glu zinc-binding motif with the catalytic site responsible for cleavage of the peptide bond (Hartl,

Pfanner et al. 1989, Kitada, Shimokata et al. 1995). The α-MPP and β-MPP dhare 48% sequence identify in *S. cerevisiae.* Moreover, the non-catalytic core1 and core2 subunits of complex III are highly homologous to the α-MPP and β-MPP subunits in the plants (Schulte, Arretz et al. 1989). Most of the MPP activity is associated with the previously mentioned complex III (Eriksson, Sjoling et al. 1996). In the case of multiple mitochondrial targeting sequences, after the processing by MPP, there is the second cleave of peptidases in the matrix (Kalousek, Hendrick et al. 1988). Friedreich's ataxia is a hereditary neurodegenerative disease caused by low level of frataxin. Frataxin is nuclear-encoded mitochondrial protein synthesized as a larger precursor and imported into the mitochondria. It undergoes two proteolytic events that result in an intermediate and mature protein forms in the mitochondria. The frataxin deficiency is associated with mitochondrial iron accumulation and high level of mitochondrial oxidative stress in yeast. MPP cleaves intermediate form of frataxin but not its mature form (Koutnikova, Campuzano et al. 1998). Therefore, MPP can have an indirect impact on iron homeostasis (Branda, Cavadini et al. 1999).

A vast of nuclearly encoded mitochondrial protein precursors are cleaved in two sequential steps by two distinct matrix MPP peptidases and mitochondrial intermediate peptidase (also known as mitochondrial intermediate precursor-processing protease, MIP, MIPEP; EC 3.4.24.-). MIPEP is monomeric mammalian metallopeptidase with is molecular the weight of 75 kDa, localized in the matrix (Kalousek, Isaya et al. 1992). It composes of two peptides of 47 and 28 kDa in equimolar amounts. Both of these are probably the products of the cleavage of MIPEP precursor (Kalousek, Isaya et al. 1992). CDNA of MIPEP encodes 710 AA protein, that contains 33 N-terminal residues where is the cleavage site recognized by the MPP (Isaya, Kalousek et al. 1992). The comparison various MIPEP sequences revealed two similarities to i) a putative MIPEP homologous yeast protein with 47% similarity and 24% identity to 712 AA long, and ii) thimet oligopeptidase (EC 3.4.24.15). They are the other members of the metallopeptidase family. MIPEP catalyses the cleavage of the canonical N-terminal octapeptid Phe-X-X-Ser-X-X-X-X (Hendrick, Hodges et al. 1989) from the intermediate preproteins. It serves as the second stage after the first ccleavage of the preprotein by MPP. Based on this revelation, the current designation of MPP is octapeptidyl aminopeptidase 1 (Oct1) by some authors (Teixeira and Glaser 2013), but for others, Oct1 is the only in the yeast and fungi (Koppen and Langer 2007). This process is neccessary interstep for the nuclear-encoded mitochondrial proteins. After the removal of this octapeptide, the mature protein is formed. It is interesting that synthetic peptides deactivate MIPEP *in vitro* with no effect on MPP. This

shows that MIPEP cleaves the octapeptide independently on the presence of the mature protein and the cleavage site is decisive for that (Isaya, Kalousek et al. 1992). MIPEP is functional in pH between 6,6 and 8,9. It requires zinc-binding motif for its activity as well as one His and two Glu residues (Isaya, Sakati et al. 1995). It can be activated by calcium, magnesium or manganese ions. It is strongly inhibited by cobalt, iron, and zinc and reversibly inhibited by ethylenediaminetetraacetic acid. MIPEP is inactivated by N-ethylmaleiminde and another chemicals with sulfhydryl group (Kalousek, Isaya et al. 1992). Physiological roles of mammalian MIPEPs are still unclear. It was showed that yeast MIPEP supports iron uptake into the mitochondria via the catalysis of ferrochelatase and iron–sulfur cluster-containing proteins maturation (Branda, Yang et al. 1999). Further, deletion of the MIPEP gene in the mouse leads to early embryonic lethality (Gakh, Cavadini et al. 2002). Mitochondrial NAD-dependent deacetylase sirtuin-3 (SIRT3) is localized in the mitochondrial matrix. It is implicated in the regulation of metabolic processes and is known for its fast increase expression in white and brown adipose tissue. SIRT3 overexpression leads to increased expression of peroxisome proliferator-activated receptor gamma coactivator 1 Alpha (PGC-1α) and thermogenin (also known as uncoupling protein 1 or UCP1). This suggests its role in adaptive thermogenesis (Shi, Wang et al. 2005, Song, Zhao et al. 2017). Mature forms of SIRT3 and MIPEP were shown upregulated in white adipose tissue during caloric restriction. It suggests that MIPEP contributes to the maintenance of mitochondrial quality via activation of SIRT3 (Kobayashi, Takeda et al. 2017). Biallelic single nucleotide variants or copy number variants of MIPEP result in left ventricular non-compaction, developmental delay, seizures, and severe hypotonia and, eventually to infantile/childhood death (Eldomery, Akdemir et al. 2016).

Mitochondrial intermediate cleaving peptidase 55 (Icp55, EC 3.4.11.-) has a molecular weight of 55 kDa (Meisinger, Sickmann et al. 2008) and is both mitochondria and nucleus localize (Naamati, Regev-Rudzki et al. 2009, Vogtle, Wortelkamp et al. 2009). Icp55 is amember of the group of aminopeptidase P family (also known as Xaa-Pro aminopeptidases, XPNPEP3). The mitochondrial fraction of Icp55 peptidase is attached to the IMM from the matrix side. Icp cuts off one destabilizing AA from the MPP-generated mitochondrial intermediate proteins (Vogtle, Wortelkamp et al. 2009). Furthermore, Icp55 catalyzes the polypeptide cleavage between Pro36 and Pro37 of cysteine desulfurase (also known as Nsf1, EC 2.8.1.-). During this process, Icp55 removes three AA residues (Tyr, Ser and Pro) from the N-terminus cleavage site of cysteine desulfurase immediately after its cleavage by MPP. This process

leads to destabilization of cystein desulfurylase (Naamati, Regev-Rudzki et al. 2009, Vogtle, Wortelkamp et al. 2009) for hampering the N-end rule pathway (Bachmair, Finley et al. 1986, Varshavsky 2011). On the other hand, the deletion of Icp55 increases the proteolytic breakdown rate of its substrates (Stames and O'Toole 2013). Based on these data, Icp55 and Oct1 are supposed to be one of the executors in the mitochondrial N-end rule pathway (Vogtle, Wortelkamp et al. 2009, Vogtle, Prinz et al. 2011). Finally, preproteins may be processed by other proteases, e.g. AAA-dependent ATPases (Azzu and Brand 2010). Previously mentioned human Xaa-Proline aminopeptidase 3 removes Pro at the position –2 from the scissile peptide bond. It is associated with cystic kidney disease and cellular tumor necrosis factor (TNF) signaling pathway (Inoue, Kamada et al. 2015). On the other hand, *in vitro* cleavage of preproteins lacking Pro was detected as well. Primary transcripts of XPNPEP3 were elevated in tumors with activated Wnt/β-catenin signaling pathway. Therefore, XPNPEP3 is suggested to be transcriptional target of Wnt/β-catenin pathway in colorectal cancer (Kumar, Kotapalli et al. 2018). In summary, it is assumed that XPNPEP3 has similar function in mammals as Icp55 in yeast (Singh, Jamdar et al. 2017).

The inner membrane peptidase (IMP, EC 3.4.99.-) is located into the IMM by its N-terminus and protrudes to the IMS by its C-terminus (Jan, Esser et al. 2000). IMP is the heterodimeric enzyme composed of Imp1 (21,4 kDa) and Imp2 (19 kDa) subunits and „sorting mitochondrial„protein (Som1). Som1 physically intertacts with Imp1 subunit and is essential for its correct function in *S. cerevisiae* (Schneider, Oppliger et al. 1994, Jan, Esser et al. 2000). Interestingly, Som1 has characteristics pattern of Cys residues Twin Cys-X_9-Cys motif instead of the N-terminal targeting sequence. This motif is typical for small nuclear-encoded proteins as subunit 17 (COX17) of complex IV (Longen, Bien et al. 2009). The IMP subunits are related not only to each other but also to other eukaryotic signal peptidases. IMP`s main function is the maturation of the preproteins in the IMS. IMP peptidase has its active site at the C-terminal domain with serine/lysine catalytic dyad (Chen, Van Valkenburgh et al. 1999). Both subunits have own non-overlapping catalytic activity. Imp1`s substrates have Asp at position -1 (Pratje and Guiard 1986) and Imp2`s substrates have Ala and Ser at positions -1 and -3 (Nunnari, Fox et al. 1993). Imp1 subunit cleaves the signal presequence at Asp21 position which is abnormal. Typical for this position is small uncharged AA. Further experiments revealed that Asp21 can be changed for Ala, Ser, Cys, Leu, or Met efficiently. But none of these mutants were cleaved by Imp2. Imp2`s substrates usually have Ala21 (Chen, Van Valkenburgh et al. 1999). Imp1 is essential for maturation of i) the mitochondrial-

encoded subunit COX2 of complex IV (Pratje, Mannhaupt et al. 1983), ii) nuclear-encoded cytochrome *b2* of complex III (Daum, Gasser et al. 1982), and iii) nuclear-encoded protein NADH-cytochrome *b5* reductase (also known as Mcr1) (Haucke, Ocana et al. 1997). Cytochrome *b2* of complex III which is gradually trimmed by MPP (Daum, Gasser et al. 1982). NADH-cytochrome *b5* reductase (known as Mcr1) is associated with the OMM and released as soluble protein after cleavaging 47 AA at the N-terminus by Imp1 (Haucke, Ocana et al. 1997). Som1 subunit is essential for the recognition of two substrates COX2 and NADH-cytochrome *b5* reductase (Esser, Pratje et al. 1996, Jan, Esser et al. 2000). Imp2 is needful for stable and functional expression of the Imp1 subunit and second splicing of nucleus-encoded cytochrome *c1* (Nunnari, Fox et al. 1993). Cytochrome *c1* is firstly cleaved by MPP. A leader peptidase process the translocation of the preprotein and, in some cases, release the mature protein from the membrane to the target compartment (Zhbanko, Zinchenko et al. 2005). Imp1 and Imp2 are members of leader peptidases type I (Behrens, Michaelis et al. 1991) with 25% homology to the leader peptidase type I in *E. coli* (Dalbey 1991, Nunnari, Fox et al. 1993). They are also membrane-associated, have similar function and require membrane phosphatidylglycerol for the translocation of proteins across the mitochondrial membrane (de Vrije, de Swart et al. 1988). The precursor of the second mitochondria-derived activator of caspases protein (Smac, also known as direct IAP binding protein with low pI, DIABLO) is mitochondrial protein which can trigger apoptosis by activation of caspases. Smac is a stop-transfer type targeting signal and was identified as a substrate of IMP (Burri, Strahm et al. 2005). Inner mitochondrial membrane peptidase 2-like (IMMP2L) is human homologue of Imp2 with homology 31%. It is predicted to be associated with Tourette syndrome. Tourette syndrome is a neuropsychiatric disorder characterized by multiple motor and vocal tics onset in childhood. This can be caused by the assumed role of IMMP2L in the biogenesis of complex III (Petek, Windpassinger et al. 2001). Further, IMMP2L ensures the cleavage of glycerol-3-phosphate dehydrogenase 2 and apoptosis-inducing factor (AIF). AIF is a positive intrinsic regulator of apoptosis and contributes to the biogenesis of the complex I in non-senescent cells. Based on this metabolic pathway, IMMP2L may increase NAD^+ levels which has pro-longevity effect (Zhang, Ryu et al. 2016). As the major AIF cleaving protease, IMMP2L may suppress the AIF-dependent cell death pathway (Sica and Kroemer 2018, Sica and Kroemer 2018, Yuan, Zhai et al. 2018).

ATP23 protease (EC 3.4.24.-) is the member of the M76 protein family. It is located in the IMS (in *S. cerevisiae*) and exhibits dual activity in the biogenesis of ATP synthase. Firstly,

ATP23 is a processing peptidase that functions in the maturation of the mitochondrial encoded ATP6 subunit by cleaving the 10 AA presequence. Secondly, ATP23 promotes the connection between mature ATP6 and ATP9 oligomers. These serve as chaperones to Atp10 subunit. Atp10 subunit is located on the opposite side of the IMM than ATP23 (Zeng, Neupert et al. 2007) and serves as an essential assembly factor in the maturation of the membrane-embedded F_O-moiety. Moreover, *ATP10* and *ATP23 genes* genetically interact with prohibitins (PHB1 and PHB2). This genetic interaction was proved by deletion ATP23 by homologous recombination. Heterozygous PHB1 or PHB2 mutants showed that meiotic progenies lacking *ATP23* and either *PHB1* or *PHB2* were not viable or displayed a severe growth defect on yeast extract–peptone–dextrose (YPD) medium. YPD is a medium where the carbon source is glucose (Osman, Wilmes et al. 2007). On the other hand, the substitution of the Glu for Gln in the Zn-binding motif revealed that abrogation of ATP23 proteolytic activity has no effect on respiratory growth in the yeast (Osman, Wilmes et al. 2007). In contrast, human ATP6 homologue is synthesized without N-terminus. Thus, it is not a proteolytic substrate of ATP23 protease. Ups1 and Ups2 (also known as Gep1) with Ups3 (Gep2) are members of the Ups1/PRELI-like protein family. They are unstable proteins localized in the IMS and coordinately modulate the amount of cardiolipin and phosphatidylethanolamine within the membrane. Their amount is regulated by mitochondrial peptidases. Ups1 contributes to the processing of dynamin-like GTPase Mgm1. Mgm1 is the major player in mitochondrial fusion that shapes mitochondrial reticulum (Sesaki, Dunn et al. 2006). Ups1 is cleaved by ATP23 and Yme1 proteases while Ups2 is cleaved only by Yme1 protease. Mitochondrial distribution and morphology protein 35 (Mdm35) is a member of the twin Cys-X_9-Cys protein family. It protects Ups1 and Ups2 against proteolysis and assures their import into the mitochondria (Potting, Wilmes et al. 2010). Such protection of Ups1 and Up2 proteins against proteolysis ensures and coordinates the amount of cardiolipin and phosphatidylethanolamine within membrane (Tamura, Onguka et al. 2012). Physiological levels of cardiolipin were preserved in cells lacking Ups2 and, on the other hand, overexpression of Ups2 led to the reduced level of cardiolipin (Osman, Haag et al. 2009, Tamura, Endo et al. 2009). Further, Ups1-Mdm35 mediates the transport of the phosphatidic acid, the precursor of cardiolipin, from OMM to IMM in *S. cerevisiae*. KO of the Ups1 protein exhibits only ~20% cellular levels of cardiolipin. Moreover, Ups2 builts up protein complex with Mdm35 and controls the phosphatidylserine transfer from the OMM to the IMM by a phosphatidylserine decarboxylase (PSD1). Phosphatidylserine is the precursor of phosphatidylethanolamine (Miyata, Goda et al. 2017).

Rhomboid protease (EC 3.4.21.-) is membrane-embedded serine protease (Urban, Lee et al. 2001) which exists in most species. Rhomboid protease has a regulatory function in mitochondrial biogenesis where it cleaves the transmembrane domains within the hydrophobic lipid bilayer (Lemberg and Freeman 2007). It was named by the embryonic lethal mutation in *D. melanogaster.* This mutation is in the *spitz* group of gene *Star*, *pointed*, *single-minded*, and *sichel*. They derive their names from the misshaped head skeletons (Mayer and Nusslein-Volhard 1988). *Spitz* was described as the first growth factor which is produced as a transmembrane preprotein. In the secretory pathway, Spitz is cleaved within its transmembrane domain to release the extracellular signaling domain. The split is sensitive only for the group of serine protease inhibitors (Urban, Lee et al. 2001). Rhomboid protease is irreplaceable as a mediator in ligand-receptor interaction in epidermal growth factor (EGF) receptor signaling pathway (Freeman 1994, Bang and Kintner 2000). Rhomboid GlpG protease was the first intramembrane proteases with solved high resolution 2.1 A˚ X-ray crystallography (in *E.coli*) (Wang, Zhang et al. 2006, Wu, Yan et al. 2006). It contains a core composed of six hydrophobic transmembrane domains S1-S6 (Urban, Lee et al. 2001). The domains are laterally protected within the lipid bilayer by a large stretch between S1 and S2. This stretch is the membrane-embedded evolutionary conserved L1 loop. GlpG core structure is representative of the whole rhomboid protease family. It is composed of S3, S4, and S6 domains with conserved AA e.g., Gly at their packing interfaces. It provides tight helical packing and stabilizing forces. The central cavity contains all conserved polar residues of S2, S4 and S6 (His 150, Asn 154, Ser 201, His 254) and there is the hydrophilic active site (Lemberg, Menendez et al. 2005). The interior aquaeous cavity is created by helix S4 and opens to extracellular side. It makes up a putative 'V-shaped' opening active site between S1 and S3 domains accessible for substrates. Previously-mentioned L1 loop has C-terminus located into the V-shape gap region with Trp and Arg residues. It serves as a gateway and is able to change conformation after binding substrate_(Wang, Zhang et al. 2006). The hydrophilic active site of rhomboid proteases are formed by Ser/His catalytic dyad (Lemberg, Menendez et al. 2005, Clemmer, Sturgill et al. 2006) where the essential residues are Ser201 and His254. These residues are connected by a short and very strong hydrogen bond (Cleland, Frey et al. 1998). His254 is sufficient for activation of Ser201 by nucleophilic atack of substrates (Voet 2010) with contributing water molecule. The molecules of water modulate hydrogen bonding between His254 and Asn251 and π-π interactions between His254 and Tyr205 (Clemmer, Sturgill et al. 2006). Generally, the substrate protein is recognized by its α-helix near the cleavage side and docked into the V-shape hydrophilic gap between S1 and S3

helices. Here, only the first parts of the substrates are unfolded and subsequently, the rhomboid protease cleaves the transmembrane substrates by only a few AAs within the membrane close to the extracellular side. The products of the cleavages are soluble and biologically active protein fragments (Urban 2006, Wang, Zhang et al. 2006). The potential substrates are characteristic by their transmembrane domain. The recognition motif is share by different rhomboid proteases. Rhomboid proteases are highly specific to the respective substrates (Fleig, Bergbold et al. 2012). Moreover, the destabilizing residues Thr-Met-Ser downstream in the substrate are also necessary for the efficient cleavage (Strisovsky, Sharpe et al. 2009). The inhibitor of this mechanism is 3,4-dichloroisocoumarin (Urban and Wolfe 2005). The processing of cytochrome c peroxidase protease (Pcp1) is one of the several rhomboid-GlpG superfamilies of intramembrane preptidases in *S.cerevisiae*. Pcp1 has two known substrates. The precursor of cytochrome c peroxidase (Ccp1) is anchored to the IMM. It is first cleaved by m-AAA protease (Tatsuta, Augustin et al. 2007) and, subsequently, by the Pcp1 protease. The second substrate Mgm1, the yeast homologue of mammalian OPA1, is cleaved by Pcp1 to short isoforms (s-Mgm1) using „alternative topogenesis“. This is the process during which approximately half of the N-terminal domains of hydrophobic segments are planted into the IMM and transferred across the membrane and the second part of hydrophobic segments are cleaved by Pcp1 generating short isoforms (Esser, Tursun et al. 2002, Herlan, Vogel et al. 2003, McQuibban, Saurya et al. 2003, Botelho, Osterberg et al. 2011). Moreover, the Mgm1 cleavage depends on the amount of cellular ATP and heat shock protein 70 (Hsp70). This suggests a possible mechanism for the cellular regulation of the mitochondrial reticulum necessary for removal of damaged mitochondria (Herlan, Bornhovd et al. 2004). Human ortholog of Pcp1 is presenilin-associated rhomboid-like (PARL) metalloprotease. It was found colocalized with amyloid-β precursore protein but coimmunoprecipitation experiments excluded direct interaction between them (Pellegrini, Passer et al. 2001). Presenilin-1 and presenilin-2 are the catalytic components of γ-secretase, an enzyme that plays major role in Alzheimer's disease. The γ-secretase carries out the last cleavage in the maturation of the amyloid-β peptide (Wolfe, Xia et al. 1999). Moreover, the mammalian homologue PARL is involved in regulation of OPA1 (McQuibban, Saurya et al. 2003) and later studies confirmed direct interaction between PARL protease and OPA1. PARL protects cells against the release of cytochrome c and thus against the apoptosis (Cipolat, Rudka et al. 2006). On the other hand, a small amount of processed OPA1 was detected in the mouse PARL-deficient cells which was probably processed by other rhomboid protease (Cipolat, Rudka et al. 2006) or by paraplegin subunit of the m-AAA protease

(Ishihara, Fujita et al. 2006, Ehses, Raschke et al. 2009). Genetical kinship of Pcp1 and PARL proteases were also proved by their substrate specificity. Both do not require helix breaking AA in the cleaved hydrophobic substrates domain (Schafer, Zick et al. 2010). Another revealed substrate of PARL is the high temperature requirement protein A2 (HtrA2, also known as Omi). During the maturation, the protein is released from the IMM to the IMS in the presence of anti-apoptotic HCLS1-associated protein X-1 (HAX-1). Maturated HtrA2 precludes the accumulation of B-cell lymphoma 2 (Bcl-2)-associated X protein (BAX), one of the initiator proteins in apoptosis (Martins, Iaccarino et al. 2002). Moreover, previously mentioned mitochondrial pro-apoptotic Smac protein, cleaved initially by IMP, is then cleaved by PARL within IMM. This second cleavage reveals the N-terminal inhibitors of apoptosis (IAPs)-binding motif which is essential for triggering the apoptosis. On the other hand, the loss of PARL activity leads to non-processed Smac and diminished apoptosis. After reintroduction of Smac protein, the apoptosis was restored (Ishihara and Mihara 2017, Saita, Nolte et al. 2017). Another function of PARL is the secondary cleavage of steroidogenic acute regulatory protein (StAR)-related lipid transfer (START) domain in the STARD7 protein (known as gestational trophoblastic tumor gene-1, GTT1). STARD7 protein is a lipid transporter that specifically binds and transports phosphatidylcholine between membranes (Horibata and Sugimoto 2010). It is first cleaved by MPP protease and, subsequently, PARL protease moderates the cleavage of STARD7 protein in the IMM allowing its partitioning between the mitochondrial IMS and the cell cytosol (Saita, Tatsuta et al. 2018). Mitochondrial serine/threonine-protein phosphatase (PGAM5) is a member of phosphoglyceromutase family involved in the conversion of 3-phosphoglycerate to 2-phosphoglycerate during glycolysis. The lost of the mutases activity and obtained N-terminal mitochondrial targeting sequence during the evolution lead to PGAM5 protein OMM localization (Lo and Hannink 2008). PGAM5 is supposed to be genuine PARL substrate and, moreover, the enhanced amount of processed PGAM5 is accompanied by increased amount of the phosphatase and tensin homologue (PTEN)-induced kinase (PINK1) (Spinazzi and De Strooper 2016). Another known substrate of PARL is the PINK1 kinase. PINK1 kinase is known to be mutated with parkin protein in some of the autosomal recessive cases of Parkinson`s disease (Clark, Dodson et al. 2006). PINK1 kinase is active in the mitochondria (Valente, Abou-Sleiman et al. 2004) but parkin is an E3 ubiquitin ligase active in cytosol (Shimura, Hattori et al. 2000). Mutations in both PINK1 and parkin lead to parkinsonism when the parkin is sequestred from cytosol to damaged mitochondria which lead to their mitophagy (Narendra, Jin et al. 2010). Moreover, PINK1 kinase moderates enzymatic activity of NdufA10 subunit of complex I (Morais,

Haddad et al. 2014). PARL is also connected with insulin resistance and thus type 2 diabetes. Lower mRNA levels of PARL and mitochondrial mass were found in skeletal muscle in mice. Knockdown (KD) of PARL leads to malformed mitochondrial cristae, lower mitochondrial content, decreased PGC-1α protein levels, and impaired insulin signaling (Walder, Kerr-Bayles et al. 2005, Civitarese, MacLean et al. 2010).

1.2.2. ATP-dependent AAA proteases

ATPases associated with diverse cellular activities (AAA proteases) are one of the main players in mitochondrial protein quality control and thus regulation of protein homeostasis by removing misfolded or no longer needed proteins. Moreover, AAA proteases participate in irreversible important cell steps such as apoptosis, etc. located into mitochondria. Their misregulation may lead to severe human diseases. AAA proteases are composed of mitochondrial targeting sequence and three main parts i) N-terminal domain that harbors one (i-AAA protease) or two (m-AAA protease) helices (Koppen and Langer 2007, Lee, Augustin et al. 2011), ii) AAA domain with Walker A motif (also known as Walker loop or P-loop), and iii) Rossman fold. Walker A and Walker B are highly evolutionary conserved protein sequence motifs in ATP-binding proteins discovered by J. E. Walker. The motifs have the pattern Gly-XXXX-Gly-Lys-Thr/Ser (Walker, Saraste et al. 1982). Rossmann fold is highly evolutionary conserved motif found by M. Rossmann in nucleotide binding proteins. It was found in FAD and NAD^+ cofactors (Rao and Rossmann 1973). So far, three types of the N-terminal domains in AAA metalloproteases were revealed: a) the Filamentous temperature sensitive H (FtsH)-like group (bacteria and eukaryotic organelles), b) in Yme1 protease (plants, fungi, and basal metazoans), and c) in Yme1 protease (Scharfenberg, Serek-Heuberger et al. 2015). The C-terminal domain is proteolytically active and belongs to the metallopeptidase of the M41 family. For this family is typical consensus metal-binding motif His-Glu-X-X-His and one Zn^{2+} ion per subunit with two His residues (Gerdes, Tatsuta et al. 2012). Ussually, C-terminal domain makes up an α-helix (Hanson and Whiteheart 2005). Active site, that usually contains Ser or Thr, is located inside cylindrical-shape multidomain complexe, often hexameric ring, with axial substrate`s input. While unstructured or small proteins can enter without assistance, larger or folded proteins or complexe multidomain proteins required ATP-dependent unfolding assistance. AAA proteases use chemical energy from ATP hydrolysis to make conformational changes themselves and in substrates and to degrade them (Erzberger and Berger 2006).

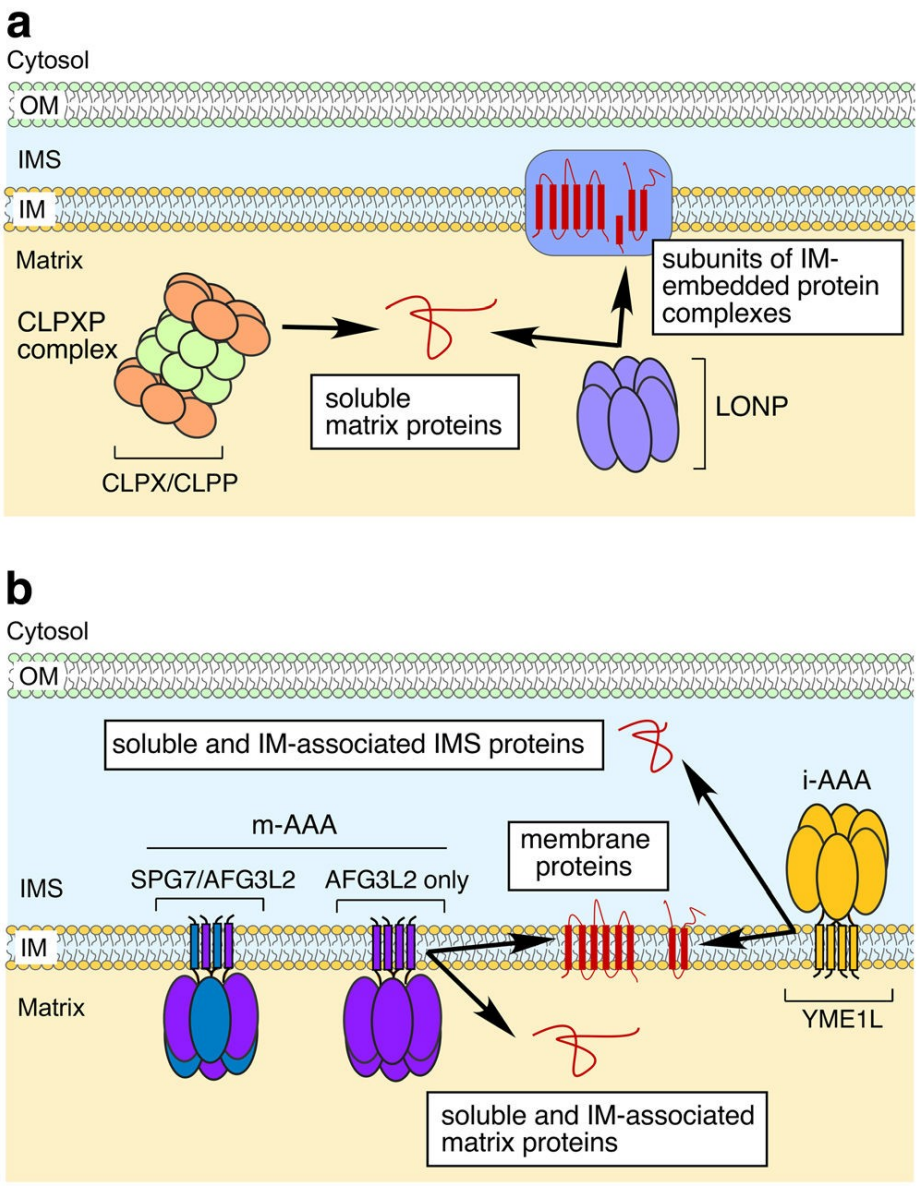

Fig.1.3. Distribution and specialization of mitochondrial AAA proteases (Levytskyy, Germany et al. 2016)

After entrance the protein substate is caught and unfolded by loop made up of AAs inside in the central pore of the AAA proteases. The unfolded protein substrate is gradually pulled into the proteolytic chamber of the AAA protease and degradated by conformational changes within both the protein substrate and the AAA protease`s proteolytic cavity. AAA ATPases carry out the chemical reaction by nucleophilic attack of the water molecule to the γ-phosphate of ATP which then leads to reposition of N-terminal domain with respect to C-terminal domain. These conformational changes are subsequently carried out by other domains in oligomeric structure. The rest of molecule serves for regulation or adaptation to different substrates (Snider, Thibault et al. 2008). So far, four main proteolytic complexes active within the various distinct mitochondrial subcompartments were identified. Both i- and

m-AAA protease complexes are found in the IMM. Whereas the i-AAA protease is active in the IMS, the homologous m-AAA protease functions on the matrix side of the IMM. The remaining two complexes, CLPXP and Lon proteases are matrix localized.

1.2.2.1. i-AAA protease

Yeast mitochondrial escape 1-like (YME1L, also known as FtsH1, Yta1l in yeast, and presenilin-associated metalloprotease PAMP in mammals, EC 3.4.24.-) is nuclear encoded ATP-dependent metalloprotease that catalyzes the degradation of the proteins with a particular degron sequence in the IMS. It plays an important role in respiration activity, protection against oxidatively damaged membrane proteins, and modulation of mitochondrial morphology. I-AAA protease is built up of six copies of YME1 subunits formed into the homohexameric complex. This complex is anchored into the IMM with protruding exerts into the IMS. YME1 protease is composed of i) ATP-binding and hydrolysis domain and ii) zinc-dependent proteolytic domain with an active site. One of the substrates of YME1 protease is COX2 of complex IV. Yeast strains lacking YME1 show elevated rate of DNA escape from mitochondria, temperature-sensitive growth, and changes in the morphology of the mitochondrial compartment (Weber, Hanekamp et al. 1996). YME1 was shown to associate with additional nonsubunit adaptor proteins, e.g. mitochondrial genome-required protein 1 (Mgr1) (Dunn, Lee et al. 2006) and mitochondrial genome-required protein 3 (Mgr3) (Dunn, Tamura et al. 2008). The i-AAA protease is composed of i) N-termini domain, ii) AAA ATPase domain, iii) the conserve second region of homology (SRH) motif, iv) the proteolytic domain, v) and C-terminal Calponin homology domain (Koppen and Langer 2007). The N-terminus of YME1 contains the targeting sequence and 19 kDa peptide. This peptide is composed of the core and loosely folded surrounding regions. The core has five helices and four of them creates tetratricopeptide repeat (TPR) hairpins that are conserved from yeast to mammals. The N-terminus of YME1 is unique among AAA proteases and mediates the hexamerization of the protease. YME1 protease has likely evolved from bacterial FtsH peptidases because *E. coli* FtsH-N contains rare α + β fold, *S.cerevisiae* contain N-terminal domain of YME1 with TPR, and *Hydra vulgaris* exhibits both the tetratricopeptide repeat region typical for metazoans and the N-terminus characteristics of animals (Scharfenberg, Serek-Heuberger et al. 2015). SRH motif is essential for the ATP hydrolysis by YME1 protease and mutants exhibit similar intramolecular conformational changes as wild-type but

show reduced or none proteolytic activity (Karata, Inagawa et al. 1999). YME1 recognizes specific degrons only in the unfolded form of the TIM9 and TIM10. TIM10 is degraded faster than TIM9 despite of their sequence and structural similarities. Moreover, the degradation is more quickly after the disruption of substrate`s disulfide bonds in the phenylalanine-rich motif (Met-Ser-Phe-Leu-Gly-Phe-Gly) (Rampello and Glynn 2017). Substrate recognition is likely ensured by two helical subdomains in the C-termini but it is assumed that N-terminus participates too. There are two substrate binding sites per one Yme1 subunit. The substrate polypeptides are identified by helices in AAA and proteolytic domains. These helices have lattice-like arrangement at the surface and serve as initial substrate binding site. The main substrate binding site is located within the AAA domain. Mutation Glu541Gln in conserved binding motif leads to loss-of-function of catalytic core and to coprecipitation with prohibitin 1 (Phb1). Cytochrome c oxidase assembly protein COX20 is essential chaperon in the assembly of complex IV and manages the initial substrate recognition of non-assembled COX2 by the i-AAA protease (Graef, Seewald et al. 2007). Another contribution to enzymatic activity is ensured by conserved Arg from the SRC domain (Karata, Inagawa et al. 1999). SRC homology domain is one of the two small protein binding domains found in Src oncoprotein, which is non-receptor proto-oncogene tyrosine-protein kinase Src. Another essential conserved motif Tyr-Val-Gly important for proteolysis is located in the central pore of the AAA domain. Mutation of the Tyr354 leads to affected proteolysis, due to hampered substrate unfolding (Graef and Langer 2006). Another substrates of YME1 are Nde1 subunit of NADH dehydrogenase and Ups2 protein. Degradation of Ups2 protein is mediated by YME1, whereas Ups1 is degraded by both YME1 protease and the Atp23 metallopeptidase. Ups2 is required for mitochondrial cristae morphogenesis and modulates the stability of mitochondrial phosphatidylethanolamine. Ups2 and Ups1 control the level of cardiolipin in mitochondria (Potting, Wilmes et al. 2010). YME1 overlaps its proteolytic activity with Mop112 metallopeptidase (also known CYM1) (Kambacheld, Augustin et al. 2005). Polynucleotide phosphorylase (PNPase) is located into IMS where it operates as a bifunctional enzyme with a phosphorolytic 3' to 5' exoribonuclease activity and a 3'-terminal poly(A)polymerase activity. Its overexpression leads to pleiotropic cellular effects that include growth inhibition and apoptosis. PNPase is translocated via TIM23 and cleaved first by MPP protease and secondly by IMP protease. The second way of its maturation goes through cleavage by MPP protease and then by chaperon activity of YME1 protease. *S.cerevisiae* strains lacking YME1 showed accumulation of PNPase in the cytosol (Rainey, Glavin et al. 2006). Moreover, the AAA domain of YME1 protease in the cell-free system binds unfolded

polypeptides and suppresses their aggregation (Leonhard, Stiegler et al. 1999). Non-assembled or defective assembled synthetic TIMs mutant variants are proteolytic degradated by YME1 protease (Baker, Mooga et al. 2012). Several other proteins were identified that are affected by YME1 deficiency which confirm the role of YME1 as an important player in the protein turnover in mitochondria (Schreiner, Westerburg et al. 2012). In eukaryotes, i-AAA protease function is high conserved in mitochondrial protein metabolism. The ectopic expression of human YME1L transcript variant 3 that shares 42% sequence identity with their yeast counterpart, can partially complement the thermosensitive respiratory growth defect of the yeast yme1 mutant (Shah, Hakkaart et al. 2000). Human YME1L is a 716 AA long polypeptide with similar tissue expression pattern as paraplegin. It is predicted to be a candidate gene for general neurodegenerative disorders (Coppola, Pizzigoni et al. 2000). YME1L may unfold termostabile protein substrates and is able to recognise different sequence-specific signals (degrons). One potential recognition signal is Phe-h-h-Phe, where „h“ means any hydrophobic AA. This signal was revealed in 21 human IMS proteins (Shi, Rampello et al. 2016). Human YME1L is required for mitochondrial fusion/fission via constitutive processing of L-OPA1 (MacVicar and Langer 2016). The depolarization of IMM and exhaustion of cellular ATP leads to activation and stabilization of OMA1 protease and thus elevated the cleavage of L-OPA1. Moreover, oxidative stress-dependent reduction of YME1 may enhance the cellular stress (Rainbolt, Saunders et al. 2015). The mitochondrial unfolded protein response (mtUPR) is a protein quality control pathway. Cells use this pathway to deal with mitochondrial stress by the retrograde signaling pathway to the nucleus and subsequent transcription of protective genes. The main transcription factor is involved CHOP which can heterodimerize with other components and serve as a promoter. MtUPR responsive genes have CHOP binding site flanked by two mitochondrial unfolded protein response elements (MURE). MURE was found, e.g. in gene for Hsp60 chaperone, NDUFB2 subunit of complex I, TIM17A of mitochondrial import complex, YME1L protease, etc. (Mottis, Jovaisaite et al. 2014). In HEK293 cells, YME1L modulates the membrane accumulation of non-assembled Ndufb6 and ND1 subunits of complex I and COX4 subunit of complex IV. The knockdown of YME1L leads to reduced cell proliferation and apoptotic resistance, altered mitochondrial ultrastructure, diminished rotenone-sensitive respiration, and increased sensitivity to oxidative damage (Stiburek, Cesnekova et al. 2012). These results show the essential role of YME1L in the maintenance and turnover of IMM proteins. The clinical impact of YME1L protease is still not clear. It was revealed that YME1L depletion in mice embryonal cells was not viable. Postimplantation-promoted deletion of YME1L in the

same cells led to activation of OMA1. This accelerated OPA1 proteolysis, mitochondrial fragmentation and metabolic alterations in cardiac tissue. Cardiomyocyte-specific deletion of YME1L causes impairment of mitochondrial morphology and dilated cardiomyopathy (Wai, Garcia-Prieto et al. 2015). Moreover, loss of YME1L protease in skeletal muscle preserves the function of YME1L-deficient hearts. Feeding a high-fat diet suppresses heart failure and restores the lifespan of YME1L knockout mice. Cells lacking both YME1L and OMA1 proteases restore their mitochondrial morphology and myocardial function (Wai, Garcia-Prieto et al. 2015). So far, only one disease-causing mutation in YME1L was described. Homozygous Arg149Trp located within a highly conserved region of the mitochondrial pre-sequence causes inhibition of YME1L precursor protein by MPP and leads to infantile-onset mitochondriopathy (Hartmann, Wai et al. 2016). Human YME1L has been repeatedly shown to be related to cancer progression and has been identified as an MYC-responsive gene (Bredel, Scholtens et al. 2009).

1.2.2.2. m-AAA protease

Nuclear-encoded ATPase family gene 3-like 2 protein (AFG3L2, EC 3.4.24.-) has molecular weight of 89 kDa. It is located into the IMM protruding to both AAA and metallopeptidase domains into the mitochondrial matrix. AFG3L2 protease, with proteolytic and chaperone functions, is responsible for maturation, maintenance, and quality control of membrane proteins on the matrix side of the IMM (Koppen, Metodiev et al. 2007). The AAA domain serves as sorting domain with chaperon-like activity. The m-AAA protease consists either of homo oligomer of six AFG3L2 subunits or hetero-oligomerize with spastic paraplegia 7 protein (also known as paraplegin, SPG7). The amount of AFG3L2 and SPG7 oligomers is tissue- and species-specific (Koppen, Metodiev et al. 2007). Moreover, SPG7 requires AFG3L2 for its maturation which is regulated by Tyr179 in AFG3L2 subunit. Arg688Gln substitution leads to insensitivity of the SPG7 subunit to AFG3L2-mediated maturation and is restored using carriers which bypass this regulation (Almontashiri, Chen et al. 2014). Mouse mitochondria harbor AFG3L1 subunit of m-AAA protease which makes up similar homo- or heterooligomeric complexes as AFG3L2 subunit. All subunits of m-AAA protease are nuclear encoded with N-terminal targeting sequences. AFG3L1 and AFG3L2 subunits are, after import into the mitochondria, processes by MPP to their intermediate forms. This form is subsequently maturated autocatalytically. Murine AFG3L1 is only a pseudogene in humans

(Koppen, Bonn et al. 2009). Heterohexameric Yta10-12 complex is a the yeast homologue of mammalian AFG3L2 complex. It has the molecular weight of 850 kDa. The Yta10-12 complex is built up of Yta10 (also known as Afg3p) and Yta12 (Rca1p) subunits with metallopeptidase activity and is responsible for the cleavage of non-assembled IMM proteins with simultaneous ATP hydrolysis. Mutant variants lead to homooligomerization of only Yta12 subunits (Lee, Augustin et al. 2011). Yta10 or Yta12 deficient cells show respiratory deficiency but are viable (Arlt, Tauer et al. 1996). The coordination between substrate cleavage and ATP hydrolysis after binding one ATP molecule is ensured by intramolecular signaling network in the AAA domain with a special role of arginine finger and loop 2 regions of Yta10 component. The enzymatic activity of each subunit is enhanced by interactions between its Walker A motif with another one in neighboring subunits. Coordinated ATP hydrolysis between subunits and thus the obtained energy of ATP is used as a mechanical force for membrane dislocation of substrates. (Augustin, Gerdes et al. 2009). Previously-mentioned Ccp1 substrate requires gradually two protease: i) the m-AAA protease and ii) the rhomboid protease Pcp1 for its maturation. While first of them ATP-dependently dislocates Ccp1 from its initial position to the correct position in the IMM, the second Pcp1 protease cleaves Ccp1 inside the IMM (Tatsuta, Augustin et al. 2007). Chaperon-like activity of Yta10-12 complex is essential for the assembly of the intergral membrane ATPase 9 subunit of ATP synthase complex. Eukaryotic m-AAA proteases show similar molecular organization. Reintroduction of human AFG3L2 and paraplegin is able to restore the respiratory competence of Yta10-12 mutant of *S.cerevisiae* (Atorino, Silvestri et al. 2003). AFG3L2 has similar AAA and metallopeptidase domains each of them made up by α + β fold of two α helices and five β sheets in human, peripherally bound to the membrane surface (Ramelot, Yang et al. 2013). The m-AAA protease is responsible, independent on the OMA1 protease, for the cleavage of OPA1 protein. Both murine AFG3L1 and AFG3L2 are essential for mitochondrial fusion via stabilization of the L-OPA1 forms. Loss of AFG3L2 leads to elevated OPA1 processing by OMA1 protease (MacVicar and Langer 2016). Complex of m-AAA protease and the m-AAA protease interacting protein 1 (MAIP1, also known as C2ORF47) was found in mouse neurons where it managed the assembly of the essential mitochondrial Ca^{2+} uniporter (MCU) regulator protein (EMRE). EMRE, metazoan-specific protein with a single transmembrane domain, has a molecular weight of 10 kDa and mediates calcium uptake into mitochondria (Sancak, Markhard et al. 2013). The m-AAA protease cleaves non-assembled EMRE components and loss of m-AAA protease leads to permanently open mitochondrial permeability transition pore. This suggest possible molecular mechanism

for neuronal disorgers associated with mutated m-AAA protease, via deregulated mitochondrial Ca^{2+} homeostasis (Konig, Troder et al. 2016). Autosomal dominant inherited spinocerebellar ataxias (SCAs) especially SCA type 28 (SCA28) is manifesting by young-adult onset, slowly progressive trait, and limb ataxia resulting in problems with coordination and balance, dysarthria, ptosis, nystagmus, and ophthalmoparesis. A predominant amount of the patients inherited SCA28 disorder from their parents. These manifestations are typical by cerebellar dysfunction mostly due to Purkinje cell degeneration. Missense substitution Glu700Lys in AFG3L2 (Edener, Wollner et al. 2010) was confirmed using human mutated AFG3L2 in *S.cerevisiae.* This mutated variant leads to AFG3L2 homocomplex with proteolytic impairment, marked reduction of respiratory chain complex IV, and loosely affected complex III and complex V (Di Bella, Lazzaro et al. 2010). So far, 17 missense mutations have been identified in Europe patients. Homozygous AFG3L2 mutations were identified in a spastic ataxia neuropathy syndrome (Pierson, Adams et al. 2011) and confirm the evolutionary conserved Tyr689 (respectively Tyr689Asn) as likely pathogenic background in SCA28 (Zuhlke, Mikat et al. 2015). Early onset spastic ataxia-neuropathy syndrome leads to lower extremity spasticity, peripheral neuropathy, ptosis, oculomotor apraxia, dystonia, cerebellar atrophy, and progressive myoclonic epilepsy. It is caused by homozygous missense mutation Tyr616Cys in AFG3L2 subunit. This mutation leads to the inability of AFG3L2 to homooligomerize in patient`s fibroblasts and experimentally also in *S.cerevisiae* (Pierson, Adams et al. 2011). COX1 subunit is incorporated into the subcomplex of complex IV and was found truncated in patient`s cells where it led to destabilization of complex IV. Synthetic dominant negative mutant Glu408Gln in Walker B leads to enhanced stability defective COX1 (Hornig-Do, Tatsuta et al. 2012). Hereditary spastic paraplegia (HSP) type 7 is characterized by aberrant structure of m-AAA protease and patient`s fibroblasts show higher sensitivity to oxidative stress and complex I deficiency. Both defects are restored by complementation of exogenous wild-type paraplegin (Atorino, Silvestri et al. 2003). Human SPG7 is composed of β sheet which is built up of five parallel strands, surrounded by two α helices and has four antiparallel α helices at the C-terminal part. Nucleotide binding site is located between these components. Mutations in catalytic centre of human SPG7 lead to complete abrogation of the enzymatic activity of m-AAA protease (Karlberg, van den Berg et al. 2009). Two other mutations were identified in two patients with HSP and confirmed by complementation experiments in yeast. These mutations Glu575Gln and Lys354Ala led to enzymatically inactive forms (Bonn, Pantakani et al. 2010). Mitochondrial ribosomal protein L32 (MRPL32) is cleaved by m-AAA protease and subsequently assemble into the

preassembled ribosomal particles and assembled ribosome. The maturation of MrpL32 protein and mitochondrial protein synthesis were defective in yeast and HSP mouse models with depletion of paraplegin (Nolden, Ehses et al. 2005).

1.2.2.3. CLPXP

Caseinolytic protease (CLPXP) is localized into the mitochondrial matrix close to the matrix side of the IMM (de Sagarra, Mayo et al. 1999). CLPXP protease participates in the mitochondrial protein quality control, and is built up of two separate components (Katayama-Fujimura, Gottesman et al. 1987). These complexes are involved in developmental changes, survival under starvation, replication of phage, and plasmids in bacteria. Moreover, related ClpA-like proteins can be divided into several additional subfamilies e.g ClpC and ClpE (Gottesman 2003). CLPAP is built up of AAA ATPase component CLPA and protease component CLPP (EC 3.4.21.-). CLPXP is built up of ATPase termed CLPX and a peptidase called CLPP. CLPP component is able to unspecifically cleave small peptides but not larger folded proteins. For the degradation of proteins, CLPP component needs the second part, CLPA or CLPP. This suggests the sorting function for this components. Moreover, CLPX alone can serve as a chaperone. CLPX subunit contains a typical N-terminal domain with C4-type zinc-binding domain and characteristic AAA motif. This motif is composed of large and small AAA domains. Two N-terminal domains fold independently of the rest of the CLPX subunit as a dimer stabilized by two zinc atoms per dimer. These N-terminal domains are essential for the cleavage of some bacterial substrates, e.g. MuA, Mu repressor, and UmuD but not for SsrA tag. The deletion of the N-terminal domain leads to inability of binding to CLPP and substrates (Wojtyra, Thibault et al. 2003). Large AAA domain comprises Walker A, Walker B, arginine finger, and several loops. Small AAA domain contains sensor II arginine. Both domains are functional together as an asymmetric hexagonal ring. This asymmetry is essential for ATP binding between small and large parts of each CLPX subunit and subsequent conformational changes of subunits. The CLPX subunits are present in two domain-domain conformational positions: four are loadable and two are unloadable for nucleotide i.e. maximum four nucleotides can be concurrently bound (Glynn, Martin et al. 2009). The second component of CLPXP is CLPP subunit with a molecular weight of 30 kDa. Its function is to bind the sorting and ATPase component and to cleave of the substrates. CLPP subunit is synthesized as a precursor with typical N-terminal targeting sequence of 14

AA which is cleaved by autocatalysis in *E. coli*. Experiments with the replacement of first 1-21 residues of N-terminus from *E. coli* to human CLPP confirmed the auto-processing (Kang, Maurizi et al. 2004). Seven CLPP subunits create barrel-shape chamber with narrow axial pore and two of these chamber folds face-to-face built up CLPP component of the CLPXP protease. CLPP component has internal proteolytic serine active site with classical Ser-His-Asp catalytic triad and oxyanion hole. The narow axial pore is enough for entrance of small peptides but is inadequate for larger proteins (Wang, Hartling et al. 1997). The activity of CLPP is partially inhibited by diisopropyl fluorophosphate. It results in several covalent modifications of single active site and in mild reduction (not typical for serine protease) of enzymatic activity. It suggests the possible heterogenity or redundancy of active sites (Thompson, Singh et al. 1994). The efficient clevage is ensured by i) high concentration of active sites in CLPP subunits and ii) by the distance of each active site which is enough for the binding of the extended substrates. Heptamer of CLPP is stable itself. Only in the presence of CLPX and ATP, CLPXP is able to built up typical tetradecamer of CLPP with two hexamers of CLPP. Final CLPXP complex possesses high peptidase activity when compared to sole CLPP. Mutations in CLPP subunit leads to dissociation of CLPXP because the CLPX component have to make the conformational changes in CLPP to stabilize the whole CLPXP molecule (Kang, Dimitrova et al. 2005). Moreover, some antibiotics such as acyldepsipeptides induces positive conformational changes in CLPP during proteolytic activation (Li, Chung et al. 2010). CLPX function is sorting coponent of CLPXP which is able to identify degradation tags called degrons e.g. ssrA tag at C-terminus in *E.coli* (Gottesman, Roche et al. 1998). SsrA tag is 11 AAs long peptide tail, exactly Ala-Ala-Asn-Asp-Glu-Asn-Tyr-Ala-Leu-Ala-Ala, attached to the incomplete nascent protein tagging the protein degradation. This mechanism depends on SsrA RNA (known as tmRNA and 10SaRNA) which is functional both as a tRNA and as mRNA. It is used to recognise the proteins whose biosynthesis has stalled or has been otherwise interrupted (Karzai, Roche et al. 2000). Generally, there are two classess of degrons tailed to the C-terminus with homology to the ssrA tags or MuA tags and three classes of tags connected at N-terminus (Baker and Sauer 2012). SsrA tag is recognised by several loops localized in different parts of CLPX component. Though the human CLPX component has the same sequences in one of this loops (Gly-Tyr-Val-Gly). It is not able to recognise ssrA tag (Martin, Baker et al. 2008). In substrate recognition two adaptor proteins were found: stringent starvation protein B (SspB) and regulator of RpoS (RssB). SspB protein modulates transport of ssrA tag proteins and facilitate the degradation of one type of N-terminal tags (Flynn, Levchenko et al. 2004). RssB regulates the turnover of sigma S factor (RpoS) by

promoting its proteolysis in exponential phase of growing cells via transport of RpoS to the CLPXP protease (Muffler, Fischer et al. 1996). After the recognition, CLPX component translocates the unfolded protein substrates into the axial pore of itself using energy from ATP. The cycle of ATP binding and hydrolysis leads to conformational changes in CLPX subunits mutually. The previously mentioned Gly-Tyr-Val-Gly loop is responsible for linking these two actions (Siddiqui, Sauer et al. 2004). Surprisingly, in accordance with different tags, CLPXP protease cleaves unfolded protein substrates from N- and C-terminus and it is not specific in side-chain chirality, polarity, and size. In addition, CLPXP is able to successfully degrade the substrate proteins with homopolymeric tracts composed of Gly, Lys, and Pro (Barkow, Levchenko et al. 2009). CLPXP protease can start degradation by cleaving disulfide bonds in the internal part of substrate protein under the condition of concurrent translocation of two or more polypeptides through the pore (Hoskins, Yanagihara et al. 2002). The enterance into the CLPP part is moderated by 20 AAs at N-terminus. This mechanism prevents the enterance of large proteins or in the absence of ATPase subunit (Bewley, Graziano et al. 2009). Final step is protein degradation into peptide fragments in peptidase chamber of the CLPP component. Multiple degradations are four-fold slower than single molecule because the protease needs another time for the engagement (Olivares, Baker et al. 2018). Cell-free expression (transcription-translation) system with purified CLPXP protease displayed low activity of this protease. The speed was elevated by the addition of exogenous ATP in *E.coli* (Shi, Wu et al. 2018). CLPXP protease participates in one or more pathways modulating β-lactam resistance in methicillin-resistant *Staphylococcus aureus* (MRSA). MRSA encodes *mecA* gene for peptidoglycan transpeptidase PBP2a, that is neccessary for the resistance. CLPX and CLPP inactivation mutants showed various types of distinct phenotypes that may elevate β-lactam tolerance (Baek, Grundling et al. 2014). The above described mechanism is typical for *E.coli*. Human CLPXP still remains unclear. Function of human CLPXP have been identified associated with SDH B of complex II and the survivin oncoprotein in tumour cells. KD of both CLPXP subunits leads to elevated level of misfolded SDH B subunit, total cellular superoxide production and activation of adenosine monophosphate (AMP)-activated protein kinase (AMPK). Similar to several other AAA proteases, CLPP subunit of CLPXP was overexpressed in breast adenocarcinoma cells and in both primary and metastatic prostatic adenocarcinoma. KD of CLPX or CLPP partially blocks the tumor cell proliferation and inhibits colony formation. It suggests CLPXP regulation of the tumor cell invasion and metastasis (Seo, Rivadeneira et al. 2016). Further, CLPXP participate in activation of δ-aminolevulinate synthase (ALAS) which catalyses the first step

of heme biosynthesis resp. the synthesis of δ-aminolevulinic acid from succinyl-CoA with glycine (Voet 2010). The mutation Gly298Asp in CLPX leads to inactivation of the ATPase activity and pathological accumulation of the protoporphyrin IX. This can lead to erythropoietic protoporphyria in erythroid cells (Yien, Ducamp et al. 2017). To this day, nine types of porphyrias were described and one of them is erythropoietic protoporphyria, which is characteristics by the accumulation of protoporphyrin IX. More than 90% of them are caused by loss-of mutations in ferrochelatase, 5% are caused by mutations in the C-terminus of ALAS2, and mutations in CLPXP protease may be the cause of the rest 5% of cases (Whitman, Paw et al. 2018). Recessive mutation Thr145Pro and Cys147Ser in CLPP component of CLPXP leads to the changes in its chamber and dysfunction of the CLPXP protease. This causes Perrault syndrome, a rare disorder characterized by loss of hearing, sense abnormalities of the ovaries, and, in some cases, neurological problems (Jenkinson, Rehman et al. 2013).

1.2.2.4. Lon

Lon protease (EC 3.4.21.-) is the member of the S16 peptidase family localized in the mitochondrial matrix. It participates in the turnover of mitochondrial matrix proteins and in the regulation and maintenance of the mitochondrial DNA. Originally, Lon protease was named „La“ by the depletion of the *lon* gene in *E.coli* mutants which leads to longer undivided filaments upon UV irradiation. It suggested the role of Lon protease in defense against radiation (Howard-Flanders, Simson et al. 1964). So far, two types of Lon proteases were identified (LonB and LonA). LonB (typical of *Archae*) has hydrophobic membrane anchor to the cytoplasmic side of the membrane, in contrast with LonA (typical for *Eubacteria* and *Eukarya*), which has large N-terminal domain between Walker A and Walker B motifs. N-terminal anchor or N-terminal domain participates in substrate binding. Other differences are in consensus sequences and in the orientation of the active sites. Both LonA and LonB contain typical AAA+ modules and the proteolytic domains on the C-terminus with typical Ser–Lys catalytic dyad (Rotanova, Botos et al. 2006). Moreover, there are two Lon proteases, mitochondrial and peroxisomal, in *Eukaria*, which are encoded by two different genes. Lon protease typically oligomerize in single-ringed shaped homo-oligomer. This is necessary for binding of the G-quadruplex DNA and for the proteolytic activity as a protector against the stress-induced protein aggregation. G-quadruplex DNA is secondary structure

typical for guanine-rich regions. Lon protease forms homohexamers with exception of yeast Lon protease which one is heptameric (Venkatesh, Lee et al. 2012). N-terminal domain is usually arranged in one trimer of dimers and links with the proteolytic domain by a narrow trimeric channel composed likely of coiled-coil helices (Kereiche, Kovacik et al. 2016). PIM1 protease, the yeast homologue of Lon with 30% of sequence identity, is 1133 AA long. Deletion of PIM1 protease leads to the inability to use nonfermentable substrates and thus maintain functional mtDNA and acceleration of the aging (Erjavec, Bayot et al. 2013). PIM1 lacking cells show elevated frequency of mtDNA deletion and thus lower level of respiration (Suzuki, Suda et al. 1994). The constitutively expressed PIM1 is elevated under thermal stress conditions, so PIM1 may be important in the heat shock response (Van Dyck, Pearce et al. 1994). As a substrate of the protease was identified ATP-dependent α-casein (Wang, Gottesman et al. 1993). The human LONP1 (EC 3.4.21.53) homologue has approximately 100 kDa molecular weight and is present in all human tissues. It is higher expressed in the brain, heart, liver, skeletal muscle, and placenta and lower in kidney, lung, and pancreas. Lon protease is synthesized in the cytosol as a 959 AAs long preprotein with typical N-terminal sequence and transported into the mitochondrial matrix (Wang, Gottesman et al. 1993). Its maturation is two steps process. Firstly, N-terminal targeting sequence is cleaved by MPP and secondly by self-assembly and autocatalytic cleavage (Wagner, van Dyck et al. 1997). For maturation is necessary the IMM electrochemical potential because the process can be stopped by 2,4-dinitrophenol (Wang, Maurizi et al. 1994). The major pool of Lon protease is found soluble in the mitochondrial matrix but a small portion of it was identified associated with mitochondrial nucleoids. In human, Lon protease has several important roles: i) DNA- and RNA-binding activity, ii) chaperone activity, and iii) proteolytic activity. Lon protease is able to bind single strand RNA, single strand DNA and double strand DNA in guanine-thymine rich sequences throughout the heavy strain of mtDNA. Moreover, it can be specifically associated with guanine-uracil sequences in RNA. This association is decreased by ATP and increased by the substrate stimulation (Liu, Lu et al. 2004). Lon protease directly interacts with other components of nucleoids, e.g. mitochondrial transcription factor A (TFAM), polymerase γ and Twinkle (Liu, Lu et al. 2004), and with chaperons heat shock protein 60 (HSP60) and heat shock protein 70 (HSP70). Only the DNA-free or nonphosphorylated TFAM is degraded by Lon protease (Lu, Lee et al. 2013). HSP60 makes up a complex with HSP70, and under stress conditions, the stability of this complex depends on Lon protease. Moreover, HSP60 binds p53 protein to inhibit the apoptosis. Lon protease co-immunoprecipitates with NDUFS8 subunit of the complex I located in the IMM (Kao,

Chiu et al. 2015). Chaperon activity of the Lon protease is ensured by ATP-binding domain and N-terminal domain. Lon protease also participates in the assembly of the subunits of OXPHOS in yeast, e.g. NDUFS8 subunit of complex I. Lon protease`s proteolytic activity is essential for maintenance of mitochondrial function and integrity. The initial mechanism of cleavage is done by Ser885–Lys896 of the catalytic dyad and it cleaves hydrophobic AAs in the interior of the substrate. Consequentialy, other cleavages are carried out processively along the polypeptide chains, at least, in the case of experimental substrates: the α-subunit of MPP and the StAR (Ondrovicova, Liu et al. 2005). The regulation of the proteolytic activity of Lon is not clear. It is known that Lon protease supports regulation of the SIRT3 and coimmunoprecipitates with it. The KD of SIRT3 leads to elevated level of Lon protease (Gibellini, Pinti et al. 2014). Human Lon protease is responsible for the degradation of ALAS (Tian, Li et al. 2011), StAR (Granot, Kobiler et al. 2007), and COX4 subunit (isoform 1) of complex IV (Fukuda, Zhang et al. 2007). Lon protease degraded misfolded protein, e.g. glutaminase C (Kita, Suzuki et al. 2012) and oxidatively-modified proteins like mitochondrial aconitase (Bota and Davies 2002) and cystathionine beta-synthase (Kita, Suzuki et al. 2012). Interestingly, the amount of the Lon protease correlates with the number of other players in mitochondrial unfolded protein response (mtUPR), e.g. CLPP component. Downregulation of the Lon protease leads to increased level of PINK1 protease (Jin and Youle 2013). The Lon protease is upregulated in genetic inherited disease the cerebral, ocular, dental, auricular, skeletal (CODAS) syndrome and in some types of the mammalian cancers characterized by short survival of patients (Pinti, Gibellini et al. 2016), e.g. breast cancer (Braso-Maristany, Filosto et al. 2016), cervical cancer (Nie, Li et al. 2013), colon cancer (Gibellini, Pinti et al. 2014), bladder cancer (Liu, Lan et al. 2014) etc. In these tumors, there are changes in the mitochondrial metabolic pathways from respiratory to glycolytic metabolism (Pinti, Gibellini et al. 2015) via remodeling of the OXPHOS. On the other hand, the homologous deletion of Lon protease causes early embryonic lethality in mice and the haploinsufficiency of Lon protease protects mice against colorectal cancer and chemically induced skin tumors (Cheng, Kuo et al. 2013, Quiros, Espanol et al. 2014). The 2-cyano-3,12-dioxoolean-1,9-dien-28-oic acid (CDDO) is known as the inhibitor of the production of nitric oxide (Honda, Rounds et al. 1998) and its derivates are used as therapeutic agent (Wang, Yang et al. 2014) causing the apoptosis via protein aggregation and inactivation of Lon protease, but not cytosolic 20S proteasome (Bernstein, Venkatesh et al. 2012). This mechanism is functional in several types of the cancer cells, e.g. hepatocarcinoma cells and in MCF7 breast carcinoma cells (Gibellini, Pinti et al. 2015).

1.2.3. Oligopeptidases

Mitochondrial oligopeptidases are only poor understood with only few exceptions. They were firstly described in isolated rat liver. During this experiment, a large fraction of various proteins synthesized in mitochondria were degraded to AAs within 1 hour without the participation of lysosomal enzymes and transported out of the mitochondria (Desautels and Goldberg 1982). Oligopeptidases complete the degradation of peptides produced by AAA protease, e.g. i-AAA and m-AAA proteases (Kambacheld, Augustin et al. 2005). The presequences of nuclear-encoded mitochondrially resident proteins, that are not degraded, are rich in basic AAs. This AAs prefer α-helical conformation and thus adopt the amphipathic structure with neutral AA along the peptide chain (Roise, Horvath et al. 1986). The amphipathic structure has the advantage of binding to the OMM. But it may be also disadvantageous because the hydrophobic AA can permeate OMM and the hydrophilic AA can interact with phospholipids, e.g. cardiolipin. This can cause lysis of the OMM and subsequently increase permeability of the IMM (Nicolay, Laterveer et al. 1994).

The rest of peptides, which are not degradated, are transported out of the mitochonria by MultiDrug resistance-Like 1 (Mdl1) ATP-binding cassette (ABC) transporter. Each *MDL* gene codes a set of transmembrane domains. ATP-binding domain depleted mutants revealed that *MDL* genes are not essential for viability of the yeast (Dean, Allikmets et al. 1994). Mdl1 is located into the IMM in *S. cerevisiae* and serves as the intracellular peptide transporter able to export 0,6-2,1 kDa peptides. i-AAA protease generates small peptides directly out of mitochondria into the IMS from which the peptides diffuse by porins or are translocated by TOMM. Mutations in Walker A or Walker B lead to decreased export of long peptides but short peptides or single AA are not affected, so the ATP-binding and its hydrolysis are essential for the function of Mdl1 transporter (Young, Leonhard et al. 2001). The released peptides may have a regulation role in cell signaling. The deletion of YME1 leads to the absence of some sort of released peptides which results in distinct alterations of nuclear gene expression (Arnold, Wagner-Ecker et al. 2006).

Thimet („Thiolsensitive metallo“) oligopeptidases (EC 3.4.24.-) are the member of the metallopeptidase M3 family and have roles in regulation processes. Their substrates are, e.g. amyloid –β, angiotensin I, and bradykinin (Knight, Dando et al. 1995, Koike, Seki et al. 1999, Pereira, Souza et al. 2013). Thimet oligopeptidese, as many other metalloproteases/peptidases possess zinc binding motif His-Glu-X-X-His (Fukasawa, Hata et al. 2011), has pH optimum

between 6.5-8.5 and needs thiol to its active form. Thimet metallopeptidase can be inhibited by N-[1-(RS)-carboxy-3-phenylpropyl]-Ala-Ala-Phe-p-aminobenzoic acid (Buchler, Tisljar et al. 1994). It was revealed that two thimet oligopeptides Prd1 (human homologue known as saccharolysis) and Mop112 (human homologue known as PreP) cleave products of the i-AAA protease.

The proteinase/oligopeptidase yeast cysteine proteinase D (yscD, also known as saccharolysin, EC 3.4.24.37 formerly EC 3.4.22.22.) has a molecular weight of 83 kDa. It is coded by *PRD1* gene in *S.cerevisiae*. Interestingly, 3-5% of its activity was detected in IMS of the mitochondria. YscD oligopeptidase cleaves the same Phe-Ser bond in bradykinin as other oligopeptidases (Orlowski, Michaud et al. 1983) and Pro-Phe and Ala-Ala bonds (Garcia-Alvarez, Teichert et al. 1987, Buchler, Tisljar et al. 1994). Further experiment with mutant variants revealed that yscD oligopeptidase is not involved in essential pathways in the mitochondria (Garcia-Alvarez, Teichert et al. 1987). Mammalian homolog is called neurolysin (known as Angiotensin II-binding protein, EC 3.4.24.16), has the molecular weight of 78 kDa and cleaves oligopeptides such as neurotensin, bradykinin and dynorphin A. In the neurotensin protein, the neurolysin peptidase cleaves preferentially Pro-Tyr in specific position (Kambacheld, Augustin et al. 2005, Barrett 2012, Vogtle, Burkhart et al. 2017).

The presequence protease (PreP, EC 3.4.24.-) was firstly described in *Arabidopsis thaliana* (Stahl, Moberg et al. 2002). It was named Cym1 in yeast *S. cerevisiae* (also known as Mop112) (Kambacheld, Augustin et al. 2005) and the official named symbol is pitrilysin metallopeptidase 1 (PITRM1) in humans (also known as hPreP or MP1) (Mzhavia, Berman et al. 1999). PreP, a member of M16C family, is a mitochondrial matrix located in contrast to *S. cerevisiae* homologue Mop112 which is in the IMS (Alikhani, Berglund et al. 2011). It is a typical zinc-metallopeptidase which binds one zinc ion per subunit by inverted Zn-binding motif. Presequences and their lengths for each PreP protease homologs are very distinct and their lengths correspond with target compartment of mitochondria, e.g. the presequences of *A. thaliana* is 85 AAs, PreP has 29 AAs, and Mop112 presequence contains only 7 residues in *S. cerevisiae* (Alikhani, Berglund et al. 2011). The Mop112 sequentially overlaps with the i-AAA protease. The knockout of Mop112 protease leads to increased amount of release peptides from the mitochondria, generated upon proteolysis of mitochondrial proteins, and altered mitochondrial morphology (Kambacheld, Augustin et al. 2005). The human hPreP is predicted to be a part of „central proteome“. The term that describe the group of 1 124 proteins that are ubiquitously and abundantly expressed in different human cell lines (HaCat,

HepG2, K562, HEK293, Namalwa, U937, HeLa) (Schirle, Heurtier et al. 2003). Human PreP has the molecular weight of 117 kDa and pH optimum 7.7 (Mzhavia, Berman et al. 1999). It is composed of PreP-N and PreP-C domains which are linked by helical hairpin. Prep protease uses the conserved mechanism of M16C protease family, the substrate selection by size-exclusion (King, Liang et al. 2014). Human brain PreP peptidasome was found to degrade amyloid-β. It is 36-43 AA long main component of amyloid plaques in brain of patients with Alzheimer`s disease. The inactivation of hPreP leads to inhibition of the proteolytic activity against amyloid-β (Falkevall, Alikhani et al. 2006). Moreover, the enhancement of PreP activity leads to the reduction of amyloid-β, attenuation of neuroinflammation, and to the improvement of mitochondrial and synaptic function (Fang, Wang et al. 2015). To summarize, PreP peptidasome has an important role in the maturation or degradation of mitochondrial targeting peptides and thus in mitochondrial protein quality control (Teixeira and Glaser 2013).

1.2.4. Other mitochondrial proteases

The last group is composed of the rest of mitochondrial proteases which do not belong to the three previous groups. The most important members of this group are the OMA1 and HtrA2 proteases.

1.2.4.1. HtrA2 protease

Oligomeric serine protease high-temperature requirement (HtrA, also known as Omi) has a molecular weight of 49 kDa and predicted monophyletic origin from α-proteobacteria (Koonin and Aravind 2002). HtrA protease is nuclear-encoded and residential into the IMS but residual fraction was detected also in the nucleus (Martins, Iaccarino et al. 2002). Bacterial HtrA (also known as DegP) is a heat-shock induced protease, regulated by signal transduction pathways and participates in the survival of macrophages. Mutations in HtrA2 reduced their lifespan (Pallen and Wren 1997). Under elevated temperature, HtrA is required for bacterial survival. It acts as a protease (Spiess, Beil et al. 1999, Goo, Rhim et al. 2017) with only limited substrate selectivity (Kolmar, Waller et al. 1996). Under low temperature, HtrA/DegP adopts a chaperonin function. Mammals have four HtrA proteases HtrA1 – HtrA4. HtrA1 (also known as L56 or PRSS11), HtrA3 (also known as PRSP), and HtrA4 have signal

peptides as well as domains known as the insulin-like growth factor binding (IGF) and protease inhibitor domains. They have roles in secretion signals and were found significantly reduced in several types of the cancers (Narkiewicz, Klasa-Mazurkiewicz et al. 2008, Chien, Campioni et al. 2009, Narkiewicz, Lapinska-Szumczyk et al. 2009). The HtrA2 has characteristic two specific domains a (chymo)trypsin-like protease domain and C-terminal PDZ domain. PDZ domain (Post synaptic density protein, Drosophila disc large tumor suppressor, and Zonula occludens-1 protein) is composed of 80-90 AAs folded into four β strands and one or two α helixes. This domain serves in anchoring of preferentially of the C-terminus of the substrate and stabilization and regulation of a trypsin-like protease domain (Clausen, Southan et al. 2002). HtrA2 is synthesized as a precursor with N-terminal mitochondrial targeting sequence and its attached to the IMM when matured. After maturation, it is able to expose its N-terminus to IAP antagonist Smac (Martins, Iaccarino et al. 2002, Verhagen, Silke et al. 2002). During the apoptosis, HtrA2 is released into the cytosol. HtrA2 plays a crucial role in cell physiology and is involved in pathological processes including neurodegenerative disease and cancer (Vande Walle, Lamkanfi et al. 2008). Missense mutations lead to highly reduced proteolytic activity of HtrA2 and to degeneration of striatal neurons. This suggests that the loss of HtrA2 changes the sensitivity of mitochondria to stress. Moreover, mice with such mutations have partly undeveloped organs such as heart, thymus, and spleen and die at the age of 3 weeks (Jones, Datta et al. 2003). Further research showed that mice with deletion of HtrA2 have no coordination, reduced mobility, and elevated tremor (Martins, Morrison et al. 2004). These manifestations are similar to the Parkinson`s disease (PD). About 2% of the population above the age of 60 is affected by this condition (Bose and Beal 2016). Two missense mutations were revealed to affect enzymatic activity of HtrA2 that are associated with PD (Strauss, Martins et al. 2005). Phosphorylation of HtrA2 is carried out by MAP kinase and depends on PINK1 kinase. PINK1 kinase was found mutated in PD and leads to decreased level of phosphorylation (Plun-Favreau, Klupsch et al. 2007). Another regulation pathway is mediated by presenilin-1 which significantly increase HtrA2 proteolytic activity. Human presenilin-1 is one of four core proteins of γ-secretase which cleaves single-pass transmembrane proteins at residues within the transmembrane domain and it is important substrate is amyloid precursor protein and the product is β-amyloid, a crucial protein of Alzheimer`s disease. Moreover, presenilin-1 is required for HtrA2-induced apoptosis (Gupta, Singh et al. 2004).

1.2.4.2. OMA1 protease

OMA1 (overlapping with the m-AAA protease 1 homologue, EC 3.4.24.-) metallopeptidase functionally overlapping with the m-AAA protease and has a molecular weight of 60 kDa. It has predicted homooligomeric structure induced by self-cleave at C-terminus (Bohovych, Donaldson et al. 2014, Zhang, Li et al. 2014). Functionally, OMA1 protease cooperates and/or complements other IMM proteases especially i-AAA and m-AAA proteases under specific conditions. As mentioned before, OMA1 protease, and i-AAA protease are regulated reciprocally. OMA1 protease may manage i-AAA protease`s proteolytic degradation and i-AAA protease controls and cleaves membrane-depolarization activated OMA1 protease. It depends on the level of mitochondrial ATP and thus on the type of cellular stress (Rainbolt, Lebeau et al. 2016). This mechanism is likely specific for mammalian cells because the reintroduction of OMA1 protease from mouse embryonic fibroblasts (MEFs) did not restore this mechanism in OMA1 depleted *S.cerevisiae* cells. Moreover, the yeast OMA1 protease is more stable than mouse homologue (Baker, Lampe et al. 2014). Mitochondrial phosphatidylserine decarboxylase 1 (Psd1) with phosphatidylserine decarboxylase 2 and 3 are responsible for catalysis of formation of phosphatidylethanolamine from phosphatidylserine. It plays a central role in phospholipid metabolism and interorganelle trafficking of phosphatidylserine. Psd1 is composed of noncovalently associated α and β subunits. The α subunits are necessary for enzymatic activity. The β subunits are autocatalyticaly removed. OMA1 protease cleaves misfolded temperature-sensitive Psd1 precursor and the rest is cleaved by i-AAA protease. The i-AAA protease alone may degrade β-subunits after their heat exposure-triggered postautocatalytical aggregation in temperature-sensitive mutants of *S.cerevisiae* (Ogunbona, Onguka et al. 2017). Similarly, OMA1 and m-AAA protease manage the proteolysis of misfolded oxidase assembly factor/protein 1 (OXA1). Its C-terminus interacts with ribosomal proteins and inserts both, mitochondrial and nuclear-encoded proteins, into the IMM. Oxa1 is essential in insertion of COX1, COX2 and COX3 subunits of complex IV, ATP6 and ATP9 subunits of ATP synthase and cytochrome *b* (Cytb) into the IMM in *S.cerevisiae* (Hennon, Soman et al. 2015). The m-AAA protease removes the matrix-located C-terminus of OXA1 protein and degrades its transmembrane domain. In absence of m-AAA protease, OMA1 protease cleaves OXA1 in cooperation with unknown peptidase (Kaser, Kambacheld et al. 2003). Moreover, OMA1 is essential for survival during the stationary phases because yeast cells with mutated OMA1 protease and i-AAA or m-AAA proteases showed slow growth at elevated temperatures. OMA1 mutated cells showed

physiological amounts of single complexes of OXPHOS but imbalanced respiration. This can be caused by affected supercomplexes of OXPHOS. *OMA1* gene were shown to interact with genes encoding factors known to influence the stability of supercomplexes of OXPHOS (Bohovych, Donaldson et al. 2014). The OMA1 protease is one of the key players in housekeeping of the mitochondrial integrity. OMA1 protease is evolutionary conserved. But there are significant differences between the N- and C-terminal regions in the yeast and mouse homologues resulting in functional differences (Baker, Lampe et al. 2014). Metallopeptidase from M48C family participates in the protein quality system in IMM (Lopez-Pelegrin, Cerda-Costa et al. 2013). Under stress conditions accompanied by decrease of membrane potential or loss of YME1L protease, OMA1 protease cleaves OPA1 to S-OPA1. OPA1 protein has eight alternatively spliced mRNA variants (Sp1-Sp8). Four spliced variants have both S1 and S2 proteolytic sites, namely Sp4, Sp6, Sp7, and Sp8. The rest four spliced variants have only S1 proteolytic site. The OPA1 preprotein is firstly processed by MPP protease which generates IMM-bound L-OPA1 isoforms. All L-OPA1 isoforms have S1 proteolytic site and half of them also have an S2 site (Song, Chen et al. 2007). Under normal conditions (limited activity of OMA1) the L-OPA1 is processed by OMA1 protease at S1 proteolytic site and by i-AAA protease at S2 proteolytic site. This creates the balanced mix of L-OPA1 and S-OPA1 forms. Under stress conditions, which leads to mitochondrial dysfunctions, the activity of OMA1 is enhanced probably via membrane depolarisation. This is associated with changes in ATP level due to ATP-independent activity of OMA1 protease. Enhancement of OMA1 protease leads to reduction in the amount of L-OPA1 isoforms and increased level of the S-OPA1 isoforms. This regulation may help to remove dysfunctional mitochondria from mitochondrial reticulum and delay eventual apoptosis (MacVicar and Langer 2016). This results in S-OPA1 isoforms accumulation which increases mitochondrial fission and thus mitochondrial network fragmentation (Wai, Garcia-Prieto et al. 2015). This process removes defective mitochondria from mitochondrial reticulum and delay apoptosis (Head, Griparic et al. 2009). After the recovery of the physiological conditions, OMA1 protease is autocatalytically degraded. The degradation starts on the both C-and N-terminus (Baker, Lampe et al. 2014). OMA1 protease is IMM-embedded by one hydrophobic transmembrane segments. Currently, it is assumed that OMA1 exposes its C-terminal metallopeptidase domain and positively charged N-terminus to the IMS and its active site into the mitochondrial matrix (Lopez-Pelegrin, Cerda-Costa et al. 2013, Baker, Lampe et al. 2014). OMA1 protease products were found on both sides of IMM (Kaser, Kambacheld et al. 2003). The second assumption is that only the N-terminus is sensitive to cell stress. This N-terminal region is presumed to participate in OMA1

activation because the mutation in this region leads to suppression of OMA1 stress-inducible activation and processing (Baker, Lampe et al. 2014). In contrast with AAA proteases, OMA1 protease has no ATPase domain so it is ATP-independent. Two missense mutations (His69, Glu272) in OMA1 protease were found in patients with familial and sporadic forms of amyotrophic lateral sclerosis. The underlying mechanism of this mutations still remains unclear. It is assumed to stall homooligomerization of matured OMA1 protease (Daoud, Valdmanis et al. 2011). OMA1 protease is a critical for neuronal survival via L-OPA1 isoforms formation. OMA1 deletion protects prohibitin 2-deficient neurons against apoptosis (Korwitz, Merkwirth et al. 2016). Intrinsic apoptosis is triggered by activation of B- cell lymphoma (Bcl2)-associated X (Bax) and Bcl2-killer (Bak) proteins. This leads to their oligomerization via activation of BH3 interacting death protein (tBID). Subsequently, Bcl-2 interacting mediator (Bim) releases the cytochrome *c*. OMA1 knockout enhanced the release of cytochrome *c* in the Bax- and Bak-dependent mode and thus activate the cascade of cysteine-dependent aspartate-directed proteases (Caspases). The activation of caspases lead to apoptosis. On the other hand, knockout of OMA1 may be bypassed by OPA1 KD (Jiang, Jiang et al. 2014). The OMA1 depletion leads to developmental abnormalities in zebrafish model. Similar results were obtained by experiments with Oma1-deficient mouse embryonic fibroblasts (Bohovych, Donaldson et al. 2014). YME1L depletion in mice embryonal cells was not viable. Postimplantation promoted YME1L deletion in the same model led to activation of OMA1 protease. This also speeds up OPA1 proteolysis, mitochondrial fragmentation, and metabolic alterations in cardiac tissue. Double-deletion of YME1L and OMA1 proteases restored mitochondrial morphology and cardiac metabolism (Wai, Garcia-Prieto et al. 2015). The Mgm1 is the yeast ortholog of human OPA1. It is not cleaved by OMA1 or i-AAA proteases but by mitochondrial rhomboid protease Pcp1 (Schafer, Zick et al. 2010).

1.3. Adaptor proteins

Adaptor proteins of the mitochondrial proteases exert their activity only in cooperation with the scaffold and docking proteins. They facilitate their enzymatic reactions. Adaptor proteins are composed of a variety of protein-binding modules that modulate the enzyme`s active site. They usually contain Src homology 2 (SH2) and Src homology 3 (SH3) domains. Both domains distinguish different specific AA sequences. SH2 protein motif is about 100 AA long

and serves to recognize substrates containing phosphotyrosine (Russell, Breed et al. 1992). SH3 domain is about 60 AA long and identifies proline-rich regions surrounded by other specific AAs (Pawson and Schlessingert 1993).

1.3.1. Mgr1 and Mgr3

The i-AAA protease supercomplex is composed of YME1L subunits and adaptors proteins mitochondrial genome-required protein 1 **(**Mgr1) and mitochondrial genome-required protein 3 (Mgr3). They are required for IMM protein turnover and for targeting of the substrates. They are necessary for growth of the cells that lack the mitochondrial genome. These adaptor proteins coprecipitate with i-AAA protease. Mgr1 mediates the link within the Mgr3-Mgr1 subcomplex and i-AAA protease. In the case of Yme1 absence, Mgr1 and Mgr3 remain associated and are able to bind substrate proteins (Dunn, Tamura et al. 2008). Yet they are defective in protein turnover of two i-AAA protease substrates Yta10(161)-dihydrofolate reductase and Nde1p-HA (Leonhard, Stiegler et al. 1999). Another substrate of the i-AAA protease, the Cox2 subunit of complex IV, is found at physiological amounts when other subunits of complex IV are present (Nakai, Yasuhara et al. 1995). In contrast, increased level of Cox2 was found in the absence of other subunits of complex IV. This suggests possible role of Mgr1 and Mgr3 in turnover of Cox2 subunit (Dunn, Tamura et al. 2008). Cox2 subunit is synthesized in mitochondrial matrix with the targeting sequence cleaved by Imp1 (MPP protease) (Cruz-Torres, Vazquez-Acevedo et al. 2012). Cox2 is then cotranslationally inserted into the IMM. The maturation comprises of the export of the hydrophilic C-terminus into the IMS by Cox18 subunit in *S. cerevisiae* (Fiumera, Broadley et al. 2007). The processing of the targeting sequence is facilitated by Cox20 an integral protein of the IMM with hydrophilic domains protruding into the IMS. After this process, Cox20 subunit remains associated with the mature unassembled Cox2 subunit. Cox20 physically interacts with Cox18 in presence of Cox2 and thus protects Cox2 against proteolytic degradation by i-AAA protease. Mutations in Yme1, Mgr1 or Mgr3 reduce the proteolytic activity of the whole YME1 complex. The absence of Cox20 leads to the processing of Cox2 by Imp1 protease (Elliott, Saracco et al. 2012). For the correct assembly of Cox2 is necessary the oxidase assembly protein 1 (Oxa1) and its paralog Cox18. Oxa1 is required for contranslation export of the N-terminus of Cox2 through the IMM. The overexpression of Oxa1 leads to increased level of unassembled Cox2 subunit after its insertion to IMM. The inactivation of Mgr1 and Mgr3 proteins was sufficient

to support growth of cox18 depleted cells. This suggests that the i-AAA protease functions as chaperone in the folding and/or assembly of Oxa1-translocated Cox2 subunit (Fiumera, Dunham et al. 2009). Mgr3 protein, similarly to Mgr1 protein, is required for mtDNA-independent yeast growth. TOM22 is anchored by its C-terminus to the OMM. The Om45 protein is anchored to the OMM by its N-terminal hydrophobic segment and the major part of the polypeptides is located in the IMS (Song, Tamura et al. 2014). Both of these proteins are degraded by i-AAA protease as Mgr1 and Mgr3 are able to recognize IMS domains of OMM proteins and assist with their proteolysis (Wu, Li et al. 2018).

Mitochondrial Mgr1 has a predicted molecular weight of 47 kDa (Sickmann, Reinders et al. 2003). It is required for normal growth of *S.cerevisiae* cells. Mgr1 depleted cells stopped after 30 hours of growth dividing and after another 70 hours recovered the growth and achieved approximately the same density as wild-type population. Mgr1 depleted cells show poor assembly of YME1 and reduced YME1 proteolytic activity and lower mitochondrial protein turnover. The Mgr1 depleted cells show milder phenotypes than YME1 depleted cells (Dunn, Lee et al. 2006).

Mitochondrial Mgr3 (Dunn, Tamura et al. 2008) has a predicted molecular weight of 58 kDa. It has one transmembrane domain at N-terminus and three coiled-coil regions. Mgr3 is similar to another *S.cerevisiae* protein encoded by YKL133C gene (35% sequence identity), but yeast cells depleted of *ykl133c* are not petite negative. Petite negative (marked as „ρ–“) mutant is a respiratory deficient mutant caused by the absence/mutations in mtDNA or mutations in nuclear-encoded subunits of OXPHOS. The majority of petite mutations are generated by treatment of the cells with ethidium bromide. They are unable to grow in medium with non-fermentable source of carbon and form only small colonies on glucose medium (Goldring, Grossman et al. 1971). The Mgr3 depletion in *S.cerevisiae* leads to reduced proteolysis by i-AAA protease.

1.3.2. LACE1

Afg1 (ATPase family gene 1) is a yeast mitochondrial ATPase, a member of the SEC18-NSF, PAS1, CDC48-VCP, TBP family of ATPases (Lee and Wickner 1992). It is a well evolutionarily conserved protein with a robust mammalian homologue LACE1 (lactation elevated 1) (Khalimonchuk, Bird et al. 2007). The protein is composed of five domains and

contains an ATP/GTP-binding Walker A motif (P-loop) (Walker, Saraste et al. 1982, Abrahams, Mak et al. 2002). Afg1 homologues structurally resemble mitochondrial FtsH/AAA family proteases but do not contain the conserved zinc protease domain (Sauer and Baker 2011). Yeast Afg1 deletion strain showed reduced respiratory growth rate and diminished activities of OXPHOS complexes III and IV. It was suggest that the protein facilitates the degradation of mitochondrially encoded complex IV subunits COX1, COX2, and COX3 (Khalimonchuk, Bird et al. 2007). RT (reverse transcription) PCR of mouse tissues showed marked tissue-dependent LACE1 expression with the highest mRNA levels in heart, kidney, and lactating compared with inactive breast tissues (Abrahams, Mak et al. 2002). LACE1 gene region was found to be downregulated in the natural killer cells (NK cells) neoplasms (Karube, Nakagawa et al. 2011). LACE1 was found associated with bipolar disorder (Knight, Rochberg et al. 2010).

2. AIMS OF STUDY

Mitochondrial proteases and their adaptor proteins are now seem to be more and more important not only for the mitochondrial structure and function, but for the whole cell and, in the case of a multicellular organism, for the whole organism. The thesis had two main goals:

1) Characterization of the functional overlap and cooperativy of proteolytic subunits AFG3L2 and YME1L of the mitochondrial inner membrane complexes m- and i-AAA in the maintenance of mitochondrial structure and respiratory chain activity using shRNAmir knockdown approach in the HEK293 cell line

2) Study the role of human LACE1 (lactation elevated 1) ATPase, the homologue of yeast Afg1 Atpase, in the mitochondrial protein homeostases using shRNAmir knockdown, protein overexpression and protein-protein interaction analyses

3. MATERIAL AND METHODS

3.1. Materials

3.1.1. Cell line

HEK293 (human embryonic kidney) cells (CRL-1573) were obtained from the A.T.C.C. (Manassas, U.S.A.).

3.2. Methods

3.2.1. Plasmid construction

The nucleotide sequences of 28 different candidate miR-30-based shRNAs [shRNAmirs (microRNA-adapted shRNAs)] targeted to human AFG3L2 (NM_006796), CLPP (NM_006012), CLPX (NM_006660), LACE1 (NM_145315) and YME1L (NM_014263; NM_139312) mRNAs were designed and with negative control (non-silencing) bought as CMV-GFP-IRESNeo expression cassette of the lentiviral pCMV-GIPZ-Zeo vector (Open Biosystem, GE Dharmacon, USA). The C-fusion Myc-FLAG-tagged ORF expression constructs pCMV6-LACE1 containing the human LACE1 cDNA ORF sequence and the pCMV6-CLPP containing the human CLPP cDNA ORF sequence (OriGene, USA) were reintroduced into the HEK293 cells. Walker A motif mutants of CLPP and LACE1 proteins were carried out using the QuikChange II Site-Directed Mutagenesis Kit (Stratagene, USA). To construct the LACE1K142A variant, 424A>G and 425A>C nucleotide substitutions were introduced; to construct the LACE1T143V variant, 427A>G and 428C>T nucleotide substitutions were introduced; to construct the LACE1K142A/T143V variant, 424A>G, 425A>C, 427A>G and 428C>T nucleotide substitutions were introduced, and finally to prepare the LACE1E214Q variant, a 640G>C substitution was introduced into the pCMV6-LACE1 expression construct. The fidelity of all constructs was confirmed by

automated DNA sequencing. Using optimized protocol the mutant variants were inserted into transforming chemically competent *E. coli* cells One Shot® MAX Efficiency DH5α^{TM} – T1^{R} (Invitrogen, Life Technologies, USA).

3.2.2. Transformation of chemically competent cells

Transformation was carried out according to the optimized protocol. *E. coli* cells One Shot® MAX Efficiency DH5α^{TM} – T1^{R} (Invitrogen, Life Technologies, USA) were thawed on ice. Into the cells were added 4 µl ligation reaction and mixed by gently tapping. The vial was incubated on ice for 30 minutes. Cells were incubated for exactly 30 second in the 42°C water bath then returned on ice back and added 250 µl of pre-warm S.O.C. medium (2% tryptone, 0.5% yeast extract, 10 mM NaCl, 2.5 mM KCl, 10 mM $MgCl_2$, 10 mM $MgSO_4$, and 20 mM glucose). Cells were shaked at 37 °C for exactly 1 hour at 225 rpm in shaking incubator and after shaking spread 20 µl to 200 µl and labeled Luria-Bertani (LB) agar plate. Inverted place was incubated at 37 °C overnight. Selected colonies were analysed and amplified with subsequent DNA isolation. Transformation cells are stored at -80 °C.

3.2.3. DNA isolation

DNA plasmids were isolated using Quiagen EndoFree Plasmid Purification Midi Kit (Quiagen, Germany) according to the optimized protocol. Finally, concentration of acquired DNA pellets was measured by NanoDrop Spectrophotometer ND-1000 (NanoDrop Technologies, USA).

3.2.4. Cell culture and transfections

Human embryonic kidney cells (HEK293, CRL-1573) were obtained from the American Type Culture Collection (ATCC, Manassas, USA) and maintained in high-glucose Dulbecco's modified Eagle's medium (DMEM, Biochrom, Germany) supplemented with 10% (v/v) fetal bovine serum (FBS, Sigma Aldrich, USA) at 37 °C in a 5% CO_2 atmosphere. Cells were grown to ~90% confluence and splitted using 0.05% (w/v) trypsin and 0.02% (w/v) EDTA (Biosera, USA). Finally, cells were harvested using icy PBS and detached cells were sedimented by centrifugation, washed twice in icy PBS (Sigma, USA) and stored at -80°C.

To generate stable HEK293 KD cell lines, subconfluent cells were transfected by electroporation using Nucleofector^{TM} (Lonza, Switzerland) programm Nucleofector®

Program Q001 with a cell-specific Amaxa® Cell Line Nucleofector® Kit V according to the optimized protocol using 5 µg DNA on each reaction. Stably expressing cells were selected 48 hours after transfection using puromycin (Sigma Aldrich, USA) at a concentration of 1.5 µg/ml and geneticin G418 (Sigma Aldrich, USA) at a concentration of 720 µg/ml over a period of 3 weeks. Western blot analysis was used to evaluate the efficiency of knockdown at the protein level in each of the stable cell lines.

To generate transiently transfected cell lines, subconfluent cells were transiently transfected with the expression constructs using the Lipofectamine® 2000 Transfection Reagent (Life Technologies, USA) according to the optimized protocol using 10 µl per WillCo wells® and 90 µl per culture flask T-75. Transfected cells were harvested 48 hours after transfection and either processed directly for analyses or stored at −80 °C.

A negative non-silencing control (scrambled) Stealth RNAi siRNA and functionally validated Stealth RNAi siRNA duplexes targeting the human LACE1 and p53 transcripts were purchased (Invitrogen, USA). The RNAiMAX Transfection reagent (Invitrogen, USA) was used for transient transfection of cells. The transfected cells were harvested 48 hours post-transfection and either stored at -80 °C or used for subsequent analysis.

3.2.5. Cell death analysis

Stably transfected HEK293 cells were cultivated in high-glucose DMEM supplemented with 10% (v/v) FBS at 37 °C in a 5% CO_2 atmosphere and treated with staurosporine (2 µM) for 0, 3, and 6 hours or TNF alpha (10 ng/ml) and INF-gamma (80 ng/ml) for 0, 3, 6, and 12 hours. Cell lysates were analyzed by SDS PAGE and subsequent immunoblotting for PARP cleavage.

3.2.6. The assessment of cell proliferation

Stably transfected HEK293 cells were seeded in six-well plates at 5×10^4 cells per well and cultured in high-glucose DMEM supplemented with 10% (v/v) FBS containing 1 µg/ml puromycin. The medium was changed on the second, fourth, and sixth days. Viable cells were counted every 24 hours for a total of 7 days using a Scepter Handheld Automated Cell Counter (Millipore, USA).

3.2.7. Immunocytochemistry

Living HEK293 cells grown on coverslips (Willco Wells, Netherlands) were fixed with 4% paraformaldehyde (Thermo Fisher Scientific, USA) in PBS (Lonza, Switzerland) at room temperature (RT) for 20 minutes and permeabilized with 0.1% Triton X-100 (Sigma Aldrich, USA) in PBS at RT for 15 minutes, followed by rinse in PBS. Cells were blocked by 10% FBS/PBS at RT for 60 min. Primary detection was performed with anti-COX1 (Abcam, United Kingdom), anti-cytochrome c (Abcam, United Kingdom) or anti-p53 (Cell Signaling; USA) primary antibodies. Cells were incubated with primary antibody in 10% FBS/PBS at 4°C over night, followed by rinse in PBS. Secondary detection was performed with Alexa Fluor® 488 IgG2α (Life Technologies, USA), Alexa Fluor® 594 IgG2α (Life Technologies, USA) or Alexa Fluor® 594 IgG (H+L)(Cell Signaling, USA). Cells were incubated with secondary antibody in 10% FBS in PBS at RT for 2 hours covered with cellophane, followed by rinse in PBS. Cells were analyzed at 24°C using a Nikon Diaphot 200 inverted microscope (Nikon, Tokyo, Japan) equipped with a Plan-Apochromat 60×, numerical aperture 0.95, oil objective (Carl Zeiss, Wetzlar, Germany). The images were acquired with an Olympus DP50 CCD camera (Olympus, Milan, Italy) and Viewfinder Lite 1.0 software (Pixera, Santa Clara, CA).

3.2.8. Fluorescence microscopy (MitoTracker® Red CMXRos)

For fluorescence staining, living, intact HEK293 cells were incubated with 10 nM MitoTracker® Red CMXRos (Thermo Fisher Scientific, USA) for 15 minutes in PBS and analyzed at 24°C using a Nikon Diaphot 200 inverted microscope (Nikon, Japan) equipped with a Plan-Apochromat 60×, numerical aperture 0.95, oil objective (Carl Zeiss, Germany). The images were acquired with an Olympus DP50 CCD camera (Olympus, Italy) and Viewfinder Lite 1.0 software (Pixera, USA).

3.2.9. Electron microscopy

For ultrastructural analysis, the cells were fixed using a modification of Luft's method (Luft, J.H., *Permanganate; a new fixative for electron microscopy.* J Biophys Biochem Cytol, 1956. 2(6): p. 799-802.). Briefly, the cells were incubated in PBS containing 2% potassium permanganate for 15 minutes, washed with PBS, and dehydrated with an ethanol series. They were then embedded in Durcupan Epon (Electron Microscopy Sciences, UK), sectioned by Ultracut microtome (Reichert, Depew, USA) to thicknesses ranging from 600 to 900 Å, and

finally stained with lead citrate and uranyl acetate. A JEOL JEM-1200 EX transmission electron microscope (JEOL, Japan) was used for imaging.

3.2.10. Mitochondrial isolation and subfractination

Mitochondrial fractions were isolated from HEK293 cells using resuspended cells in STE solution (10mM Tris-HCl, 250mM sucrose, 1mM EDTA and 1% (v/v) Protease inhibition coctail (PIC), pH 7.4) and disruption by hypo-osmotic swelling coupled to Dounce homogenization at 4°C. Nuclear contamination was removed by low-speed centrifugation 600 g and by ultracentrifugation 10 000 g for 25 minutes at 4°C. The resulting pelets were resuspended in STE solution (100 mM NaCl, 10 mM Tris-Cl, pH 8.0, 1 mM EDTA) and analyzed by sodium dodecyl sulfate–polyacrylamide gel electrophoresis (SDS PAGE) and subsequent immunoblotting.

To prepare submitochondrialfractions, mitochondria at a protein concentration of 1 mg/ml were either sonicated (Ultrasonic Homogenizer 4710 Series; Cole-Parmer, USA) or treated with 100 mM sodium carbonate (pH 11.5) and were then centrifuged at 144000 g for 1 hour. The resulting supernatant fractions were precipitated with trichloroacetic acid (TCA) and subsequently dissolved in SDS PAGE sample buffer along with the washed pellet fractions and using Western Blot.

3.2.11. Preparation of nuclear extracts

The cells were washed with PBS, pelleted by centrifugation and resuspended in the cell lysis buffer (10 mM HEPES (pH 7.5), 10 mM KCl, 0.1 mM EDTA, 1 mM dithiothreitol, 0.5% Nonidet-40, and 0.5 mM PMSF) along with 1% (v/v) PIC (Sigma Aldrich, USA) and allowed to swell on ice for 20 min. The cells were then vortexed to disrupt cell membranes and then centrifuged at 12 000 g at 4°C for 10 min. The pelleted nuclei were washed with the cell lysis buffer and resuspended in the nuclear extraction buffer (20 mM HEPES (pH 7.5), 400 mM NaCl, 1 mM EDTA, 1 mM DTT, and 1 mM PMSF) with 1% (v/v) PIC and incubated in ice for 30 minutes. The nuclear extract was collected by centrifugation at 12 000 g for 15 min at 4°C.

3.2.12. Immunoprecpitation of LACE1-FLAG protein (Co-immunoprecipitation and affinity purification)

For anti-FLAG co-immunoprecipitation, the LACE1-KD cells were transiently transfected with the LACE1–FLAG construct, with the CLPP–FLAG construct or with their mutant variants (as descripted in chapter Plasmid construction) or with the empty parental pCMV6 vector. Equivalent transfection efficiency was monitored by Western blotting with the anti-FLAG M2 monoclonal antibody. The transfected cells were harvested 48 hours after transfection and then used to prepare mitochondrial fractions. Isolated mitochondria were solubilized using 1% Triton X-100 in Tris-Buffered Saline (TBS) containing 1% (v/v) PIC at a protein concentration of 2 mg/ml. The resulting cleared extracts were incubated for 2 hours with washed anti-FLAG M2 affinity beads (Sigma–Aldrich, USA) at 4 °C with gentle agitation on rotating mixer (Torrey Pines Scientific, USA). The affinity beads containing the bound antigens were then washed five times with TBS containing 0.1% Triton X-100 and the bound material was eluted under non-denaturing conditions with 3× FLAG® peptide solution and routinely processed for electrophoresis and Western blotting. For affinity purification of LACE1–FLAG, wild-type (wt) HEK-293 cells were transiently transfected with the pCMV6-LACE1 construct. The anti-FLAG affinity purification of LACE1 was performed essentially as described above, except that digitonin 1% (w/v) was used instead of Triton X-100 to solubilize mitochondrial fractions.

3.2.13. Electrophoresis

Blue Native Polyacrylamide Gel Electrophoresis (Schagger and von Jagow 1991) was used for separation of mitochondrial membrane protein complexes on polyacrylamide 8–16 % (w/v) gradient gels using a Mini Protean® 3 System (Bio-Rad Laboratories, USA). Mitochondria were pelled by centrifugation 14000 g for 10 minutes at 4 °C and the pellets were solubilized with 10% (w/v) n-dodecyl β-D-maltoside (DDM, Sigma Aldrich, USA) with a final DDM/protein ratio of 1.0 mg/mg in extraction buffer (1.5 M aminocaproic acid, 2 mM EDTA, and 50 mM Bis-Tris (pH 7.0)) at 4 °C for 20 min on ice with gently vortex every 5 minutes. Samples were centrifuged at 51 000 G for 20 min and Serva Blue G (Serva, USA) was added to solubilized protein at a concentration of 0,1 mg/mg of detergent, and approximately 20 µg of protein was loaded for each lane. The electrophoresis was performed at 40 V at 4 °C for 1 h and then at 100 V at 4 °C.

Tricine sodium dodecyl sulfate–polyacrylamide gel electrophoresis (SDS PAGE) was carried out under standard conditions with 10% polyacrylamide, 0.1% (w/v) SDS and 5.5 M urea gels. Whole cell lysates or mitochondrial fractions were resuspended in RIPA Buffer (50 mM Tris-HCl (pH 7.4), 150mM NaCl, 1 mM phenylmethylsulfonyl fluoride, 1 mM EDTA, 1% (w/v) Triton X-100, 0.1% (w/v) SDS, 1% (w/v) sodium deoxycholate, and 1% (w/v) PIC) for 20 minutes on ice with gently vortex every 5 minutes and centrifuged at 15 000 g for 10 minutes at 4 °C. Sample buffer (50 mM Tris-HCl (pH 6,8), 12% (v/v) glycerol, 4% (w/v) SDS, 0,01% (w/v) Bromphenol Blue, and 2% 2-Mercaptoethanol) was added in ratio of 3 portions of sample : 1 portion of sample buffer and incubated for 30 minutes at 37 °C, and approx. 10 µg of protein was loaded for each lane.

For two-dimensional BN/SDS PAGE, strips of the first-dimension gels were incubated for 40 min in 1% 2-mercaptoethanol and 1% SDS and then for 10 minutes in 1% SDS, and denatured proteins were then resolved in the second dimension on 12% polyacrylamide, 0.1% SDS and 5.5 M urea gels.

3.2.14. Western blot analysis and antibodies

Proteins were electroblotted from the gels on to Immobilon®-P PVDF membranes (Merck Millipore, USA) using semi-dry transfer for 1 hour at a constant current of 0.8 mA/cm2. Membranes were air-dried overnight, rinsed twice with 100% (v/v) methanol and blocked in PBS and 1% (w/v) I-Block™ Protein-Based Blocking Reagen (ThermoFisher Scientific, USA) for 1 hours. Primary detection was performed with mouse/rabbit/goat monoclonal/polyclonal antibodies as detailed below by incubating blots with primary antibodies in PBS, 0.1% (v/v) Tween 20 and 1% (w/v) I-Block™ Protein-Based Blocking Reagen for 2 hours or over night. Secondary detection was carried out with goat anti-mouse IgG–horseradish peroxidase conjugate (Sigma Aldrich, USA) or with goat anti-rabbit IgG-horseradish peroxidase conjugate (Sigma Aldrich, USA) in PBS, 0.1% Tween 20 and 1% (w/v) I-Block™ Protein-Based Blocking Reagen for 1 hour. The blots were developed with West Pico Chemiluminescent substrate (ThermoFisher Scientific, USA) and visualised by G:Box (Syngene, USA).

The monoclonal antibody against human AFG3L2, ATPase F1-α , citrate synthase, CLPP, CORE 2, COX1, COX2, COX4, COX5A, COX6A, cytochrome c, Drp1, Histone H3, LACE1, LON, NDUFA9, NDUFB6, OMA1, Omi/HTRA2, OXA1L, PARL, PNPase, SDH A, Spg7,

and TIMM50 were obtained from Abcam (UK). Antibody to mtHSP70 was obtained from Lonza (Switzerland). The antibody to OPA1 was purchased from BD Biosciences (UK). Antibody to YME1L was from previous study (Stiburek, Cesnekova et al. 2012). The M2 monoclonal antibody to FLAG epitope and Histone H3 was obtained from Sigma Aldrich (USA). Antibody to mtHSP70 was from Lonza (Switzerland) and antibodies to α-tubulin, β-actin, Bax, Cleaved PARP, p53, and PUMA were from Cell Signaling Technology (USA).

3.2.15. Enzyme activity assays

The activities of the mitochondrial enzymes complex I (NQR, NADH:Coenzyme Q10 oxidoreductase), complex II (SQR, succinate:coenzyme Q10 oxidoreductase), complex III (QCCR, coenzyme Q10:cytochrome c reductase), and complex IV (COX, cytochrome c oxidase) were measured spectrophotometrically with the UV-2401PC instrument (Shimadzu, Japan) by standard methods at 37°C in isolated HEK293 mitochondria. In mitochondria, rotenone-sensitive complex I activity was measured by incubating 45 μg of mitochondrial protein in 1 ml of assay medium (50 mMTris-HCl (pH 8.1), 2.5 mg/ml BSA, 50 μM decylubiquinone, 0.3 mM KCN, and 0.1 mM NADH without or with 3 μM rotenone). The decrease in absorbance at 340 nm due to the NADH oxidation was followed. Complex II activity was measured by incubating 20 μg of mitochondrial extract in 1 ml of assay medium (10 mM potassium phosphate (pH 7.8), 2 mM EDTA, 1 mg/ml BSA, 0.3 mM KCN, 10 mM succinate, 3 μM rotenone, 0.2 mM ATP, 80 μM 2,6-dichloroindophenol, 1 μM antimycin, and 50 μM decylubiquinone). The decrease in absorbance at 600 nm due to the reduction of 2,6-dichloroindophenol was monitored. Complex III activity was measured by incubating 20 μg of mitochondrial protein in 1 ml of assay medium (10 mMKpi, 2mM EDTA, 1mg/1ml BSA, 3μM rotenone, 10mM succinate, 0.2mM ATP, 0.3 mM KCN, and reaction started with 40μM COX). Added 10 μL malonate, after 1 minute added 5 μL DBH_2, after another 1 minute added 10μL 10mM malonate, and measured after 1 minute. Then added 10 μL 1μM Antimycin A (Sigma Aldrich, USA) and measured. Complex IV activity was measured by incubating 15–18 μg of mitochondrial protein in 1 ml of assay medium (40 mM potassium phosphate (pH 7), 0.1 mg/ml BSA, 25 μM reduced cytochrome c, and 2.5 mM DDM) and the oxidation of cytochrome c at 550 nm was monitored. All assays were performed at 37°C. The total protein was determined using the method of Lowry (Lowry *et al.* 1951).

Mitochondria (5-20 μg/ml protein) were incubated in a medium containing 40 mM Tris (pH 7,4), 5 mM $MgCl_2$, 10 mM KCl, 2 mM phosphoenolpyruvate, 0.2 mM NADH, 1 μg/ml

rotenone, 0.1% (w/v) BSA, 5 units of pyruvate kinase and 5 units of lactate dehydrogenase for 2 minutes. The reaction was started by the addition of 1 mM ATP and the rate of NADH oxidation, equimolar to ATP hydrolysis, was monitored as the decrease in absorbance at 340 nm. Sensitivity to aurovertin was determined by parallel measurements in the presence of 2 μM inhibitor.

3.2.16. High-resolution oxygraphy

The cells were permeabilized with 30 μg/ml digitonin, and oxygen consumption was measured at 37 °C using an OROBOROS Oxygraph-2k (OROBOROS INSTRUMENTS Corp, Austria) in 2 ml chamber with KCl-based medium containing 80mM KCl, 10mM Tris, 3mM $MgCl_2$, 1mM EDTA, 5mM potassium phosphate (pH 7.4). The measurements were carried out after permeabilization of cells (manual titration) by approximately 4 μM digitonin, protein load per chamber ranging between 0.5 – 0.9 mg, with final concentrations of substrates and inhibitors as follows: 10mM glutamate, 2.5mM malate (CI-ADP), 1mM ADP (complex I/+ADP), 10mM succinate (complex II), 4mM ascorbate, and 0.4mM TMPD (N,N,N′,N′-tetramethyl-1,4-phenylenediamine) (complex IV), 0.5μM rotenone, and 1μM antimycine A. To control for intactness of mitochondrial membranes, cytochrome *c* (2.5μM) was added after succinate. Respiration was uncoupled by 200 nM carbonilcyanide p-triflouromethoxyphenylhydrazone (FCCP) titration steps, maximum 1.5 μM (complex IV), and finally inhibited by the addition of sodium azide (10 mM).

3.2.17. Statistic analysis

All experiments were performed in at least triplicate. The Western blots shown are representative of at least three independent experiments. Statistical analyses were performed using a two-tailed Student's *t* test in Excel (Microsoft, USA). The results are expressed as mean ± SD. $p < 0.05$ was considered statistically significant; asterisks are used to denote significance as follows: *$p < 0.05$, ** $p < 0.01$, ***$p < 0.001$.

4. RESULTS AND DISCUSSION

4.1. Results and discussion related to aim A)

Mitochondrial protein quality control is crucial for the maintenance of correct mitochondrial homeostasis. It is ensured by several specific mitochondrial proteases located across the various mitochondrial subcompartments. Here we have focused on characterization of functional overlap and cooperativity of proteolytic subunits AFG3L2 and YME1L of the mitochondrial inner membrane complexes m- and i-AAA in the maintenance of mitochondrial structure and respiratory chain activity.

4.1.1. Knockdown of YME1L and/or AFG3L2 leads to increased accumulation of complex I, IV and V subunits

We have generated stable HEK293 cell lines with shRNA-downregulated expression of single YME1L (NM_014263) and AFG3L2 (NM_006796.1) as well as a double-KD cells expressing both YME1L and AFG3L2 shRNAs (Open Biosystems). Control cell line was prepared by transfecting HEK293 cells with commercially available scrambled (non-silencing) shRNAmir-containing expression vector RHS436 (Open Biosystems). Western blot analysis with antibodies to YME1L and AFG3L2 confirmed that all three produced cell lines contained less than 10% of residual target protein levels (Figure 4.1. A). We have previously demonstrated that YME1L protease affects stability of Cox4 and Ndufb6 respiratory chain subunits by mediating their proteolytic degradation (Stiburek, Cesnekova et al. 2012). However, not much is known of AFG3L2 protease function in oxidative phosphorylation system biogenesis and of the possible substrate overlap or cooperation between AFG3L2 and YME1L in this process (Stiburek, Cesnekova et al. 2012).

We have performed SDS-PAGE western blotting screen using mitochondrial fractions isolated from the KD cell lines to identify affected respiratory chain and ATP synthase subunits. The screen was clearly limited by the number of available antibodies, but we were able to identify several affected OXPHOS subunits in the KD cells (Figure 4.1. B).

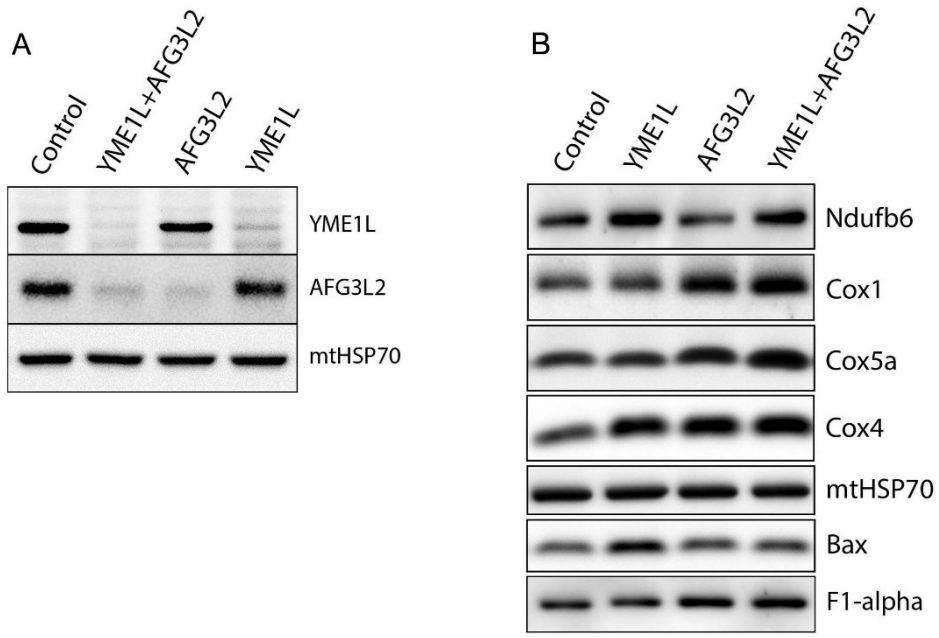

Figure 4.1. Knockdown of AFG3L2 and YME1L by shRNA leads to increased accumulation of complex I, IV and V subunits. (**A**) Knockdown of YME1L, AFG3L2 or both by stable shRNA expression leads to efficient reduction of corresponding protein levels. Whole-cell lysates from the shRNA knockdown cell lines were immunoblotted with antibodies to YME1L, AG3L2 or mtHSP70. The control cell line was prepared by transfecting HEK293 cells with the non-silencing (scrambled) shRNAmir vector. (**B**) Altered accumulation of respiratory chain subunits and Bax in YME1L and/or AFG3L2 KD cells. Whole cell lysates were immunoblotted with antibodies to Ndufb6, Cox1, Cox5a, Cox4, mtHSP70, Bax and F1-alpha.

In YME1L KD mitochondria, both Ndufb6 and Cox4 subunits were found to be increased, which is consistent with our previous report (Stiburek, Cesnekova et al. 2012). On the other hand, western blots of mitochondrial fraction from AFG3L2 KD cells revealed increased levels of Cox1, Cox4 and Cox5a subunits, as well as of the F1-alpha subunit of ATP synthase. Finally, mitochondria from the double knockdown YME1L/AFG3L2 cells showed markedly increased levels of Ndufb6, Cox1, Cox4, Cox5a and F1-alpha subunits (Figure 4.1. B). Additionally, immunoblot of single YME1L KD mitochondria showed increased amount of BAX protein (Figure 4.1. B.)

We have previously demonstrated that loss of YME1L results in reduced growth rate of the cells attributed either to their reduced apoptotic resistance or diminished respiratory capacity. To assess the overall effect of AFG3L2 and YME1L knockdown on cell viability, we examined the growth rates of AFG3L2 and AFG3L2/YME1L knockdown cells over a time course of 7 days. We found significant growth retardation associated with the loss of either single AFG3L2 or both AFG3L2 and YME1L (Figure 4.2.).

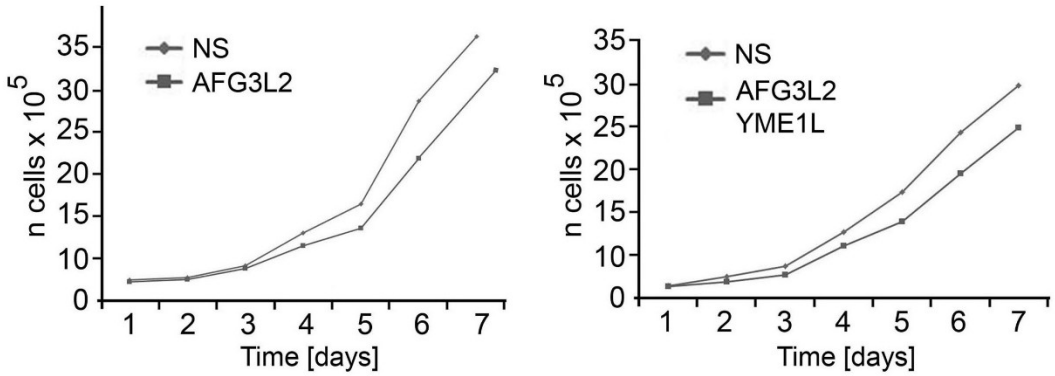

Figure 4.2. Knockdown of AFG3L2 and YME1L by shRNA leads to reduced growth rate. Stable knockdown cells were seeded in six-well plates at 5 x 10^4 cells per well and cultured in DMEM containing 1 ug/ml puromycin. Viable cells were counted every 24 hours for a total of 7 days.

4.1.2. Loss of both YME1L and AFG3L2 leads to mitochondrial fragmentation and severely attenuated and disorganized cristae architecture

To compare the impact of single and simultaneous knockdown of YME1L and AFG3L2 on mitochondrial morphology and ultrastructure we used fluorescent mitochondrial imaging and transmission electron microscopy of knockdown cells. MitoTracker Red fluorescence microscopy showed that whereas mitochondria in AFG3L2 KD cells showed only moderate fragmentation, mitochondrial network in YME1L KD and YME1L/AFG3L2 KD cells was severely fragmented (Figure 4.3.).

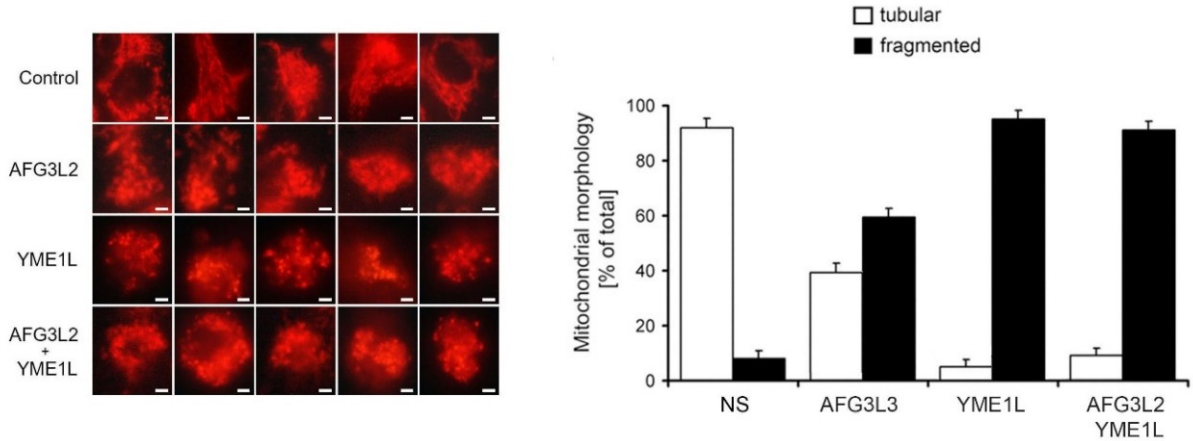

Figure 4.3. Loss of AFG3L2 and/or YME1L leads to mitochondrial fragmentation (A) AFG3L2 and YME1L KD cells exhibit markedly fragmented mitochondrial reticulum. Cells were analyzed using a Nikon Diaphot 200 inverted microscope equipped with an Olympus DP50 camera. Bar, 10 μM.

Transmission electron microscopy revealed altered and attenuated cristae architecture in all three KD cell lines (Figure 4.4.). AFG3L2 KD cells showed most severe cristae depletion of all three examined cell lines. In contrast, YME1L KD mitochondria showed marked cristae disorganization. The mitochondria of double YME1L/AFG3L2 KD cells appeared to combine these ultrastructural defects, containing low number of markedly disorganized cristae structures (Figure 4.4.)

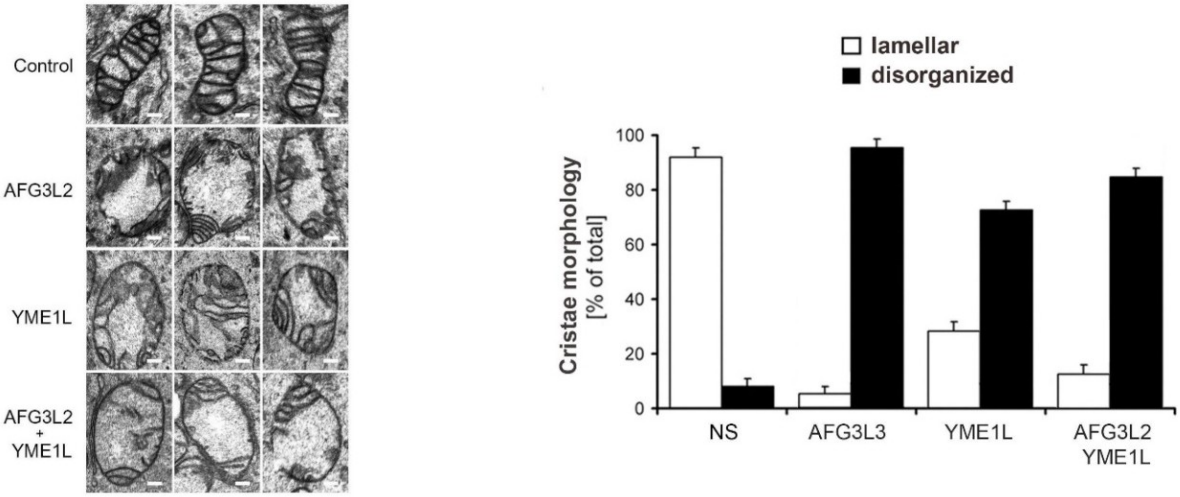

Figure 4.4. Loss of AFG3L2 and/or YME1L leads to severely disorganized and attenuated cristae architecture AFG3L2 and YME1L KD cells exhibit markedly altered and attenuated cristae architecture. The cells were incubated in PBS containing 2% potassium permanganate for 15 min, washed with PBS, and dehydrated with an ethanol series. They were then embedded in Durcupan Epon, sectioned by microtome to thicknesses ranging from 600 to 900 Å, and stained with lead citrate and uranyl acetate. The sections were viewed with a JEOL JEM-1200 EX transmission electron microscope. Bars correspond to 200 nM.

4.1.3. Loss of YME1L and/or AFG3L2 leads to marked accumulation of OPA1 protein forms, diminished Spg7 and elevated Oma1

Mitochondrial shape and cristae architecture depends on balanced accumulation of the dynamin-related GTPase Optic atrophy 1 (OPA1) protein forms. Mitochondrial inner-membrane proteases were shown to mediate proteolytic processing of OPA1 protein, which directly influence mitochondrial fusion and cristae architecture (Anand, Langer et al. 2013). We have therefore analyzed the levels of OPA1 protein forms as well as of Spg7 and Oma1 proteases in whole-cell lysates of the knockdown cells. The OPA1 alterations found in single knockdown cells were limited to short OPA1 forms (S-OPA1), with increase in band c and band e in AFG3L2 KD cells, and increase in band c and band e accompanied by reduction in

band d in YME1L KD cells (Figure 4.5.). In contrast, the YME1L/AFG3L2 double KD cells showed marked increase in all five detectable OPA1 bands, with the most prominent increase in L-OPA1 band b and S-OPA1 band d (Figure 4.5.).

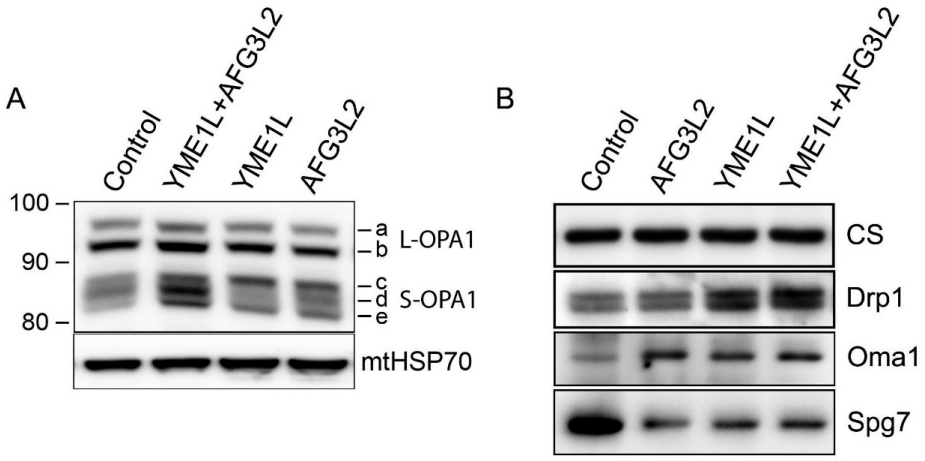

Figure 4.5. Loss of AFG3L2 and/or YME1L is associated with elevated OMA1, diminished SPG7, and markedly altered of OPA1 protein forms. Whole cell lysates were resolved using SDS-PAGE and western blotted with antibody to OPA1 (**A**); Drp1, Oma1 and Spg7 (**B**). Detection of mtHSP70 and citrate synthase (CS) was used to control for equal protein loading.

4.1.4. AFG3L2/YME1L KD cells show reduced complex I holoenzyme and impaired activity of complexes I, III and IV

We used blue-native immunoblotting to analyze holoenzyme levels and assembly profiles of OXPHOS complexes. In agreement with our previous report, loss of YME1L resulted in accumulation of Ndufb6 subunit leading to appearance of multiple complex I subcomplexes and increased amount of complex I holoenzyme (Figure 4.6. A). Interestingly, although the profile of Ndufb6-subcomplexes in YME1L/AFG3L2 KD cells resembled that of single YME1L KD cells, complex I holoenzyme levels were not elevated in double protease knockdowns, but significantly reduced (Figure 4.6. A). In addition, the low molecular weight subcomplexes were found reduced and high molecular weight Ndufb6 subcomplex was elevated in YME1L/AFG3L2 cells, when compared to single YME1L KD profile (Figure 4.6. A). Blue-native immunoblotting of Cox4 revealed increased accumulation of Cox4-containing subcomplex in AFG3L2 KD and YME1L/AFG3L2 KD cells, when compared to YME1L KD and control cells (Figure 4.6. B). Blue-native immunoblotting of F1-alpha, SDH A and Core protein 2 did not show any significant assembly alterations of complexes V, II and III in these cells (Figure 4.6. C).

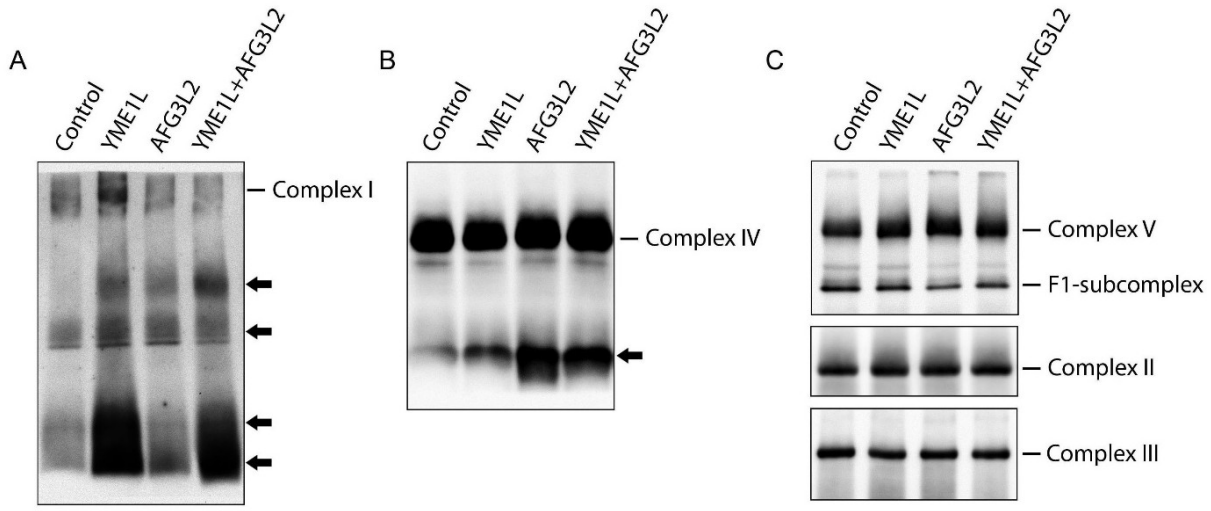

Figure 4.6. Accumulation of complex I and IV subcomplexes due to loss of AFG3L2 and/or YME1L. Isolated mitochondrial fractions were solubilized with 1% dodecyl maltoside, and equal amounts of protein extracts were resolved using BN-PAGE and then immunoblotted with antibodies to NDUFB6 (**A**) COX4 (**B**) and ATPase F1-alpha, SDH A or Core 2 (**C**).

Spectrophotometric measurements of respiratory chain (RC) enzyme activities showed markedly reduced activity of complexes I (54% of control), III (36% of control) and IV (42% of control) in YME1L/AFG3L2 knockdown cells (Figure 4.7.). Whereas in YME1L KD cells were RC activities largely unaffected (except for markedly elevated complex I activity), AFG3L2 KD cells showed significantly reduced activity of complexes III and IV (Figure 4.7.).

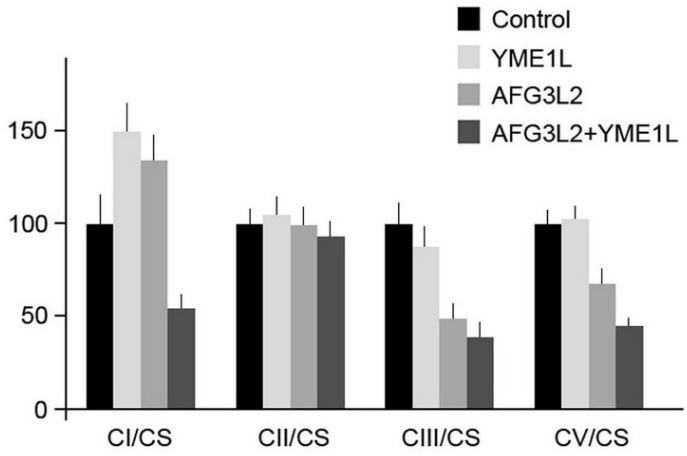

Figure 4.7. Impaired activity of respiratory chain complexes I, III and IV due to loss of AFG3L2 and/or YME1L. Enzyme activities of respiratory chain complexes I-IV were measured spectrophotometrically in isolated mitochondria. The values (mean ± SD) were normalized to the activity of mitochondrial enzyme citrate synthase (CS).

The main points related to aim A)

Loss of both AFG3L2 and YME1L leads to respiratory chain deficiency and impaired mitochondrial dynamics and ultrastructure. Our results show that:

- Knockdown of YME1L and/or AFG3L2 leads to increased accumulation of complex I, IV and V subunits and Exhibit reduced growth rate
- Loss of both YME1L and AFG3L2 leads to mitochondrial fragmentation and severely attenuated and disorganized cristae architecture
- Loss of YME1L and/or AFG3L2 leads to marked accumulation of OPA1 protein forms, diminished Spg7 and elevated Oma1
- AFG3L2/YME1L KD cells show reduced complex I holoenzyme and impaired activity of complexes I, III and IV and Accumulation of complex I and IV subcomplexes

4.2. Results and discussion related to aim B)

Mitochondrial protein homeostasis is crucial for cellular function and integrity and is therefore maintained by several classes of proteins possessing chaperone and/or proteolytic activities. In the present study, we focused on characterization of LACE1 (lactation elevated 1) function in mitochondrial protein homeostasis.

4.2.1. LACE1 is a mitochondrial integral membrane protein which exist as part of three protein complexes of approximately 500, 400 and 140 kDa

The yeast LACE1 homologue (Afg1) was shown to be an inner mitochondrial membrane protein. MitoFates (http://mitf.cbrc.jp/MitoFates), a mitochondrial targeting prediction returned a high score for the presence of mitochondrial presequence in human LACE1 and identified MPP and Icp55 cleavage sites within the sequence (Fukasawa, Tsuji et al. 2015). By performing subcellular fractionation with subsequent immunoblot detection using anti-LACE1 antibody (Abcam), we found that the endogenous processed LACE1 (~50 kDa) is highly enriched in mitochondrial fractions of human embryonic kidney 293 (HEK293) cells (Figure 4.8. A). Immunodetection of mtHSP70 and β-actin was used to control for mitochondrial fractionation efficiency.

By subjecting mitochondrial fractions from HEK-293 cells to either sonic treatment or alkaline carbonate extraction with subsequent ultracentrifugation and immunoblotting (Fujiki, Hubbard et al. 1982), we found that the majority of endogenous LACE1 (~50 kDa) remained in the mitochondrial pellet fraction after both treatments (Figure 4.8. B). This indicates that, similarly to its yeast counterpart (Afg1), the endogenous LACE1 is an integral mitochondrial membrane protein. To verify whether overexpression of wild-type LACE1-FLAG (NM_145315) leads to the same mitochondrial targeting of the fusion protein, we have transiently transfected wild-type HEK293 cells with a C-FLAG-fusion human LACE1 ORF construct (GenBank® accession number NM_145743; OriGene Technologies). The cells were harvested 48 hours post-transfection and used to prepare mitochondrial fractions. Subjecting mitochondrial fractions to either sonic treatment or alkaline carbonate extraction with subsequent ultracentrifugation and immunoblotting (Fujiki, Hubbard et al. 1982), we verify that the majority of LACE1-FLAG protein remained in mitochondrial pellet fractions (Figure 4.8. C). CLPP immunoblotting was used as an example of soluble mitochondrial matrix

protein, whereas PNPase immunoblotting was used as an example of membrane-associated intermembrane space protein.

To determine the native molecular mass of LACE1, the resulting LACE1-FLAG mitochondria (as described above) were solubilized with non-ionic detergent dodecylmaltoside (1% w/v) and resolved using two-dimensional blue-native/denaturing PAGE. The immunoblots were developed with anti-FLAG antibody. To enable estimation of the molecular mass of the LACE1 protein complex, the immunoblots were subsequently developed with antibodies against the NDUFA9 (NADH:ubiquinone 1 α subunit 9) subunit of complex I, SDH A subunit of complex II and COX2 subunit of complex IV. Under the conditions used, these antibodies recognized complex I holoenzyme (970 kDa), complex IV monomer (205 kDa) and complex II monomer (130 kDa) respectively. The direct size comparison revealed that the LACE1 protein complex has an apparent molecular mass of ∼140 kDa under conditions of 1% dodecyl maltoside (Figure 4.8.D). Given the apparent molecular mass of LACE1 (∼50 kDa), this result pointed to the existence of either LACE1 containing heteromeric complex or a homodimer of two LACE1 subunits.

Since AAA family members typically function as homohexamers, we performed the blue native PAGE Western blotting experiment using mitochondria solubilized with digitonin (1% w/v). In contrast with dodecyl maltoside, digitonin was shown to better preserve high-molecularmass inner membrane protein complexes, including respiratory supercomplexes, probably due to its lower delipidating properties (D'Aurelio, Gajewski et al. 2006). Detection of LACE1–FLAG on digitonin gels revealed, in addition to the previously identified ∼140 kDa complex, two complexes of∼400 and 500 kDa respectively (Figure 4.8.E). To find out whether similar species would be seen with affinity-purified LACE1–FLAG protein under the same solubilizing conditions,we have performed the blue native PAGE Western blotting experiment using LACE1–FLAG protein that has been affinity-purified (anti- FLAG) from isolated mitochondrial fractions. Indeed, all three previously identified LACE1 complexes could be observed on purified LACE1–FLAG protein gels (Figure 4.8. E). The lower amount of the ∼500 kDa complex on the purified protein gel, when compared with solubilized mitochondria gel, is likely to be due to destabilization of the protein complex during the affinity purification process.

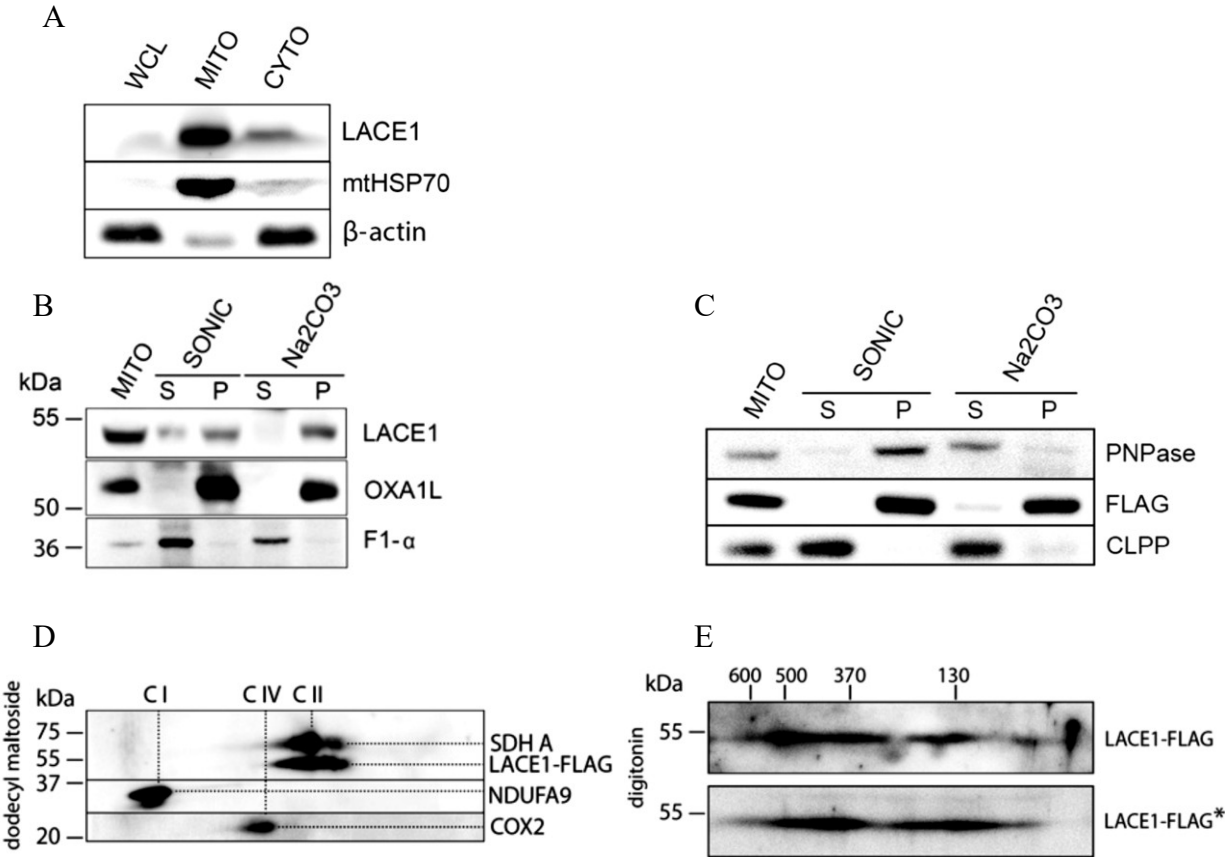

Figure 4.8. LACE1 is a mitochondrial integral membrane protein found in complexes of ~140, 400 and 500 kDa. (**A**) LACE1 is a mitochondrial protein. Whole cell lysate (WCL), mitochondrial (MITO) and cytosolic (CYTO) fractions were prepared from HEK293 cells and immunoblotted with antibody to LACE1 (Abcam, UK), to mitochondrial matrix heat shock protein mtHsp70 (Lonza, Switzerland) and to β-actin. (**B**) Human LACE1 is an integral mitochondrial membrane protein with an apparent molecular mass of ~50 kDa. Submitochondrial fractions were prepared from mitochondria from HEK-293 cells using either sonic disruption (SONIC) or extraction with 100 mM sodium carbonate (pH 11.5; Na2CO3). The resulting supernatant (S) and pellet (P) fractions and untreated mitochondria (MITO) were immunoblotted with antibodies against LACE1 (Abcam) and against OXA1L and F1-*α* subunit of ATP synthase. (**C**) LACE1-FLAG expressed in HEK293 cells is a mitochondrial integral membrane protein. Wild-type HEK293 cells were transiently transfected with a C-FLAG-fusion human LACE1 (NM_145315) ORF construct (OriGene). Submitochondrial fractions were prepared from isolated mitochondria using either sonic disruption (SONIC) or extraction with 100 mM sodium carbonate (pH 11.5). The resulting supernatant (S) and pellet (P) fractions and untreated mitochondria (MITO) were immunoblotted with M2 monoclonal antibody to FLAG epitope (Sigma Aldrich, Germany), and with antibodies to intermembrane space protein PNPase and matrix localized ClpP (Abcam, UK). (**D**) When solubilized with 1% dodecyl maltoside, LACE1 exists in a ~140 kDa complex. Mitochondria from HEK-293 cells transiently transfected with wt LACE1–FLAG construct were solubilized with 1% (w/v) dodecyl maltoside and resolved using two-dimensional blue native (5–15% polyacrylamide gradient)/10% denaturing PAGE. The resulting immunoblots were first incubated with antibody against FLAG epitope (Sigma–Aldrich), and subsequently with antibodies against the NDUFA9 subunit of complex I, COX2 subunit of complex IV and SDH A subunit of complex II. Under the conditions used, these antibodies recognize complex I (970 kDa), complex IV (205 kDa) and complex II (130 kDa) respectively. (**E**) Digitonin-solubilized LACE1–FLAG migrates in high-molecular-mass complexes of ~400 and 500 kDa respectively. Mitochondria from LACE1–FLAG-expressing cells (top) and anti-FLAG affinity-purified LACE1–FLAG (bottom*) solubilized with 1% (w/v) digitonin were resolved using two-dimensional blue native (6–15%) polyacrylamide gradient)/10% denaturing PAGE. The resulting Western blot was developed with anti-FLAG antibody. Subsequently, the Western blot was developed with antibodies against ATPase subunit α, Core 2, COX2 and SDH A. Under the conditions used, these antibodies recognize ATP synthase holoenzyme (600 kDa), residual free complex III dimer (500 kDa), F1-ATPase subcomplex (370 kDa), complex IV (205 kDa) and complex II (130 kDa) respectively. Molecular masses are indicated in kDa.

4.2.2. LACE1 variants with a T143V substitution in their Walker A motif fail to accumulate in mitochondria

To define cellular activities of the LACE1 protein, five different HEK-293 cell lines stably expressing *miR-30*- based shRNAs (shRNAmirs) targeting the human LACE1 transcript (GenBank® accession number NM_145315) were constructed. Control cell line was prepared by transfectingHEK-293 cells with commercially available scrambled (nonsilencing) shRNAmir-containing expression vector RHS436 (Open Biosystems, USA). Western blot analysis with antibody against LACE1 confirmed that two of the KD cell lines produced, denoted LACE1sh4 and LACE1sh5 (V3LHS_344953, V3LHS_344954; Open Biosystems), exhibit less than 10% of residual LACE1 protein (Figure 4.9. A).

To test the specificity of the RNAi KD obtained and to assess the significance of the putative P-loop motif of LACE1, we constructed three LACE1 variants in which either one or both of the conserved lysine and threonine residues of the Walker A motif (G/A)XXXXGK(T/S) were replaced by neutral AA (Deyrup, Krishnan et al. 1998). In the first mutant variant, Lys142 was replaced with alanine (K142A), whereas in the second variant Thr143 was replaced with valine (T143V). Finally, the last variant combined mutations of the previous two variants in a single ORF (K142A, T143V). The three LACE1 mutants and the wt LACE1–FLAG were transiently expressed in a LACE1-KD background. The control cell line expressing scrambled shRNA was transfected with the empty expression vector pCMV6-ENTRY. Despite the fact that the wt LACE1 as well as the K142A single mutant accumulated in mitochondria at high levels and in the correctly processed form, both of the variants harbouring the T143V substitutions were found to accumulate in mitochondria at ∼10-fold lower levels (Figure 14.10. B). At the same time, all mutant variants exhibited disproportionately high levels of the unprocessed protein form (*). To extend these structure–function data, we constructed a Walker B motif LACE1 mutant variant. In this variant, the conserved Glu214 of the Walker B motif (consensus sequence hhhhDE; h = hydrophobic residue) of LACE1 was replaced by glutamine (Hanson and Whiteheart 2005). Ectopic expression of this variant in a LACE1-KD backgroundmresulted in correct mitochondrial targeting and normal stability ofmthe E214Q LACE1 protein (Figure 4.9. B).

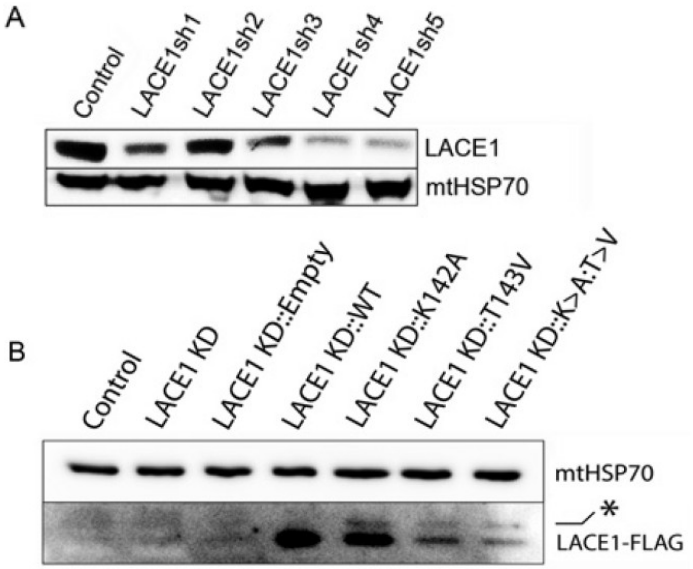

Figure 4.9. The T143V substitution in Walker A motif of LACE1 abrogates its mitochondrial accumulation (**A**) LACE1 protein is efficiently down-regulated in HEK-293 cells using the stable shRNAmir KD approach. Mitochondrial lysates (~10 μg of protein) from five different cell lines (denoted LACE1sh1–LACE1sh5) with stable vector-based expression of shRNAmirs targeting the LACE1 transcript were separated using SDS/PAGE (10% gel) and immunoblotted with antibodies against LACE1 and mtHSP70. The appropriate control cell line was generated by transfecting HEK-293 cells with non-silencing (scrambled) shRNAmir vector. Two of the cell lines, denoted LACE1sh4 and LACE1sh5, exhibited LACE1 protein levels of<10%of control values. (**B**) LACE1 variant with a T143V substitution in Walker A (P-loop) motif fail to accumulate in mitochondria of LACE1-KD cells. Three LACE1 mutant variants (K142A, T143V and K142A+T143V) in which one or two of the conserved residues of the Walker A (P-loop) motif (G/A)XXXXGK(T/S) were replaced with neutral amino acids were constructed using site-directed mutagenesis. These mutants were along with the wt LACE1 transiently expressed in a LACE1-KD background and the resulting whole-cell lysates were analysed by immunoblotting using anti-FLAG antibody. Antibody against mtHSP70 was used as a loading control. The asterisk (*) denotes the location of the LACE1–FLAG precursor protein band.

4.2.3. Loss of LACE1 leads to fragmented mitochondrial reticulum and aberrant mitochondrial ultrastructure

To assess the effects of LACE1 silencing on mitochondrial morphology, we used mitochondrial reticulum imaging and electron microscopy. MitoTracker Red fluorescence microscopy showed that LACE1-KD cells have significantly fragmented mitochondrial

reticulum, compared with the mostly tubular mitochondrial reticulum of control cells (Figure 4.10. A).

Importantly, reintroduction ofwt LACE1–FLAGinto LACE1-KD cells led to the reappearance of a correctly fused mitochondrial network (Figure 4.10. B). Transmission electron microscopy of LACE1-KD cells showed markedly altered mitochondrial shape and cristae morphology. Instead of rich lamellar cristae structure within tubularmitochondria of control cells, almost round-shaped mitochondria containing attenuated and unstructured cristae were found (Figure 4.10. B).

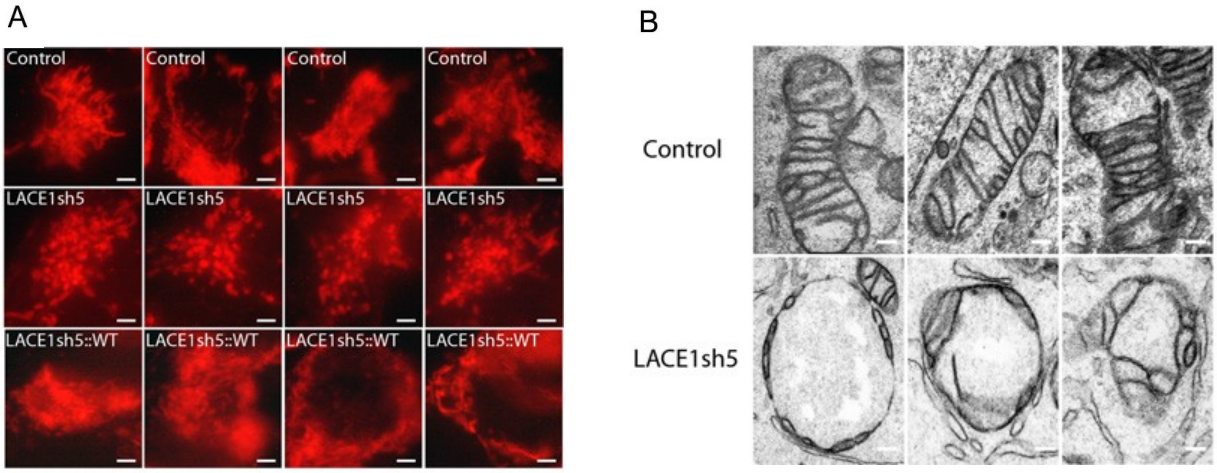

Figure 4.10. Loss of LACE1 leads to fragmented mitochondrial reticulum and aberrant mitochondrial ultrastructure. (**A**) LACE1-KD cells exhibit fragmented mitochondrial reticulum, and reintroduction of wt LACE1 200 inverted microscope equipped with an Olympus DP50 camera. Scale bar, 10 μm. (**B**) LACE1-KD cells exhibit a markedly altered mitochondrial shape and ultrastructure. The cells were incubated in PBS containing 2% potassium permanganate for 15 min, washed with PBS and dehydrated with an ethanol series. They were then embedded in Durcupan Epon, sectioned by mi leads to correction ofmitochondrial fusion. Control cells, LACE1-KD cells transfected with empty vector and LACE1-KD cells transfected with wt LACE1 were visualized with MitoTracker Red and analysed using a Nikon Diaphot crotome to thicknesses ranging from 600 to 900 A° , and stained with lead citrate and uranyl acetate. The sections were viewed with a JEOL JEM-1200 EX transmission electron microscope. Scale bars, 200 nm

4.2.4. Loss of LACE1 leads to increased accumulation of nuclear-encoded complex IV subunits, increased PARL and K142A substitution in Walker A motif and E214Q substitution in Walker B motif of LACE1 abrogate LACE1-mediated clearance of complex IV subunits

As yeast LACE1 homologue Afg1was found to facilitate turnover of mitochondrially encoded cytochrome *c* oxidase (complex IV) subunits (Khalimonchuk, Bird et al. 2007), we therefore assessed levels of complex IV subunits in whole-cell lysates of LACE1-KD cells using Western blot analysis. We found unaffected levels of mitochondrially encoded complex IV

subunits, but markedly increased levels of three (COX4, COX5A and COX6A) of the nuclear-encoded components of complex IV (Figure 4.11. A). In contrast, steadystate levels of other respiratory chain subunits were found to be unaltered in LACE1-KD cells (Figure 4.11. A).

OPA1, a dynamin-like GTPase protein, plays a central role in regulating mitochondrial fusion and cristae morphology (Stiburek, Cesnekova et al. 2012, Anand, Langer et al. 2013, Anand, Wai et al. 2014, Mishra, Carelli et al. 2014). Thus fragmented mitochondrial reticulum and altered mitochondrial ultrastructure of LACE1-KD cells prompted us to analyse the profile of OPA1 protein forms in whole-cell lysates from LACE1-KD cells using SDS/PAGE Western blotting. We found a general increase in short OPA1 forms in LACE1-KD whole-cell lysates, when compared with controls (Figure 4.11. C). In addition, the amount of the smaller of the two detectable long OPA1 forms was found to be reduced in the cells (Figure 4.11. C).

To address functional significance of both Walker A and Walker B motifs of LACE1 and to confirm the specificity of the RNAi phenotypes observed, we expressed wt LACE1 as well as K142A and E214Q LACE1 in a LACE1-KD background. Whereas expression of wt LACE1 led to significantly reduced mitochondrial accumulation of COX4, COX5A and COX6A, ectopic expression of both LACE1 variants did not lead to suppression of this phenotype (Figures 4.11. B and D). Western blots of identical samples also showed diminished levels of LON protease and increased levels of YME1L protease inmitochondria of LACE1-KD cells (Figures 4.11. B and D). In contrast with the requirement of wt LACE1 re-expression for clearance of excess COX4, COX5A and COX6A, alterations of LON and YME1L in LACE1-KD cells were effectively suppressed by expression of both LACE1 variants (Figures 4.11. B and D).

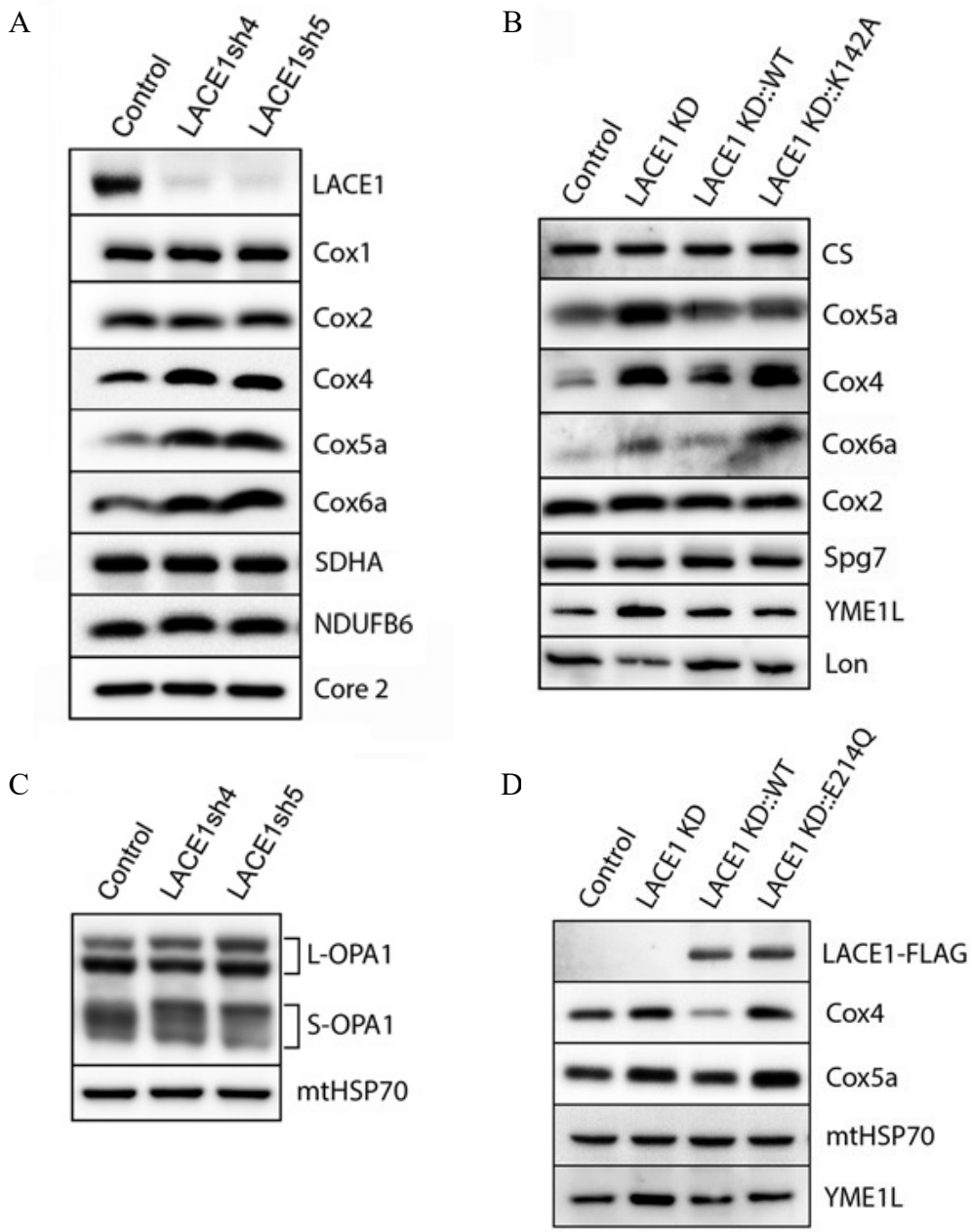

Figure 4.11. Loss of LACE1 leads to increased accumulation of COX4, COX5A and COX6A and ectopic expression of wt LACE1 but not of K142A or E214Q variants rescues the increased accumulation of complex IV subunits. (**A**) COX4, COX5A and COX6A subunits of complex IV are markedly up-regulated in LACE1-KD cells. Equal amounts of whole-cell lysates from LACE1sh4 and LACE1sh5 cell lines were separated by SDS/PAGE (10% gel) and immunoblotted with antibodies against LACE1, COX1, COX2, COX4, COX5A, COX6A, SDH A, NDUFB6 and Core 2. (**B**) Increased accumulation of nuclear-encoded complex IV subunits is reversed upon reintroduction of wt LACE, but not of the K142A variant. Whole-cell lysates were prepared from control cell line (Control) and from the LACE1-KD cell line transfected with empty vector (LACE1 KD), wt LACE1–FLAG (WT) or K142A LACE1 variant, and immunoblotted using antibodies against COX5A, COX4, COX6A, COX2, SPG7, LON and YME1L. Antibody against citrate synthase (CS) was used to control for equal protein loading. (**C**) Loss of LACE1 is associated with an increased amount of short OPA1 isoforms (S OPA1) (L-OPA1 is long OPA1 isoforms). Whole-cell lysates from control and LACE1-KD cells were separated by SDS/PAGE and Western blotted with antibody against OPA1. Antibody against mtHSP70 was used to control for equal protein loading. (**D**) Ectopic expression of E214Q LACE1 variant fails to rescue the increased accumulation of nuclear-encoded complex IV subunits in the LACE1 RNAi background. Whole-cell lysates were prepared from a control cell line (Control) and from a LACE1-KD cell line transfected with empty vector (LACE1 KD), wt LACE1–FLAG (WT) or E214Q LACE1–FLAG, and immunoblotted using antibodies against FLAG, COX5A, COX4 and YME1L. Antibody against mtHSP70 was used to control equal protein loading.

4.2.5. Knockdown of LACE1 by shRNA leads to diminished activity of mitochondrial respiratory chain and enzyme activity of complexes of electron transport chain

To assess the effects of LACE1 knockdown on cell viability, we examined the growth rate of LACE1 KD cells over a time course of 7 days. We found only moderate growth impairment associated with the loss of LACE1 (Figure 4.12. A).

Mitochondria are at the center of cellular bioenergetics harboring the energy-converting respiratory chain. Therefore, we next assessed the functional state of mitochondrial respiration in LACE1 KD cells by measuring the oxygen consumption of digitonin-permeabilized cells with the OROBOROS Oxygraph-2k device (OROBOROS INSTRUMENTS Corp, Innsbruck, Austria). We found significantly diminished activity of respiratory chain complex IV in LACE1 KD cells (Figure 4.12. C). However, the activity of complexes II and III was also significantly reduced. In contrast, the activity of respiratory complex I appeared unaffected (Figure 4.12. C).

To assess the effects of loss of LACE1 on respiratory chain function, we measured the activities of respiratory complexes I–IV using spectrophotometry on isolated mitochondria. We found significantly reduced activity of complex III (68.9% of controls) and complex IV (67.5% of controls) in mitochondria of LACE1-KD cells (Figure 4.12. D). The activity of complex I was not significantly affected in these cells, but the activity of complex II was markedly elevated (138.5% of controls) (Figure 4.12. D).

To find out whether the respiratory deficiency and reduced activity were due to diminished amount of selected respiratory complexes in LACE1 KD cells, we performed BN PAGE immunoblotting analysis of mitochondria isolated from LACE1 KD cells. Isolated mitochondria were solubilized with 1% (w/v) dodecyl maltoside, resolved on 5-15% BN PAGE gels and immunoblotted with antibodies to Cox1, Ndufb6, Core 2 and SDH A. The immunoblots revealed mostly unaffected levels of respiratory chain complexes in LACE1 KD mitochondria, with only moderate increase of complex I and slight reduction of complex III (Figure 4.12. B).

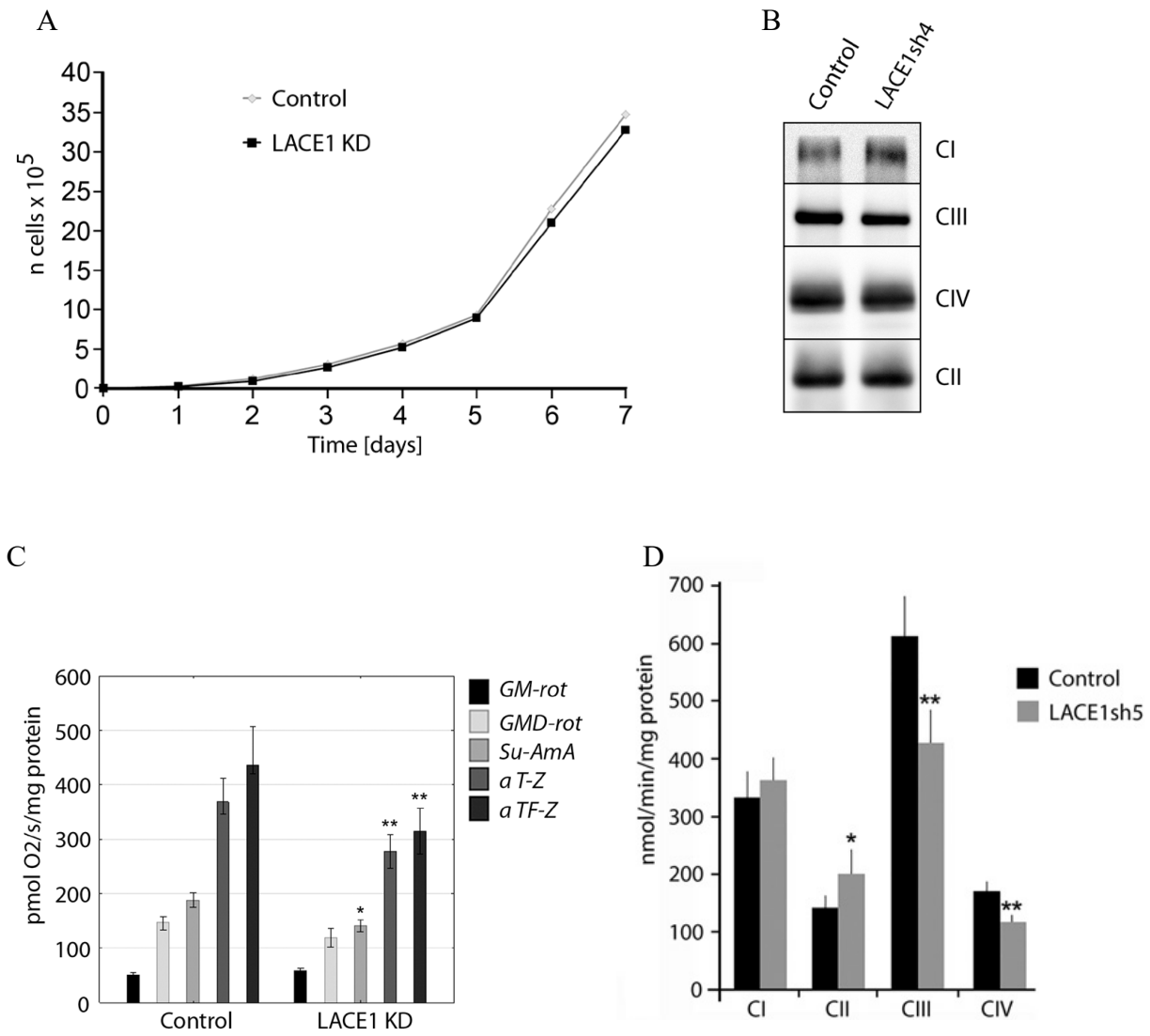

Figure 4.12. LACE1 knockdown by shRNA leads to diminished activity of respiratory chain complexes II-IV. and to diminished enzyme activity of complexes III and IV. (A) LACE1 KD cells exhibit moderate growth impairment. Stably transfected HEK293 cells were seeded in six-well plates at 5×10^4 cells per well and cultured in DMEM containing 1 µg/ml puromycin. Viable cells were counted every 24 h for a total of 7 d using a Scepter Handheld Automated Cell Counter. (**B)** LACE1 KD cells have moderately increased content of complex I and slightly reduced content of complex III. Blue-native PAGE immunoblotting analysis of mitochondria isolated from LACE1 KD cells were performed. Isolated mitochondria were solubilized with 1% (w/v) dodecyl maltoside, resolved on 5-15% blue-native PAGE gels and immunoblotted with antibodies to Ndufb6 (CI), Core 2 (CIII), Cox1 (CIV) and SDH A (CII). CI-CIV denotes four mitochondrial respiratory chain complexes. (**C**) Loss of LACE1 leads to diminished activity of respiratory chain complexes II-IV. The oxygen consumption of digitonin-permeabilized cells was measured at 37 °C using an OROBOROS Oxygraph-2k (OROBOROS INSTRUMENTS Corp, Innsbruck, Austria) in 2ml chamber by substrate-inhibitor titration. * $p<0.05$; ** $p<0.01$. (**D**) Loss of LACE1 leads to diminished activity of complexes III and IV and increased activity of complex II. Enzyme activities of respiratory chain complexes in isolated mitochondria were measured using spectrophotometry. The plotted values were normalized to protein content and are expressed as means+— S.D. *P <0.05; **P <0.01.

4.2.6. Loss of LACE1 leads to increased PARL and reduced Omi/HTRA2, whereas its overexpression leads to accumulation of p53 in mitochondria and concomitant p53 reduction in nucleus

Western blotting screen for proteins affected by manipulation of cellular LACE1 levels revealed markedly reduced Omi/HTRA2 and increased PARL in mitochondria of LACE1 KD cells (Figure 4.13. B). Reintroduction of LACE1 ORF into LACE1 KD background led to suppression of the observed protein phenotypes (Figure 4.13. B). Furthermore, overexpression of LACE1-FLAG in LACE1 KD cells led to dramatic mitochondrial accumulation of the p53 tumor suppressor and OMA1 protease and to marked cellular reduction of PUMA and Bax protein levels (Figure 4.13. A). Importantly, the nuclear p53 protein levels were found significantly reduced in LACE1-FLAG overexpressing cells (Figure 4.13. A).

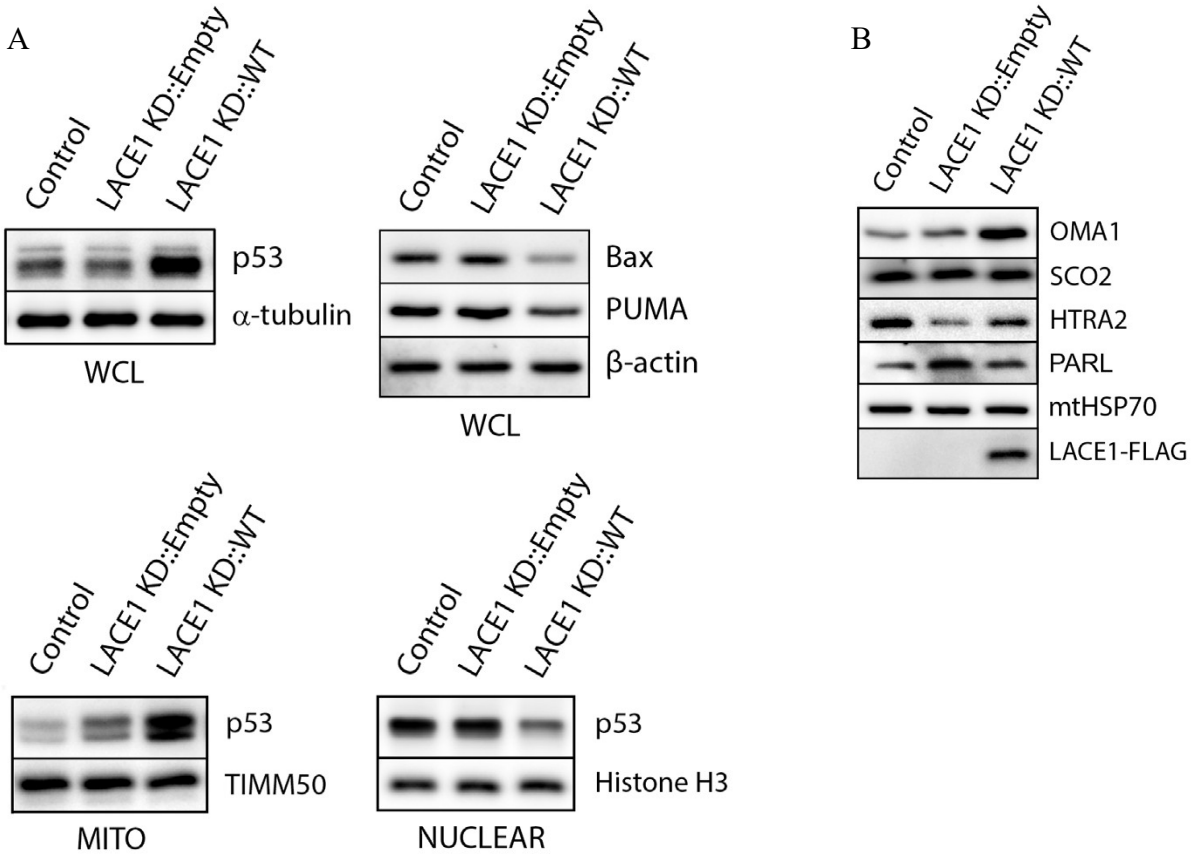

Figure 4.13. LACE1 expressed in LACE1 KD background promotes its increased mitochondrial accumulation and nuclear reduction. (A) Overexpression of LACE1 leads to increased mitochondrial accumulation of p53 and its nuclear reduction. Whole-cell lysates (WCL), mitochondrial protein lysates (MITO) and nuclear extracts (NUCLEAR) were prepared from control cell line (Control) and from LACE1 KD cell line transfected with either the empty expression vector or LACE1-FLAG construct and subsequently immunoblotted with antibodies to p53, Bax and PUMA. Equal protein loading and fractionation efficiency was monitored using antibodies to TIMM50, histone H3 and a-tubulin. (**B**) Loss of LACE1 leads to upregulation of PARL and downregulation of HTRA2. Mitochondrial protein lysates (MITO) were prepared from control cell line (Control) and from LACE1 KD cell line transfected with either the empty expression vector or LACE1-FLAG construct and subsequently immunoblotted with antibodies to OMA1, SCO2, HTRA2, FLAG, PARL and mtHSP70.

4.2.7. COX4, COX5A, YMEL and p53 co-purify with wt LACE1 expressed in LACE1-KD cells

To find out which of the observed effects associated with manipulation of cellular LACE1 levels are based on direct protein–protein interactions, we usedmitochondria from LACE1-KD cells transfected with wt LACE1–FLAG construct to perform anti-FLAG affinity purification. To control for possible nonspecific results, we used mitochondria from LACE1-KD cells transfected with CLPP–FLAG (GenBank® accession number NM_006012) construct. CLPP is a proteolytic subunit of matrix-localized CLPXP complex and thus unlikely to share common interacting partners with LACE1, which is predicted to be an inner membrane protein (Khalimonchuk, Bird et al. 2007). Mitochondria were solubilized using 0.5% Triton X-100, and co-purifying components were analysed using SDS/PAGE immunoblotting with a battery of validated antibodies against mitochondrial proteins. We obtained highly efficient FLAG pull-down with both LACE1 and CLPP proteins (Figure 4.14. B). Subsequent Western blot analysis revealed significant amounts of COX4 and COX5A subunits to specifically co-purify with LACE1–FLAG but not CLPP–FLAG protein (Figure 4.14. A).

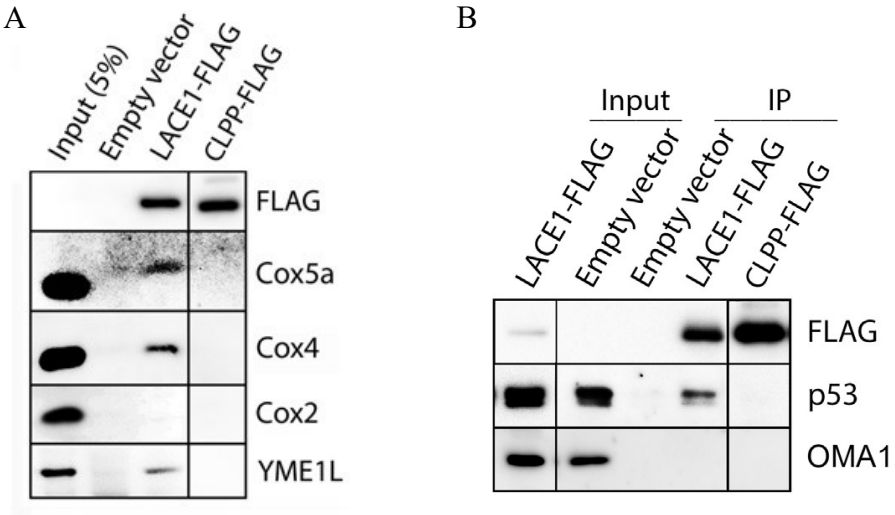

Figure 4.14. LACE1 co-immunoprecipitates with COX4, COX5A, YME1L protease and p53 tumor suppresor protein. (**A**) COX4, COX5A and YME1L and (**B**) p53 tumor supppresor protein co-immunoprecipitates with LACE1–FLAG expressed in LACE1-KD cells. LACE1-KD cells were transientlytransfected with empty expression vector, wt LACE1–FLAG construct and CLPP–FLAG construct. Isolated mitochondrial fractions were solubilized with 1% Triton X-100 and subjected to anti-FLAG affinity purification. The bound antigens were eluted with 3× FLAG peptide solution under native conditions and processed for SDS/PAGE immunoblotting. A 5% (v/v) amount of the purification input was loaded on the gel along with the purified samples and immunoblotted with antibodies against (**A**) FLAG, COX4, COX5A, YME1L and COX2 and against (**B**) FLAG, p53 and CLPP.

Importantly, additional Western blotting screening also identified a significant amount of YME1L protease (Figure 4.14. A) and the p53 tumor suppresor protein (Figure 4.14. B) in LACE1–FLAG purification samples. We were not able to identify any of the mitochondrially encoded complex IV subunits or additional nuclear-encoded complex IV components in LACE1–FLAG affinity preparations using Western blot analysis.

4.2.8. Loss of LACE1 leads to increased apoptotic resistance whereas its overexpression results in increased apoptotic sensitivity

Since LACE1 KD cells showed substantially diminished constitutive PARP cleavage (Figure 4.15. A), we next assessed staurosporine (STS)-induced apoptosis in these cells. Both control and LACE1 KD cells were treated with 0, 3 and 6 hours exposures to staurosporine (2 μM) and used either for preparation of whole cell lysates or for direct immunofluorescence staining. Whole cell lysates were subsequently processed for western blotting with antibody to cleaved PARP (Figure 4.15. B). For immunofluorescence, the cells were stained with antibody to cytochrome c and with DAPI (Figure 4.15. D). Consistently, western blotting of staurosporine treated cells showed reduced levels of cleaved PARP and cytochrome c-immunofluorescence microscopy revealed significantly milder apoptotic changes in STS-treated LACE1 KD cells, compared to identically treated controls (Figure 4.15. B and D). To confirm the cytochrome c immunofluorescence results, staurosporine treated cells were subjected to subcellular fractionation and the resulting cytoplasmic fractions were immunoblotted with antibody to cytochrome c. Western blotting detection of alfa-tubulin was used to control for equal cytoplasmic protein loading. The western blots revealed higher cytoplasmic cytochrome c content in control cells, when compared to identically treated LACE1 KD cells, confirming the immunofluorescence results (Figure 4.15. C).

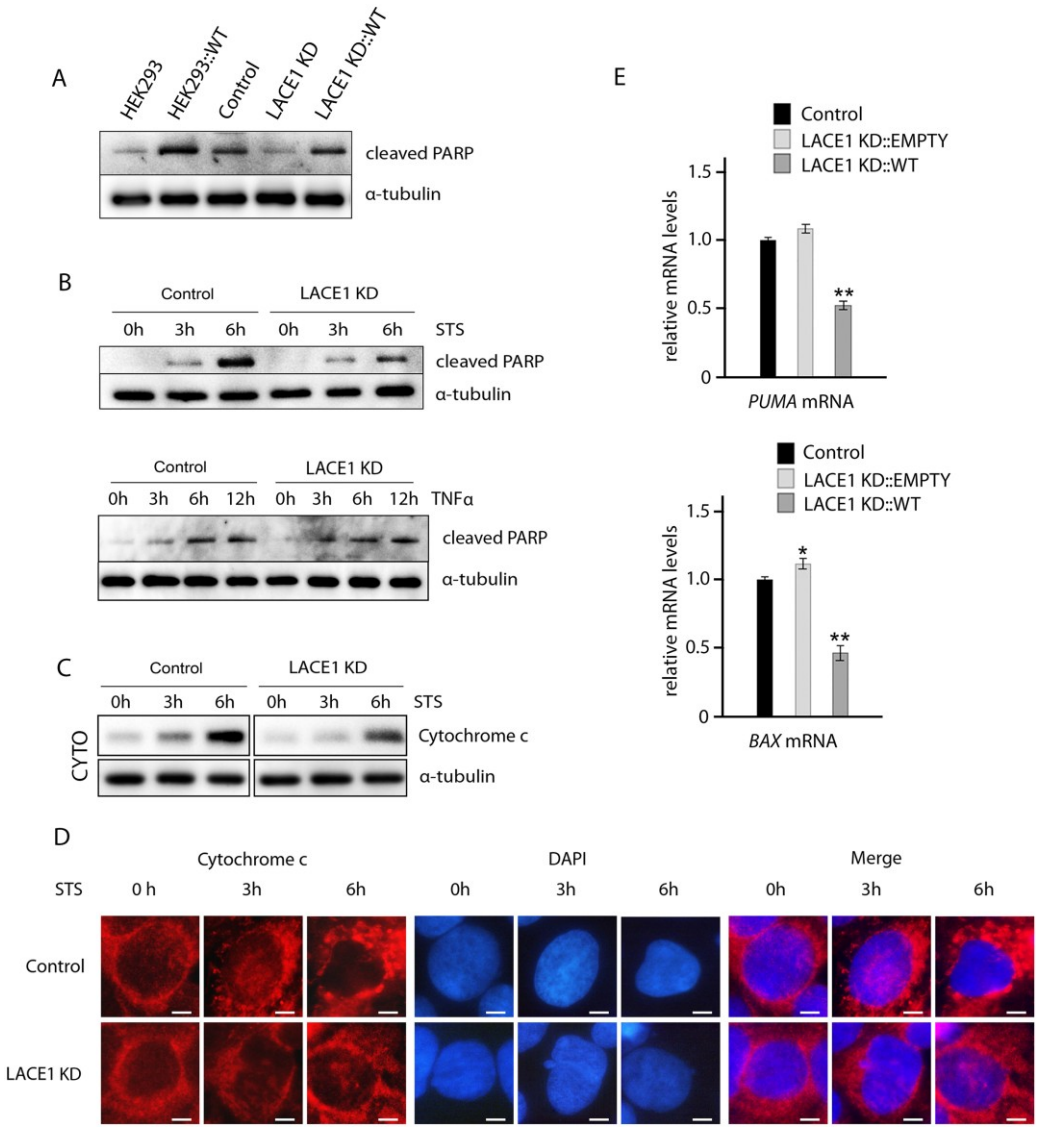

Figure 4.15. Loss of LACE1 leads to increased apoptotic resistance whereas its overexpression results in increased apoptotic sensitivity. (A) Overexpression of LACE1-FLAG in both wild-type HEK293 cells and LACE1 KD cells results in increased PARP cleavage. Wild-type HEK293 cells and LACE1 KD cells were transfected with LACE1-FLAG expression vector or with the empty vector. Whole-cell lysates were analyzed with western blotting using antibody to cleaved PARP. Antibody to α -tubulin was used to monitor equal protein loading. **(B)** LACE1 KD cells exhibit increased resistance to staurosporine-induced apoptosis but respond normally to TNFalpha-treatment. Control and LACE1 KD cells were treated with staurosporine (STS; 2 μM) or TNF alpha (10 ng/ml) and IFN-gamma (80 ng/ml) for 0, 3 and 6 hours. Whole cell lysates were prepared from treated cells and used for immunoblotting with antibody to cleaved PARP. Antibody to α-tubulin was used to control for equal protein loading. **(C)** Cells were treated with staurosporine (STS; 2 μM) for 0, 3 and 6 hours and then harvested and used for subcellular fractionation using dounce homogenization and differential centrifugation. The resulting cytoplasmic fractions were subjected to SDS-PAGE western blotting with antibody to cytochrome c. Western blotting of alpha-tubulin was used as loading control. **(D)** Cells grown on coverslips were treated with staurosporine (STS; 2 μM) for 0, 3 and 6 hours and then fixed with 4% paraformaldehyde at room temperature and permeabilized with 0.1% Triton X-100. Cells were blocked by 10% Fetal Bovine Serum and primary detection was performed with anti-cytochrome c antibody. After secondary fluorescent detection, cells were analyzed at 24°C using a Nikon Diaphot 200 inverted microscope equipped with a Plan-Apochromat 60×, numerical aperture 0.95, oil objective. The images were acquired with an Olympus DP50 CCD camera and Viewfinder Lite 1.0 software. Bar, 10 μM. **(E)** Whereas knockdown of LACE1 leads to moderate upregulation of *PUMA* and *BAX* mRNAs, overexpression of LACE1-FLAG results in their significant downregulation. Relative mRNA quantification was performed using TaqMan Gene Expression Assays according to the manufacturer's instructions (Applied Biosystems). Data were collected in duplicate in two separate runs using a 7300 Real-Time PCR System (Applied Biosystems). HPRT1 (hypoxanthine phosphoribosyltransferase 1), TUBA1A (tubulin, alpha 1a) and TBP (TATA box– binding protein) were used as reference genes.

4.2.9. LACE1 is required for mitomycin c-induced translocation of p53 to mitochondria and its concomitant reduction in nucleus

To confirm the LACE1-induced mitochondrial accumulation of p53, we performed immunofluorescence imaging of wild-type HEK293 cells transfected with the LACE1 ORF construct. Again we found dramatic increase in mitochondrial p53 content in cells with high expression of LACE1-FLAG, as inferred from co-localization of p53 fluorescence signal with that of complex IV subunit COX1 (Figure 4.16. A and B). In addition, LACE1-overexpressing HEK293 cells revealed markedly swelled and disrupted mitochondria and leaked mitochondrial content, compared with unaffected mitochondrial reticulum of cells transfected with the empty vector. This is consistent with augmented PARP cleavage after LACE1 overexpression in both wild-type and LACE1 KD HEK293 cells (Figure 4.16. A).

The DNA damage agent mitomycin c (MMC) can induce mitochondrial accumulation of p53 protein. As our results have indicated that LACE1 may be required for mitochondrial translocation and/or accumulation of p53, we used MMC treatment to find out whether mitochondrial translocation of p53 is compromised in LACE1 KD cells. Both control and LACE1 KD cells were treated with MMC (5g/mL) for 0, 3, 6 and 12hours and then analyzed with anti-p53 and DAPI immunofluorescence microscopy. The resulting images revealed marked cytoplasmic (mitochondrial) accumulation of p53 in control cells after 6- and 12-h exposures to MMC. This increase in cytoplasmic p53 protein was accompanied by marked reduction in nuclear p53 protein content (Figure 4.16. C). In contrast, neither the increase in cytoplasmic p53 nor the concomitant reduction in nuclear p53 content could be seen in identically treated LACE1 KD cells (Figure 4.16. C). Additionally, the immunofluorescence images of untreated (0h) cells revealed markedly altered nuclear distribution pattern of p53 protein in LACE1 KD cells, compared to untreated (0h) control cells. In contrast to highly localized nuclear distribution of p53 protein in control cells, the nuclear p53 signal was significantly more scattered in LACE1 KD cells, with multiple dots representing the p53 protein signal (Figure 4.16. C). Similar redistribution of p53 protein signal could be seen in control cells only after 3 and 6hours treatment with MMC.

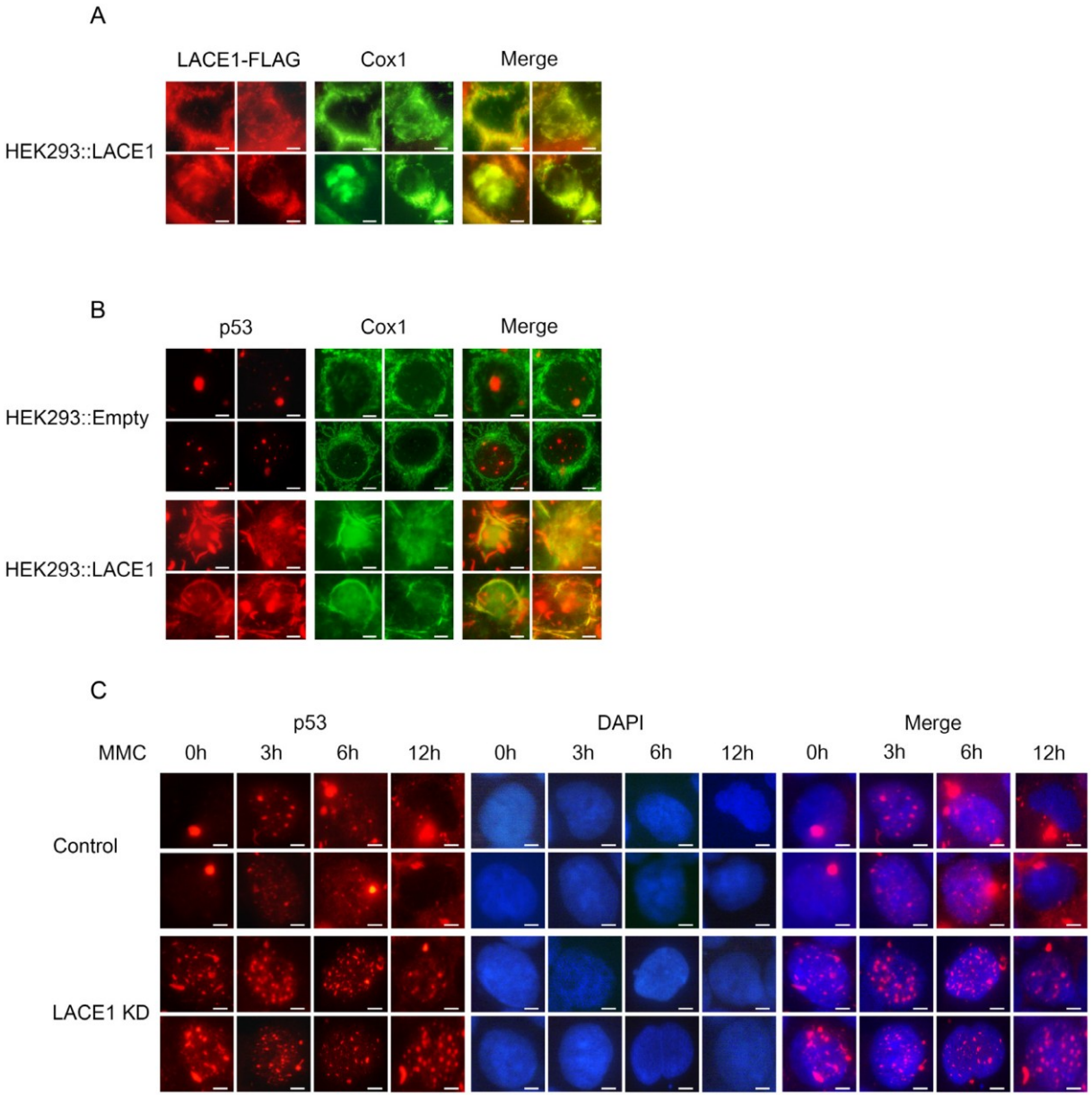

Figure 4.16. Loss of LACE1 abrogates mitomycin c-induced translocation of p53 into mitochondria whereas its overexpression promotes mitochondrial translocation of p53. (A-B) Overexpression of LACE1-FLAG in wild-type HEK293 cells promotes increased mitochondrial accumulation of p53. Cells grown on coverslips were transfected with the LACE1-FLAG construct or the empty vector and 48 hours post-transfection were fixed with 4% paraformaldehyde and permeabilized with 0.1% Triton X-100. Cells were then blocked by 10% Fetal Bovine Serum and primary detection was performed with antibodies to FLAG, p53 and COX1. After fluorescent secondary detection, cells were analyzed at 24°C using a Nikon Diaphot 200 inverted microscope equipped with a Plan- Apochromat 60×, numerical aperture 0.95, oil objective. The images were acquired with an Olympus DP50 CCD camera and Viewfinder Lite 1.0 software. Bar, 10 µM. **(C)** Loss of LACE1 abrogates mitomycin c-induced mitochondrial translocation of p53. Cells grown on coverslips were treated with mitomycin c (MMC; 5g/mL) for 0, 3, 6 and 12h and then processed for immunofluorescence microscopy essentially as describe in (A-B) except that anti-p53 antibody and DAPI staining were used. Bar, 10 µM.

4.2.10. The LACE1-mediated apoptosis is dependent on p53

To find out whether the pro-apoptotic activity of LACE1 requires p53 and to verify the previous results using cells with normal p53 signaling, we used Stealth™ siRNA knockdown in normal human dermal fibroblasts (NHDFs). First, the NHDFs were transfected with LACE1 siRNA and the staurosporine (STS)-induced apoptosis was assessed. Both control siRNA and LACE1 siRNA NHDFs were treated with 0, 3 and 6 hours exposures to 2 μM staurosporine. Whole-cell lysates were subsequently processed for western blotting with antibody to cleaved PARP. Consistent with the results on HEK293 cells, siRNA-mediated knockdown of LACE1 in NHDFs resulted in significantly increased resistance of the cells to STS-induced apoptosis (Figure 4.17. A and B).

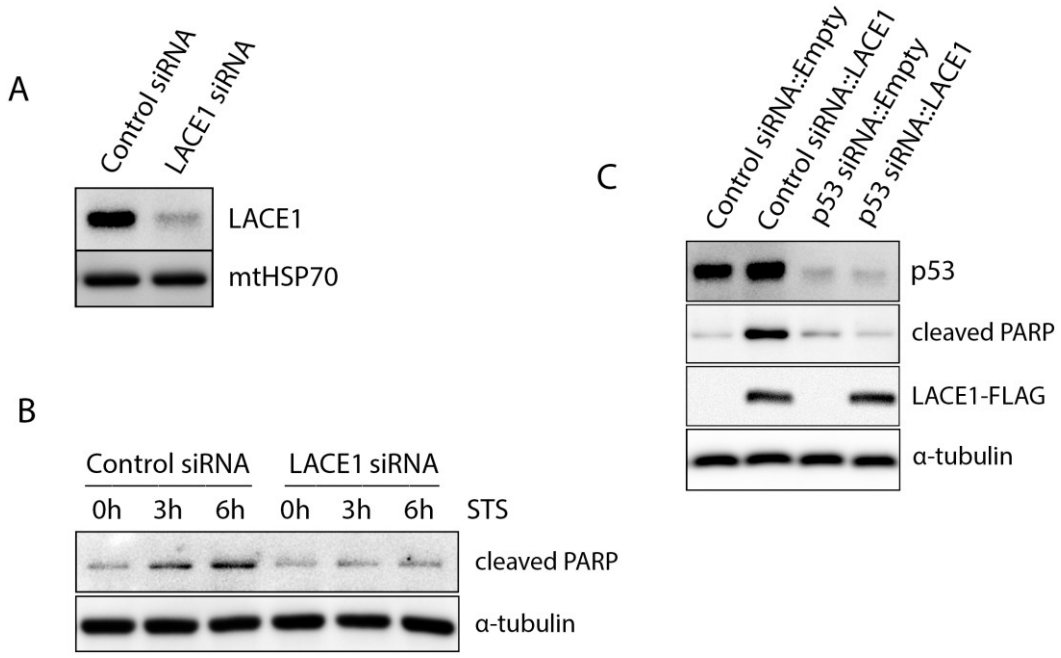

Figure 4.17. The LACE1-mediated apoptosis is dependent on p53. (A) Transfection of human dermal fibroblasts with LACE1 stealth siRNA leads to efficient knockdown of LACE1 protein. Normal human dermal fibroblasts (NHDFs) were transfected with control and LACE1 siRNA, harvested 48 hours post-transfection and processed for western blotting. The blots were developed with antibodies to LACE1 and mtHSP70. (**B)** Knockdown of LACE1 in NHDFs by siRNA renders cells resistant towards STS-induced apoptosis. Both control siRNA- and LACE1 siRNA-transfected NHDFs were treated with 0-h, 3-h and 6-h exposures to staurosporine (2 μM). Whole-cell lysates were subsequently western blotted with antibody to cleaved PARP. Equal protein loading was controlled with antibody to α-tubulin. (**C)** The LACE1-mediated apoptosis is dependent on p53. NHDFs in which p53 was downregulated using siRNA as well as appropriate siRNA control NHDFs were transfected with either LACE1-FLAG or empty vector constructs. The resulting whole-cell extracts were western blotted with antibodies to p53, cleaved PARP, FLAG. Equal protein loading was monitored with α-tubulin detection.

Next, we generated p53 siRNA knockdown NHDFs as well as appropriate siRNA control cells. Again, substantial p53 protein downregulation was obtained using stealth siRNA expression (Figure 4.17. C). Both p53 knockdown cells and the appropriate siRNA control cells were subsequently transfected with either LACE1-FLAG or empty vector constructs. The resulting whole-cell extracts were western blotted with antibodies to p53, cleaved PARP, FLAG and α-tubulin. Consistent with previous results, the western blots showed markedly increased amount of cleaved PARP in control siRNA cells overexpressing LACE1- FLAG (Figure 4.17. C). Importantly, the LACE1-FLAG overexpression failed to induce PARP cleavage in p53 knockdown cells (Figure 4.17.C).

The main points related to aim B)

Human LACE1 protein mediates degradation of nuclear-encoded complex IV subunits, interact with p53 and mediates its mitochondrial translocation and apoptosis. Our results show that:

- LACE1 is a mitochondrial integral membrane protein which exist as part of three protein complexes of approximately 500, 400 and 140 kDa
- LACE1 variants with a T143V substitution in their Walker A motif fail to accumulate in mitochondria
- Loss of LACE1 leads to fragmented mitochondrial reticulum and aberrant mitochondrial ultrastructure
- Loss of LACE1 leads to increased accumulation of nuclear-encoded complex IV subunits, increased PARL, associated with increased amount of short OPA1 isoforms and K142A substitution in Walker A motif and E214Q substitution in Walker B motif of LACE1 abrogate LACE1-mediated clearance of complex IV subunits
- Knockdown of LACE1 by shRNA leads to diminished activity of mitochondrial respiratory chain and enzyme activity of complexes of electron transport chain
- Loss of LACE1 leads to increased PARL and reduced Omi/HTRA2, whereas its overexpression leads to accumulation of p53 in mitochondria and concomitant p53 reduction in nucleus
- COX4, COX5A, YME1L and p53 co-purify with wt LACE1 expressed in LACE1-KD cells
- Loss of LACE1 leads to increased apoptotic resistance whereas its overexpression results in increased apoptotic sensitivity
- LACE1 is required for mitomycin c-induced translocation of p53 to mitochondria and its concomitant reduction in nucleus
- The LACE1-mediated apoptosis is dependent on p53

5. DISCUSSION AND COCLUSIONS

Mitochondrial protein quality control is essential for the maintenance of the cell integrity. This is ensured by sequential use of a large system of mitochondrial proteases and proteolytic complexes located across the various mitochondrial subcompartments. Errors in this system may lead to mitochondrial damage and ending with apoptosis. Moreover, mitochondrial proteases were found altered in many serious diseases. The exact cause of their occurrence is not yet clear.

Based on our previous results, we have focused on characterization of functional overlap and cooperativity of proteolytic subunits AFG3L2 and YME1L of the IMM complexes m- and i-AAA in the maintenance of mitochondrial structure and respiratory chain activity. We demonstrate that loss of AFG3L2 and YME1L both, alone and in combination, results in significant growth retardation in HEK293 cells. We have previously demonstrated that loss of YME1L results in reduced growth rate of the cells attributed either to their reduced apoptotic resistance or diminished respiratory capacity (Stiburek, Cesnekova et al. 2012). Knockdown of YME1L in mouse embryonic fibroblasts (MEFs) was shown to cause increase in mitochondrial fission factor (MFF) and mitochondrial dynamics protein 49 (Mid49), which is known to recruit mitochondrial fission protein Drp1 to mitochondria (Ruan, Li et al. 2013). Interestingly, both YME1L and YME1L/AFG3L2 knockdown mitochondria contained significantly increased levels of Drp1. In contrast, mitochondrial fraction from single AFG3L2 KD cells showed normal Drp1 levels.

Markedly diminished Spg7 levels were found in all three knockdown cell lines analyzed. Spg7 forms a hetero-oligomeric m-AAA protease isoenzyme together with AFG3L2 subunit. In the absence of AFG3L2 the stability of Spg7 might be compromised. However, the markedly diminished Spg7 levels found in YME1L KD cells are difficult to explain. In addition to YME1L, OMA1 protease mediates the processing of OPA1 (Baker, Lampe et al. 2014, Korwitz, Merkwirth et al. 2016). Whereas YME1L-dependent OPA1 processing promotes tubular mitochondrial morphology, OMA1-dependent processing induces mitochondrial fragmentation (Anand, Wai et al. 2014, Rainbolt, Lebeau et al. 2016). We found elevated OMA1 in all three knockdown cell lines with the most prominent change in AFG3L2 KD cells. Indeed, OMA1 was first identified in yeast as a peptidase with overlapping activities with the m-AAA protease (Khalimonchuk, Jeong et al. 2012).

The dynamic mitochondrial network fragments under stress conditions allowing the segregation of damaged mitochondria (Baker, Lampe et al. 2014). We have previously demonstrated that loss of YME1L leads to mitochondrial fragmentation and mitochondrial cristae disorganization (Stiburek, Cesnekova et al. 2012). YME1L directly influences the stability of OPA1, whereas loss of function of AFG3L2 triggers OPA1 processing by OMA1 protease (Ehses, Raschke et al. 2009). Whereas YME1L is active constitutively, activity of OMA1 markedly increases after stress insults such as after mitochondrial membrane depolarization (Baker, Lampe et al. 2014, Zhang, Li et al. 2014). Under normal conditions, proteolytic cleavage of long isoforms of OPA1 by YME1L results in balanced accumulation of both long and short OPA1 protein forms (Song, Chen et al. 2007). Constitutive processing of OPA1 by YME1L is required to maintain normal morphology of mitochondria (Stiburek, Cesnekova et al. 2012). Stress-induced OPA1 processing by OMA1 inhibits fusion and leads to mitochondrial fragmentation (Twig, Elorza et al. 2008). Knockdown of AFG3L2 led to the most severe mitochondrial ultrastructure defects of our KD cells, yet its effect on mitochondrial morphology appeared rather mild. Conversely, whereas loss of YME1L resulted in severe mitochondrial fragmentation, its effect on mitochondrial ultrastructure was relatively mild.

We have previously shown that YME1L is directly involved in turnover of non-assembled Ndufb6 and Cox4 (Stiburek, Cesnekova et al. 2012). Here we show that loss of AFG3L2 results in even more pronounced accumulation of non-assembled Cox4 than that seen in YME1L KD cells, suggesting the direct role of m-AAA protease in proteolysis of non-assembled Cox4. Simultaneous knockdown of YME1L and AFG3L2 did not seem to exacerbate the accumulation of non-assembled Cox4 in the mitochondria. In contrast to loss of YME1L, loss of AFG3L2 did not lead to marked mitochondrial accumulation of Ndufb6-containing subcomplexes. However, simultaneous knockdown of AFG3L2 and YME1L led to reduction in complex I holoenzyme and elevation in high molecular weight Ndufb6-subcomplex, when compared with single YME1L KD cells. Both the elevation of complex I holoenzyme in YME1L KD cells as well as its marked reduction in double AFG3L2/YME1L cells corresponds with the elevated and markedly diminished enzyme activity of NADH:ubiquinone oxidoreductase in these cells. The activity impairment of cytochrome oxidase in AFG3L2 and AFG3L2/YME1L cells further implicates the involvement of m-AAA protease in maintenance of correct complex IV biogenesis.

LACE1 protein is human homologue of yeast Afg1 ATPase. Afg1 protein has an ATPase domain but lacks a proteolytic domain. The highly evolutionary conserved Afg1 ATPase probably acts as a chaperon in degradation of unassembled or misfolded complex IV subunits (Lee and Wickner 1992, Khalimonchuk, Bird et al. 2007). On the basis of its similarity with Cdc48 (VCP/p97), the yeast Afg1 was suggested to form homohexameric complexes in the IMM (Elsasser and Finley 2005, Khalimonchuk, Bird et al. 2007). Mammalian VCP/p97 functions in a wide range of biological processes including protein degradation, cell cycle regulation, gene expression, apoptosis and DNA replication. Importantly, p97 extracts polytopic membrane proteins from the endoplasmic reticulum membrane and thus facilitates their turnover by the 20S proteasome with which it associates (Carlson, Pitonzo et al. 2006). The human LACE1 ortholog consists of ATP/GTP binding Walker A motif and has predicted ATPase activity too. LACE1 protein is built up of a common five domain structure and shows high level of expression in active mammary gland, myocardium, kidney and liver tissue. Likewise, physical interaction and co-operation of the LACE1 complex with YME1L may stimulate proteolysis of nuclear-encoded complex IV subunits by the i-AAA complex. Two adaptor proteins, Mgr1 and Mgr3, were identified for the yeast i-AAA complex. Similar to LACE1, Mgr1 and Mgr3 were shown to bind substrates even in the absence of protease and to stimulate their proteolysis by the i-AAA complex (Dunn, Tamura et al. 2008). However, since only a fraction of YME1L was found to interact with LACE1, a rather transient type of interaction between LACE1 and YME1L is proposed. In contrast, both Mgr1 and Mgr3 were shown to stably associate with the i-AAA complex in yeast.

We show that mitochondrial integral membrane protein LACE1 exists as a part of three complexes of approximately 140, 400 and 500 kDa. The native molecular mass of approximately 140 kDa observed with dodecyl maltoside-treated mitochondria rather suggested a homodimeric complex or low-molecular-mass heteromeric LACE1 complex. However, using digitonin for protein solubilization instead of dodecyl maltoside, two high-molecular-mass LACE1 complexes of approximately 500 and 400 kDa were detected using two dimensional immunoblots in both mitochondrial and purified protein samples. It is likely that the higher delipidating properties of dodecylmaltoside, comparedwith digitonin, may have affected the stability of high-molecular-mass LACE1 complexes. Indeed, both of the observed high-molecular-mass complexes might contain the expected homohexameric LACE1 ATPase complex. The slightly higher apparent molecular mass of these complexes than expected for the pure LACE1 homohexamer, could stem from bound membrane lipids

and/or interacting proteins (D'Aurelio, Gajewski et al. 2006, Stiburek, Cesnekova et al. 2012, Crichton, Harding et al. 2013).

The ectopic expression of the K142A LACE1 mutant shows the essential character of the Walker A motif for LACE1's involvement in degradation of excess nuclear-encoded complex IV subunits. Indeed, the essential lysine residue of Walker A motif is known to support binding of nucleotides. The role of the flanking threonine residue is much less understood (Nagy, Wu et al. 2009). Owing to failure of both T143V LACE1 mutants to accumulate in mitochondria, we were not able to assess their effects on clearance of excess nuclear-encoded complex IV subunits. However, a significantly increased amount of the unprocessed protein form found in all LACE1 Walker A motif variants suggests that ATP binding may be required for efficient mitochondrial import/processing of LACE1 protein. Despite high intramitochondrial protein levels, the Glu214Gln Walker B mutant also failed to rescue the increased accumulation of nuclearencoded complex IV subunits in the LACE1 RNAi background. The conserved glutamate residue of theWalker B motif is required for ATP hydrolysis (Hanson and Whiteheart 2005). Thus ATP binding and hydrolysis appear to be essential for LACE1-mediated degradation of nuclearencoded complex IV subunits.

LACE1 protein is essential for maintenance of fused mitochondrial reticulum and lamellar cristae morphology just like YME1L KD HEK293 cell line. Generally, the change of lamellar cristae morphology were observed in all cell lines with knockdown of mitochondrial proteases so far e.g. AFG3L2 KD, CLPX KD, CLPP KD, YME1L and LACE1 in HEK293. Moreover, YME1L was elevated in the LACE1 KD cell line and using method of co-immunoprecipitation, we confirmed directly interation between LACE1 protein and YME1L protease. The balanced accumulation of L-OPA1 and S-OPA1 protein regulates mitochondrial dynamics and ultrastructure (Frezza, Cipolat et al. 2006, Anand, Langer et al. 2013). The S-OPA1 forms, which induce mitochondrial fission directly, are proteolytically generated from OPA1 isoforms by the action of YME1L and OMA1 proteases (Stiburek, Cesnekova et al. 2012, Anand, Wai et al. 2014). Thus, the increased amount of short OPA1 forms accompanied by increased YME1L protease levels could explain the fragmented mitochondrial reticulum of LACE1-KD cells. In addition to the control of mitochondrial dynamics, OPA1 was found to affect mitochondrial cristae remodelling, independently of its profusion activity (Frezza, Cipolat et al. 2006). Thus the imbalanced accumulation of OPA1 protein forms could also explain the aberrant mitochondrial ultrastructure of LACE1-KD cells.

We demonstrate that LACE1, similarly as its yeast ortholog, mediates degradation of nuclear-encoded complex IV subunits COX4, COX5A and COX6A, and moreover using affinity purification we revealed direct interation with COX4 and COX5a. LACE1 protein is required for normal activity of complexes III and IV of OXPHOS. We demonstrate by ectopic expression of both Lys142Ala Walker A and Glu214Gln Walker B mutants that an intact ATPase domain is essential for LACE-mediated degradation of nuclear-encoded complex IV subunits. Yeast Afg1 was shown to facilitate degradation of mitochondrially encoded complex IV subunits COX1, COX2 and COX3, and a yeast Afg1 deletion strain showed respiratory growth impairment and diminished activities of respiratory complexes III and IV (Khalimonchuk, Bird et al. 2007). The fact that nuclear-encoded complex IV subunits COX4, COX5A and COX6A were markedly elevated in LACE1-KD cells, but the mitochondrially encoded subunits were completely unaffected, suggests changes in substrate specificity of LACE1 throughout evolution. A similar, but more profound, shift in substrate specificity between yeast and mammalian orthologues concerning complex IV subunits was found for the inner membrane translocase OXA1L (Stiburek, Fornuskova et al. 2007). LACE1 is shown to interact physically with COX4 and COX5A subunits of complex IV and with the inner membrane protease YME1L. In addition, loss of LACE1 is associated with marked up-regulation of YME1L. Indeed, COX4 subunit is one of the previously identified proteolytic substrates of YME1L protease. This fact provides a further functional link between LACE1 and YME1L (Stiburek, Cesnekova et al. 2012). On the other hand, the matrix-localized LON protease, which was reported to degrade COX4 and COX5A, exhibited a marked reduction in LACE1-KD cells (Lee and Suzuki 2008). In contrast with increased YME1L that could stem from a simple compensatory response to LACE1 deficiency, the observed downregulation of LON is more difficult to explain. On the basis of its structure–function characteristics, yeast Afg1 was suggested to resemble cytosolic Cdc48 (VCP/p97) (Khalimonchuk, Bird et al. 2007).

The reduced enzyme activity of complex IV found in LACE1- KD cells can be explained by accumulation of excess and/or damaged nuclear-encoded subunits COX4, COX5A and COX6A that is likely to lead to perturbation of the assembly process and/or enzyme function. Hence normal or even mildly increased amounts of complex III and IV holoenzymes were found to be associated with loss ofLACE1. Similarly, KD of YME1L protease in HEK293 cells that led to accumulation of excess complex I subunit NDUFB6 was associated with markedly reduced complex I activity, yet normal holoenzyme levels (Stiburek, Cesnekova et

al. 2012). On the other hand, the diminished activity of complex III in LACE1-KD cells remains to be clarified as both Core 1 and Core 2 subunits of complex III were found to be unaffected in these cells. Moreover, the yeast Afg1 deletion strain had diminished activity of complex III, but normal levels of the mitochondrially encoded subunit cytochrome *b* (Khalimonchuk, Bird et al. 2007). Thus possibly some of the remaining nuclear-encoded complex III subunit(s) may be affected by LACE1/Afg1 deficiency. The markedly increased activity of complex II is frequently encountered in systems with respiratory chain deficiency where it is thought to serve as a compensatory mechanism for maintaining optimal electron flow through the chain (DeHaan, Habibi-Nazhad et al. 2004, Claus, Schonefeld et al. 2013).

Amongst the most obvious features of LACE1 KD cells is the increased resistance to apoptosis and diminished activity of the mitochondrial respiratory chain. Since overexpression of LACE1 in both LACE1 KD cells as well as wild-type HEK293 cells led not only to suppression of the apoptotic defect but to major apoptotic phenotype point to significant pro-apoptotic character of human LACE1. Importantly, the LACE1 mediated apoptosis is shown to depend on p53 in normal human dermal fibroblasts. Furthermore, although increasingly resistant to intrinsic apoptosis, the LACE1 KD cells are fully susceptible to TNFalpha-induced cell death. The mitochondrial rhomboid protease PARL functions anti-apoptotic in mammalian cells by controlling cristae remodeling and cytochrome c release (Cipolat, Rudka et al. 2006). Hence, the markedly increased levels of PARL in LACE1 KD cells are consistent with their increased apoptotic resistance. Conversely, the intermembrane space serine protease Omi/HTRA2 shows significant pro apoptotic activity, mainly through degradation of IAP (inhibitors of apoptosis) proteins (Hegde, Srinivasula et al. 2002). Thus, the downregulation of Omi/HTRA2 along with concomitant upregulation of PARL is also consistent with the increased apoptotic resistance of LACE1 deficient cells.

The tumor suppressor protein p53 is activated upon various stress stimuli to either support cell survival or promote apoptosis. Besides its well established nuclear, transcription-dependent function, p53 was shown to act also extranuclearly. Indeed, in response to acute cellular stress or even acute exercise, p53 can rapidly translocate into mitochondria and activate here apoptosis via fast, transcription-independent manner. Several lines of experimental evidence support the direct involvement of LACE1 in mitochondrial partition of p53 protein. First, overexpression of LACE1 leads to dramatic increase in mitochondria-associated p53 and to concomitant reduction in nuclear p53 content accompanied by reduced expression of p53 transcription target genes BAX and PUMA. Second, the DNA damage agent mitomycin c

fails to induce mitochondrial translocation and concomitant nuclear reduction of p53 in LACE1 knockdown cells. Finally, LACE1-FLAG protein expressed in LACE1 knockdown cells physically interacts with p53. The role of LACE1 in mitochondrial partition of p53 is consistent with both the significant pro-apoptotic character of LACE1 protein and with the previously reported tumor-suppressor properties of LACE1 gene region (Karube, Nakagawa et al. 2011). The unaffected levels of SCO2 in LACE1 overexpressing cells further confirm the extranuclear, transcription-independent character of LACE1-induced p53 upregulation. Besides its function in complex IV assembly, the SCO2 metallochaperone was identified as a p53 transcription target gene required for shift of cellular metabolism from glycolysis to increased OXPHOS utilization (Bensaad, Tsuruta et al. 2006, Matoba, Kang et al. 2006, Madan, Gogna et al. 2013). On the other hand, positive genetic interaction between the mitochondrial metallopeptidase OMA1 and p53 was observed in OVCA cells, which is consistent with LACE1-induced OMA1 upregulation seen in our HEK293 knockdown model (Kong, Wang et al. 2014). Besides its specific role in mitochondrial homeostasis and apoptosis, the subcellular partitioning of p53 into mitochondria has the potential to substantially affect its nuclear activity (Zhuang, Wang et al. 2013). Indeed, the pattern of nuclear distribution of p53 protein is substantially affected in LACE1 KD cells. On the other hand, expression of p53 transcription target genes BAX and PUMA was found significantly diminished in LACE1 overexpressing cells. Several mechanisms have been proposed to drive the mitochondrial translocation of p53 (Ahn, Trinh et al. 2010, Trinh, Elwi et al. 2010, Zhuang, Wang et al. 2013). Similarly to our report, one of them utilizing the mitochondrial disulfide relay protein CHCHD4 was shown to be connected to mitochondrial respiratory capacity (Zhuang, Wang et al. 2013) . The yeast homologue of human LACE1 (Afg1) was shown to be required for normal activity of respiratory complexes III and IV (Khalimonchuk, Bird et al. 2007). Similar to the yeast Afg1 deletion strain, the rather moderate respiratory defect of human LACE1 KD cells suggests possible redundant character of LACE1 role in respiratory chain maintenance. Given that ATP- or ADP-binding state may change biochemical property of LACE1, it is interesting to speculate that LACE1-p53 interaction could serve as an immediate apoptotic response to altered mitochondrial ATP levels. Further work is required to address the effects of LACE1-mediated subcellular p53 partitioning towards cell metabolism and proliferation.

Collectively, our results establish a crucial role for LACE1 in mitochondrial protein homeostasis and identify a possible novel accessory protein of the IMM i-AAA complex.

Future studies will be focused on the identification of additional interacting partners of LACE1 protein.

6. REFERENCES

Abrahams, B. S., G. M. Mak, M. L. Berry, D. L. Palmquist, J. R. Saionz, A. Tay, Y. H. Tan, S. Brenner, E. M. Simpson and B. Venkatesh (2002). "Novel vertebrate genes and putative regulatory elements identified at kidney disease and NR2E1/fierce loci." Genomics **80**(1): 45-53.

Ahn, B. Y., D. L. Trinh, L. D. Zajchowski, B. Lee, A. N. Elwi and S. W. Kim (2010). "Tid1 is a new regulator of p53 mitochondrial translocation and apoptosis in cancer." Oncogene **29**(8): 1155-1166.

Alberts, B., Johnson, A., Lewis, J., Raff, M., Roberts, K., Walter, P. (2002). Molecular Biology of the Cell. 4th Edition., New York: Garland Science; 2002.

Alikhani, N., A. K. Berglund, T. Engmann, E. Spanning, F. N. Vogtle, P. Pavlov, C. Meisinger, T. Langer and E. Glaser (2011). "Targeting capacity and conservation of PreP homologues localization in mitochondria of different species." J Mol Biol **410**(3): 400-410.

Almontashiri, N. A., H. H. Chen, R. J. Mailloux, T. Tatsuta, A. C. Teng, A. B. Mahmoud, T. Ho, N. A. Stewart, P. Rippstein, M. E. Harper, R. Roberts, C. Willenborg, J. Erdmann, C. A. Consortium, A. Pastore, H. M. McBride, T. Langer and A. F. Stewart (2014). "SPG7 variant escapes phosphorylation-regulated processing by AFG3L2, elevates mitochondrial ROS, and is associated with multiple clinical phenotypes." Cell Rep **7**(3): 834-847.

Anand, R., T. Langer and M. J. Baker (2013). "Proteolytic control of mitochondrial function and morphogenesis." Biochim Biophys Acta **1833**(1): 195-204.

Anand, R., T. Wai, M. J. Baker, N. Kladt, A. C. Schauss, E. Rugarli and T. Langer (2014). "The i-AAA protease YME1L and OMA1 cleave OPA1 to balance mitochondrial fusion and fission." J Cell Biol **204**(6): 919-929.

Anderson, S., A. T. Bankier, B. G. Barrell, M. H. de Bruijn, A. R. Coulson, J. Drouin, I. C. Eperon, D. P. Nierlich, B. A. Roe, F. Sanger, P. H. Schreier, A. J. Smith, R. Staden and I. G. Young (1981). "Sequence and organization of the human mitochondrial genome." Nature **290**(5806): 457-465.

Andrews, R. M., I. Kubacka, P. F. Chinnery, R. N. Lightowlers, D. M. Turnbull and N. Howell (1999). "Reanalysis and revision of the Cambridge reference sequence for human mitochondrial DNA." Nat Genet **23**(2): 147.

Arlt, H., R. Tauer, H. Feldmann, W. Neupert and T. Langer (1996). "The YTA10-12 complex, an AAA protease with chaperone-like activity in the inner membrane of mitochondria." Cell **85**(6): 875-885.

Arnold, I., M. Wagner-Ecker, W. Ansorge and T. Langer (2006). "Evidence for a novel mitochondria-to-nucleus signalling pathway in respiring cells lacking i-AAA protease and the ABC-transporter Mdl1." Gene **367**: 74-88.

Atorino, L., L. Silvestri, M. Koppen, L. Cassina, A. Ballabio, R. Marconi, T. Langer and G. Casari (2003). "Loss of m-AAA protease in mitochondria causes complex I deficiency and increased sensitivity to oxidative stress in hereditary spastic paraplegia." J Cell Biol **163**(4): 777-787.

Augustin, S., F. Gerdes, S. Lee, F. T. Tsai, T. Langer and T. Tatsuta (2009). "An intersubunit signaling network coordinates ATP hydrolysis by m-AAA proteases." Mol Cell **35**(5): 574-585.

Azzu, V. and M. D. Brand (2010). "Degradation of an intramitochondrial protein by the cytosolic proteasome." J Cell Sci **123**(Pt 4): 578-585.

Baek, K. T., A. Grundling, R. G. Mogensen, L. Thogersen, A. Petersen, W. Paulander and D. Frees (2014). "beta-Lactam resistance in methicillin-resistant Staphylococcus aureus USA300 is increased by inactivation of the ClpXP protease." Antimicrob Agents Chemother **58**(8): 4593-4603.

Bachmair, A., D. Finley and A. Varshavsky (1986). "In vivo half-life of a protein is a function of its amino-terminal residue." Science **234**(4773): 179-186.

Baker, M. J., P. A. Lampe, D. Stojanovski, A. Korwitz, R. Anand, T. Tatsuta and T. Langer (2014). "Stress-induced OMA1 activation and autocatalytic turnover regulate OPA1-dependent mitochondrial dynamics." EMBO J **33**(6): 578-593.

Baker, M. J., V. P. Mooga, B. Guiard, T. Langer, M. T. Ryan and D. Stojanovski (2012). "Impaired folding of the mitochondrial small TIM chaperones induces clearance by the i-AAA protease." J Mol Biol **424**(5): 227-239.

Baker, T. A. and R. T. Sauer (2012). "ClpXP, an ATP-powered unfolding and protein-degradation machine." Biochim Biophys Acta **1823**(1): 15-28.

Bang, A. G. and C. Kintner (2000). "Rhomboid and Star facilitate presentation and processing of the Drosophila TGF-alpha homolog Spitz." Genes Dev **14**(2): 177-186.

Barkow, S. R., I. Levchenko, T. A. Baker and R. T. Sauer (2009). "Polypeptide translocation by the AAA+ ClpXP protease machine." Chem Biol **16**(6): 605-612.

Barrett, A., Rawlings, N., Woessner, J. (2012). Handbook of Proteolytic Enzymes

3rd Edition, Academic Press.

Becker, L., M. Bannwarth, C. Meisinger, K. Hill, K. Model, T. Krimmer, R. Casadio, K. N. Truscott, G. E. Schulz, N. Pfanner and R. Wagner (2005). "Preprotein translocase of the outer mitochondrial membrane: reconstituted Tom40 forms a characteristic TOM pore." J Mol Biol **353**(5): 1011-1020.

Behrens, M., G. Michaelis and E. Pratje (1991). "Mitochondrial inner membrane protease 1 of Saccharomyces cerevisiae shows sequence similarity to the Escherichia coli leader peptidase." Mol Gen Genet **228**(1-2): 167-176.

Benard, G., B. Faustin, E. Passerieux, A. Galinier, C. Rocher, N. Bellance, J. P. Delage, L. Casteilla, T. Letellier and R. Rossignol (2006). "Physiological diversity of mitochondrial oxidative phosphorylation." Am J Physiol Cell Physiol **291**(6): C1172-1182.

Bensaad, K., A. Tsuruta, M. A. Selak, M. N. Vidal, K. Nakano, R. Bartrons, E. Gottlieb and K. H. Vousden (2006). "TIGAR, a p53-inducible regulator of glycolysis and apoptosis." Cell **126**(1): 107-120.

Berman, S. B., F. J. Pineda and J. M. Hardwick (2008). "Mitochondrial fission and fusion dynamics: the long and short of it." Cell Death Differ **15**(7): 1147-1152.

Bernhard, W. and C. Rouiller (1956). "Close topographical relationship between mitochondria and ergastoplasm of liver cells in a definite phase of cellular activity." J Biophys Biochem Cytol **2**(4 Suppl): 73-78.

Bernstein, S. H., S. Venkatesh, M. Li, J. Lee, B. Lu, S. P. Hilchey, K. M. Morse, H. M. Metcalfe, J. Skalska, M. Andreeff, P. S. Brookes and C. K. Suzuki (2012). "The mitochondrial ATP-dependent Lon protease: a novel target in lymphoma death mediated by the synthetic triterpenoid CDDO and its derivatives." Blood **119**(14): 3321-3329.

Bewley, M. C., V. Graziano, K. Griffin and J. M. Flanagan (2009). "Turned on for degradation: ATPase-independent degradation by ClpP." J Struct Biol **165**(2): 118-125.

Bohovych, I., G. Donaldson, S. Christianson, N. Zahayko and O. Khalimonchuk (2014). "Stress-triggered activation of the metalloprotease Oma1 involves its C-terminal region and is important for mitochondrial stress protection in yeast." J Biol Chem **289**(19): 13259-13272.

Bonn, F., K. Pantakani, M. Shoukier, T. Langer and A. U. Mannan (2010). "Functional evaluation of paraplegin mutations by a yeast complementation assay." Hum Mutat **31**(5): 617-621.

Bose, A. and M. F. Beal (2016). "Mitochondrial dysfunction in Parkinson's disease." J Neurochem **139 Suppl 1**: 216-231.

Bota, D. A. and K. J. Davies (2002). "Lon protease preferentially degrades oxidized mitochondrial aconitase by an ATP-stimulated mechanism." Nat Cell Biol **4**(9): 674-680.

Botelho, S. C., M. Osterberg, A. S. Reichert, K. Yamano, P. Bjorkholm, T. Endo, G. von Heijne and H. Kim (2011). "TIM23-mediated insertion of transmembrane alpha-helices into the mitochondrial inner membrane." EMBO J **30**(6): 1003-1011.

Branda, S. S., P. Cavadini, J. Adamec, F. Kalousek, F. Taroni and G. Isaya (1999). "Yeast and human frataxin are processed to mature form in two sequential steps by the mitochondrial processing peptidase." J Biol Chem **274**(32): 22763-22769.

Branda, S. S., Z. Y. Yang, A. Chew and G. Isaya (1999). "Mitochondrial intermediate peptidase and the yeast frataxin homolog together maintain mitochondrial iron homeostasis in Saccharomyces cerevisiae." Hum Mol Genet **8**(6): 1099-1110.

Braso-Maristany, F., S. Filosto, S. Catchpole, R. Marlow, J. Quist, E. Francesch-Domenech, D. A. Plumb, L. Zakka, P. Gazinska, G. Liccardi, P. Meier, A. Gris-Oliver, M. C. Cheang, A. Perdrix-Rosell, M. Shafat, E. Noel, N. Patel, K. McEachern, M. Scaltriti, P. Castel, F. Noor, R. Buus, S. Mathew, J. Watkins, V. Serra, P. Marra, A. Grigoriadis and A. N. Tutt (2016). "PIM1 kinase regulates cell death, tumor growth and chemotherapy response in triple-negative breast cancer." Nat Med **22**(11): 1303-1313.

Bratic, I., J. Hench, J. Henriksson, A. Antebi, T. R. Burglin and A. Trifunovic (2009). "Mitochondrial DNA level, but not active replicase, is essential for Caenorhabditis elegans development." Nucleic Acids Res **37**(6): 1817-1828.

Bredel, M., D. M. Scholtens, G. R. Harsh, C. Bredel, J. P. Chandler, J. J. Renfrow, A. K. Yadav, H. Vogel, A. C. Scheck, R. Tibshirani and B. I. Sikic (2009). "A network model of a cooperative genetic landscape in brain tumors." JAMA **302**(3): 261-275.

Buchler, M., U. Tisljar and D. H. Wolf (1994). "Proteinase yscD (oligopeptidase yscD). Structure, function and relationship of the yeast enzyme with mammalian thimet oligopeptidase (metalloendopeptidase, EP 24.15)." Eur J Biochem **219**(1-2): 627-639.

Burri, L. and P. J. Keeling (2007). "Protein targeting in parasites with cryptic mitochondria." Int J Parasitol **37**(3-4): 265-272.

Burri, L., Y. Strahm, C. J. Hawkins, I. E. Gentle, M. A. Puryer, A. Verhagen, B. Callus, D. Vaux and T. Lithgow (2005). "Mature DIABLO/Smac is produced by the IMP protease complex on the mitochondrial inner membrane." Mol Biol Cell **16**(6): 2926-2933.

Campo, M. L., P. M. Peixoto and S. Martinez-Caballero (2017). "Revisiting trends on mitochondrial mega-channels for the import of proteins and nucleic acids." J Bioenerg Biomembr **49**(1): 75-99.

Canfield, D. E., E. Kristensen and B. Thamdrup (2005). "Aquatic geomicrobiology." Adv Mar Biol **48**: 1-599.

Carlson, E. J., D. Pitonzo and W. R. Skach (2006). "p97 functions as an auxiliary factor to facilitate TM domain extraction during CFTR ER-associated degradation." EMBO J **25**(19): 4557-4566.

Cipolat, S., T. Rudka, D. Hartmann, V. Costa, L. Serneels, K. Craessaerts, K. Metzger, C. Frezza, W. Annaert, L. D'Adamio, C. Derks, T. Dejaegere, L. Pellegrini, R. D'Hooge, L.

Scorrano and B. De Strooper (2006). "Mitochondrial rhomboid PARL regulates cytochrome c release during apoptosis via OPA1-dependent cristae remodeling." Cell **126**(1): 163-175.

Civitarese, A. E., P. S. MacLean, S. Carling, L. Kerr-Bayles, R. P. McMillan, A. Pierce, T. C. Becker, C. Moro, J. Finlayson, N. Lefort, C. B. Newgard, L. Mandarino, W. Cefalu, K. Walder, G. R. Collier, M. W. Hulver, S. R. Smith and E. Ravussin (2010). "Regulation of skeletal muscle oxidative capacity and insulin signaling by the mitochondrial rhomboid protease PARL." Cell Metab **11**(5): 412-426.

Clark, I. E., M. W. Dodson, C. Jiang, J. H. Cao, J. R. Huh, J. H. Seol, S. J. Yoo, B. A. Hay and M. Guo (2006). "Drosophila pink1 is required for mitochondrial function and interacts genetically with parkin." Nature **441**(7097): 1162-1166.

Claus, C., K. Schonefeld, D. Hubner, S. Chey, U. Reibetanz and U. G. Liebert (2013). "Activity increase in respiratory chain complexes by rubella virus with marginal induction of oxidative stress." J Virol **87**(15): 8481-8492.

Clausen, T., C. Southan and M. Ehrmann (2002). "The HtrA family of proteases: implications for protein composition and cell fate." Mol Cell **10**(3): 443-455.

Cleland, W. W., P. A. Frey and J. A. Gerlt (1998). "The low barrier hydrogen bond in enzymatic catalysis." J Biol Chem **273**(40): 25529-25532.

Clemmer, K. M., G. M. Sturgill, A. Veenstra and P. N. Rather (2006). "Functional characterization of Escherichia coli GlpG and additional rhomboid proteins using an aarA mutant of Providencia stuartii." J Bacteriol **188**(9): 3415-3419.

Coppola, M., A. Pizzigoni, S. Banfi, M. T. Bassi, G. Casari and B. Incerti (2000). "Identification and characterization of YME1L1, a novel paraplegin-related gene." Genomics **66**(1): 48-54.

Crichton, P. G., M. Harding, J. J. Ruprecht, Y. Lee and E. R. Kunji (2013). "Lipid, detergent, and Coomassie Blue G-250 affect the migration of small membrane proteins in blue native gels: mitochondrial carriers migrate as monomers not dimers." J Biol Chem **288**(30): 22163-22173.

Cruz-Torres, V., M. Vazquez-Acevedo, R. Garcia-Villegas, X. Perez-Martinez, G. Mendoza-Hernandez and D. Gonzalez-Halphen (2012). "The cytosol-synthesized subunit II (Cox2) precursor with the point mutation W56R is correctly processed in yeast mitochondria to rescue cytochrome oxidase." Biochim Biophys Acta **1817**(12): 2128-2139.

Csordas, G., C. Renken, P. Varnai, L. Walter, D. Weaver, K. F. Buttle, T. Balla, C. A. Mannella and G. Hajnoczky (2006). "Structural and functional features and significance of the physical linkage between ER and mitochondria." J Cell Biol **174**(7): 915-921.

D'Aurelio, M., C. D. Gajewski, G. Lenaz and G. Manfredi (2006). "Respiratory chain supercomplexes set the threshold for respiration defects in human mtDNA mutant cybrids." Hum Mol Genet **15**(13): 2157-2169.

Dalbey, R. E. (1991). "Leader peptidase." Mol Microbiol **5**(12): 2855-2860.

Daoud, H., P. N. Valdmanis, F. Gros-Louis, V. Belzil, D. Spiegelman, E. Henrion, O. Diallo, A. Desjarlais, J. Gauthier, W. Camu, P. A. Dion and G. A. Rouleau (2011). "Resequencing of 29 candidate genes in patients with familial and sporadic amyotrophic lateral sclerosis." Arch Neurol **68**(5): 587-593.

Daum, G., S. M. Gasser and G. Schatz (1982). "Import of proteins into mitochondria. Energy-dependent, two-step processing of the intermembrane space enzyme cytochrome b2 by isolated yeast mitochondria." J Biol Chem **257**(21): 13075-13080.

de Sagarra, M. R., I. Mayo, S. Marco, S. Rodriguez-Vilarino, J. Oliva, J. L. Carrascosa and J. G. Casta n (1999). "Mitochondrial localization and oligomeric structure of HClpP, the human homologue of E. coli ClpP." J Mol Biol **292**(4): 819-825.

de Vrije, T., R. L. de Swart, W. Dowhan, J. Tommassen and B. de Kruijff (1988). "Phosphatidylglycerol is involved in protein translocation across Escherichia coli inner membranes." Nature **334**(6178): 173-175.

Dean, M., R. Allikmets, B. Gerrard, C. Stewart, A. Kistler, B. Shafer, S. Michaelis and J. Strathern (1994). "Mapping and sequencing of two yeast genes belonging to the ATP-binding cassette superfamily." Yeast **10**(3): 377-383.

DeHaan, C., B. Habibi-Nazhad, E. Yan, N. Salloum, M. Parliament and J. Allalunis-Turner (2004). "Mutation in mitochondrial complex I ND6 subunit is associated with defective response to hypoxia in human glioma cells." Mol Cancer **3**: 19.

Desautels, M. and A. L. Goldberg (1982). "Liver mitochondria contain an ATP-dependent, vanadate-sensitive pathway for the degradation of proteins." Proc Natl Acad Sci U S A **79**(6): 1869-1873.

Desmond, E., C. Brochier-Armanet, P. Forterre and S. Gribaldo (2011). "On the last common ancestor and early evolution of eukaryotes: reconstructing the history of mitochondrial ribosomes." Res Microbiol **162**(1): 53-70.

Deyrup, A. T., S. Krishnan, B. N. Cockburn and N. B. Schwartz (1998). "Deletion and site-directed mutagenesis of the ATP-binding motif (P-loop) in the bifunctional murine ATP-sulfurylase/adenosine 5'-phosphosulfate kinase enzyme." J Biol Chem **273**(16): 9450-9456.

Di Bella, D., F. Lazzaro, A. Brusco, M. Plumari, G. Battaglia, A. Pastore, A. Finardi, C. Cagnoli, F. Tempia, M. Frontali, L. Veneziano, T. Sacco, E. Boda, A. Brussino, F. Bonn, B. Castellotti, S. Baratta, C. Mariotti, C. Gellera, V. Fracasso, S. Magri, T. Langer, P. Plevani, S.

Di Donato, M. Muzi-Falconi and F. Taroni (2010). "Mutations in the mitochondrial protease gene AFG3L2 cause dominant hereditary ataxia SCA28." Nat Genet **42**(4): 313-321.

Dunn, C. D., M. S. Lee, F. A. Spencer and R. E. Jensen (2006). "A genomewide screen for petite-negative yeast strains yields a new subunit of the i-AAA protease complex." Mol Biol Cell **17**(1): 213-226.

Dunn, C. D., Y. Tamura, H. Sesaki and R. E. Jensen (2008). "Mgr3p and Mgr1p are adaptors for the mitochondrial i-AAA protease complex." Mol Biol Cell **19**(12): 5387-5397.

Dvorakova-Hola, K., A. Matuskova, M. Kubala, M. Otyepka, T. Kucera, J. Vecer, P. Herman, N. Parkhomenko, E. Kutejova and J. Janata (2010). "Glycine-rich loop of mitochondrial processing peptidase alpha-subunit is responsible for substrate recognition by a mechanism analogous to mitochondrial receptor Tom20." J Mol Biol **396**(5): 1197-1210.

Edener, U., J. Wollner, U. Hehr, Z. Kohl, S. Schilling, F. Kreuz, P. Bauer, V. Bernard, G. Gillessen-Kaesbach and C. Zuhlke (2010). "Early onset and slow progression of SCA28, a rare dominant ataxia in a large four-generation family with a novel AFG3L2 mutation." Eur J Hum Genet **18**(8): 965-968.

Ehses, S., I. Raschke, G. Mancuso, A. Bernacchia, S. Geimer, D. Tondera, J. C. Martinou, B. Westermann, E. I. Rugarli and T. Langer (2009). "Regulation of OPA1 processing and mitochondrial fusion by m-AAA protease isoenzymes and OMA1." J Cell Biol **187**(7): 1023-1036.

Eldomery, M. K., Z. C. Akdemir, F. N. Vogtle, W. L. Charng, P. Mulica, J. A. Rosenfeld, T. Gambin, S. Gu, L. C. Burrage, A. Al Shamsi, S. Penney, S. N. Jhangiani, H. H. Zimmerman, D. M. Muzny, X. Wang, J. Tang, R. Medikonda, P. V. Ramachandran, L. J. Wong, E. Boerwinkle, R. A. Gibbs, C. M. Eng, S. R. Lalani, J. Hertecant, R. J. Rodenburg, O. A. Abdul-Rahman, Y. Yang, F. Xia, M. C. Wang, J. R. Lupski, C. Meisinger and V. R. Sutton (2016). "MIPEP recessive variants cause a syndrome of left ventricular non-compaction, hypotonia, and infantile death." Genome Med **8**(1): 106.

Ellenrieder, L., L. Opalinski, L. Becker, V. Kruger, O. Mirus, S. P. Straub, K. Ebell, N. Flinner, S. B. Stiller, B. Guiard, C. Meisinger, N. Wiedemann, E. Schleiff, R. Wagner, N. Pfanner and T. Becker (2016). "Separating mitochondrial protein assembly and endoplasmic reticulum tethering by selective coupling of Mdm10." Nat Commun **7**: 13021.

Elliott, L. E., S. A. Saracco and T. D. Fox (2012). "Multiple roles of the Cox20 chaperone in assembly of Saccharomyces cerevisiae cytochrome c oxidase." Genetics **190**(2): 559-567.

Elsasser, S. and D. Finley (2005). "Delivery of ubiquitinated substrates to protein-unfolding machines." Nat Cell Biol **7**(8): 742-749.

Eriksson, A. C., S. Sjoling and E. Glaser (1996). "Characterization of the bifunctional mitochondrial processing peptidase (MPP)/bc1 complex in Spinacia oleracea." J Bioenerg Biomembr **28**(3): 285-292.

Erjavec, N., A. Bayot, M. Gareil, N. Camougrand, T. Nystrom, B. Friguet and A. L. Bulteau (2013). "Deletion of the mitochondrial Pim1/Lon protease in yeast results in accelerated aging and impairment of the proteasome." Free Radic Biol Med **56**: 9-16.

Erzberger, J. P. and J. M. Berger (2006). "Evolutionary relationships and structural mechanisms of AAA+ proteins." Annu Rev Biophys Biomol Struct **35**: 93-114.

Esser, K., E. Pratje and G. Michaelis (1996). "SOM 1, a small new gene required for mitochondrial inner membrane peptidase function in Saccharomyces cerevisiae." Mol Gen Genet **252**(4): 437-445.

Esser, K., B. Tursun, M. Ingenhoven, G. Michaelis and E. Pratje (2002). "A novel two-step mechanism for removal of a mitochondrial signal sequence involves the mAAA complex and the putative rhomboid protease Pcp1." J Mol Biol **323**(5): 835-843.

Falkevall, A., N. Alikhani, S. Bhushan, P. F. Pavlov, K. Busch, K. A. Johnson, T. Eneqvist, L. Tjernberg, M. Ankarcrona and E. Glaser (2006). "Degradation of the amyloid beta-protein by the novel mitochondrial peptidasome, PreP." J Biol Chem **281**(39): 29096-29104.

Fang, D., Y. Wang, Z. Zhang, H. Du, S. Yan, Q. Sun, C. Zhong, L. Wu, J. R. Vangavaragu, S. Yan, G. Hu, L. Guo, M. Rabinowitz, E. Glaser, O. Arancio, A. A. Sosunov, G. M. McKhann, J. X. Chen and S. S. Yan (2015). "Increased neuronal PreP activity reduces Abeta accumulation, attenuates neuroinflammation and improves mitochondrial and synaptic function in Alzheimer disease's mouse model." Hum Mol Genet **24**(18): 5198-5210.

Fearnley, I. M. and J. E. Walker (1986). "Two overlapping genes in bovine mitochondrial DNA encode membrane components of ATP synthase." EMBO J **5**(8): 2003-2008.

Fiumera, H. L., S. A. Broadley and T. D. Fox (2007). "Translocation of mitochondrially synthesized Cox2 domains from the matrix to the intermembrane space." Mol Cell Biol **27**(13): 4664-4673.

Fiumera, H. L., M. J. Dunham, S. A. Saracco, C. A. Butler, J. A. Kelly and T. D. Fox (2009). "Translocation and assembly of mitochondrially coded Saccharomyces cerevisiae cytochrome c oxidase subunit Cox2 by Oxa1 and Yme1 in the absence of Cox18." Genetics **182**(2): 519-528.

Fleig, L., N. Bergbold, P. Sahasrabudhe, B. Geiger, L. Kaltak and M. K. Lemberg (2012). "Ubiquitin-dependent intramembrane rhomboid protease promotes ERAD of membrane proteins." Mol Cell **47**(4): 558-569.

Flynn, J. M., I. Levchenko, R. T. Sauer and T. A. Baker (2004). "Modulating substrate choice: the SspB adaptor delivers a regulator of the extracytoplasmic-stress response to the AAA+ protease ClpXP for degradation." Genes Dev **18**(18): 2292-2301.

Freeman, M. (1994). "The spitz gene is required for photoreceptor determination in the Drosophila eye where it interacts with the EGF receptor." Mech Dev **48**(1): 25-33.

Frezza, C., S. Cipolat, O. Martins de Brito, M. Micaroni, G. V. Beznoussenko, T. Rudka, D. Bartoli, R. S. Polishuck, N. N. Danial, B. De Strooper and L. Scorrano (2006). "OPA1 controls apoptotic cristae remodeling independently from mitochondrial fusion." Cell **126**(1): 177-189.

Fujiki, Y., A. L. Hubbard, S. Fowler and P. B. Lazarow (1982). "Isolation of intracellular membranes by means of sodium carbonate treatment: application to endoplasmic reticulum." J Cell Biol **93**(1): 97-102.

Fukasawa, K. M., T. Hata, Y. Ono and J. Hirose (2011). "Metal preferences of zinc-binding motif on metalloproteases." J Amino Acids **2011**: 574816.

Fukasawa, Y., J. Tsuji, S. C. Fu, K. Tomii, P. Horton and K. Imai (2015). "MitoFates: improved prediction of mitochondrial targeting sequences and their cleavage sites." Mol Cell Proteomics **14**(4): 1113-1126.

Fukuda, R., H. Zhang, J. W. Kim, L. Shimoda, C. V. Dang and G. L. Semenza (2007). "HIF-1 regulates cytochrome oxidase subunits to optimize efficiency of respiration in hypoxic cells." Cell **129**(1): 111-122.

Gabaldon, T. and M. A. Huynen (2003). "Reconstruction of the proto-mitochondrial metabolism." Science **301**(5633): 609.

Gakh, O., P. Cavadini and G. Isaya (2002). "Mitochondrial processing peptidases." Biochim Biophys Acta **1592**(1): 63-77.

Garcia-Alvarez, N., U. Teichert and D. H. Wolf (1987). "Proteinase yscD mutants of yeast. Isolation and characterization." Eur J Biochem **163**(2): 339-346.

Gerdes, F., T. Tatsuta and T. Langer (2012). "Mitochondrial AAA proteases--towards a molecular understanding of membrane-bound proteolytic machines." Biochim Biophys Acta **1823**(1): 49-55.

Gibellini, L., M. Pinti, R. Bartolomeo, S. De Biasi, A. Cormio, C. Musicco, G. Carnevale, S. Pecorini, M. Nasi, A. De Pol and A. Cossarizza (2015). "Inhibition of Lon protease by triterpenoids alters mitochondria and is associated to cell death in human cancer cells." Oncotarget **6**(28): 25466-25483.

Gibellini, L., M. Pinti, F. Beretti, C. L. Pierri, A. Onofrio, M. Riccio, G. Carnevale, S. De Biasi, M. Nasi, F. Torelli, F. Boraldi, A. De Pol and A. Cossarizza (2014). "Sirtuin 3 interacts with Lon protease and regulates its acetylation status." Mitochondrion **18**: 76-81.

Gibellini, L., M. Pinti, F. Boraldi, V. Giorgio, P. Bernardi, R. Bartolomeo, M. Nasi, S. De Biasi, S. Missiroli, G. Carnevale, L. Losi, A. Tesei, P. Pinton, D. Quaglino and A. Cossarizza (2014). "Silencing of mitochondrial Lon protease deeply impairs mitochondrial proteome and function in colon cancer cells." FASEB J **28**(12): 5122-5135.

Giordano, F. (2018). "Non-vesicular lipid trafficking at the endoplasmic reticulum-mitochondria interface." Biochemical Society Transactions **46**: 437-452.

Glynn, S. E., A. Martin, A. R. Nager, T. A. Baker and R. T. Sauer (2009). "Structures of asymmetric ClpX hexamers reveal nucleotide-dependent motions in a AAA+ protein-unfolding machine." Cell **139**(4): 744-756.

Goldring, E. S., L. I. Grossman and J. Marmur (1971). "Petite mutation in yeast. II. Isolation of mutants containing mitochondrial deoxyribonucleic acid of reduced size." J Bacteriol **107**(1): 377-381.

Goo, H. G., H. Rhim and S. Kang (2017). "Pathogenic Role of Serine Protease HtrA2/Omi in Neurodegenerative Diseases." Curr Protein Pept Sci **18**(7): 746-757.

Gottesman, S. (2003). "Proteolysis in bacterial regulatory circuits." Annu Rev Cell Dev Biol **19**: 565-587.

Gottesman, S., E. Roche, Y. Zhou and R. T. Sauer (1998). "The ClpXP and ClpAP proteases degrade proteins with carboxy-terminal peptide tails added by the SsrA-tagging system." Genes Dev **12**(9): 1338-1347.

Graef, M. and T. Langer (2006). "Substrate specific consequences of central pore mutations in the i-AAA protease Yme1 on substrate engagement." J Struct Biol **156**(1): 101-108.

Graef, M., G. Seewald and T. Langer (2007). "Substrate recognition by AAA+ ATPases: distinct substrate binding modes in ATP-dependent protease Yme1 of the mitochondrial intermembrane space." Mol Cell Biol **27**(7): 2476-2485.

Granot, Z., O. Kobiler, N. Melamed-Book, S. Eimerl, A. Bahat, B. Lu, S. Braun, M. R. Maurizi, C. K. Suzuki, A. B. Oppenheim and J. Orly (2007). "Turnover of mitochondrial steroidogenic acute regulatory (StAR) protein by Lon protease: the unexpected effect of proteasome inhibitors." Mol Endocrinol **21**(9): 2164-2177.

Gray, M. W., G. Burger and B. F. Lang (1999). "Mitochondrial evolution." Science **283**(5407): 1476-1481.

Gupta, S., R. Singh, P. Datta, Z. Zhang, C. Orr, Z. Lu, G. Dubois, A. S. Zervos, M. H. Meisler, S. M. Srinivasula, T. Fernandes-Alnemri and E. S. Alnemri (2004). "The C-terminal tail of presenilin regulates Omi/HtrA2 protease activity." J Biol Chem **279**(44): 45844-45854.

Hanson, P. I. and S. W. Whiteheart (2005). "AAA+ proteins: have engine, will work." Nat Rev Mol Cell Biol **6**(7): 519-529.

Harner, M., C. Korner, D. Walther, D. Mokranjac, J. Kaesmacher, U. Welsch, J. Griffith, M. Mann, F. Reggiori and W. Neupert (2011). "The mitochondrial contact site complex, a determinant of mitochondrial architecture." Embo Journal **30**(21): 4356-4370.

Hartl, F. U., N. Pfanner, D. W. Nicholson and W. Neupert (1989). "Mitochondrial protein import." Biochim Biophys Acta **988**(1): 1-45.

Hartmann, B., T. Wai, H. Hu, T. MacVicar, L. Musante, B. Fischer-Zirnsak, W. Stenzel, R. Graf, L. van den Heuvel, H. H. Ropers, T. F. Wienker, C. Hubner, T. Langer and A. M. Kaindl (2016). "Homozygous YME1L1 mutation causes mitochondriopathy with optic atrophy and mitochondrial network fragmentation." Elife **5**.

Haucke, V., C. S. Ocana, A. Honlinger, K. Tokatlidis, N. Pfanner and G. Schatz (1997). "Analysis of the sorting signals directing NADH-cytochrome b5 reductase to two locations within yeast mitochondria." Mol Cell Biol **17**(7): 4024-4032.

Hawlitschek, G., H. Schneider, B. Schmidt, M. Tropschug, F. U. Hartl and W. Neupert (1988). "Mitochondrial protein import: identification of processing peptidase and of PEP, a processing enhancing protein." Cell **53**(5): 795-806.

He, J., H. C. Ford, J. Carroll, C. Douglas, E. Gonzales, S. Ding, I. M. Fearnley and J. E. Walker (2018). "Assembly of the membrane domain of ATP synthase in human mitochondria." Proc Natl Acad Sci U S A **115**(12): 2988-2993.

Head, B., L. Griparic, M. Amiri, S. Gandre-Babbe and A. M. van der Bliek (2009). "Inducible proteolytic inactivation of OPA1 mediated by the OMA1 protease in mammalian cells." J Cell Biol **187**(7): 959-966.

Hegde, R., S. M. Srinivasula, Z. Zhang, R. Wassell, R. Mukattash, L. Cilenti, G. DuBois, Y. Lazebnik, A. S. Zervos, T. Fernandes-Alnemri and E. S. Alnemri (2002). "Identification of Omi/HtrA2 as a mitochondrial apoptotic serine protease that disrupts inhibitor of apoptosis protein-caspase interaction." J Biol Chem **277**(1): 432-438.

Hendrick, J. P., P. E. Hodges and L. E. Rosenberg (1989). "Survey of amino-terminal proteolytic cleavage sites in mitochondrial precursor proteins: leader peptides cleaved by two matrix proteases share a three-amino acid motif." Proc Natl Acad Sci U S A **86**(11): 4056-4060.

Hennon, S. W., R. Soman, L. Zhu and R. E. Dalbey (2015). "YidC/Alb3/Oxa1 Family of Insertases." J Biol Chem **290**(24): 14866-14874.

Herlan, M., C. Bornhovd, K. Hell, W. Neupert and A. S. Reichert (2004). "Alternative topogenesis of Mgm1 and mitochondrial morphology depend on ATP and a functional import motor." J Cell Biol **165**(2): 167-173.

Herlan, M., F. Vogel, C. Bornhovd, W. Neupert and A. S. Reichert (2003). "Processing of Mgm1 by the rhomboid-type protease Pcp1 is required for maintenance of mitochondrial morphology and of mitochondrial DNA." J Biol Chem **278**(30): 27781-27788.

Herrmann, J. M. (2011). "MINOS is plus: a Mitofilin complex for mitochondrial membrane contacts." Dev Cell **21**(4): 599-600.

Herrmann, J. M. and W. Neupert (2000). "Protein transport into mitochondria." Curr Opin Microbiol **3**(2): 210-214.

Herrmann, R. G. (2012). Cell organelles, Springer Science & Business Media.

Honda, T., B. V. Rounds, G. W. Gribble, N. Suh, Y. Wang and M. B. Sporn (1998). "Design and synthesis of 2-cyano-3,12-dioxoolean-1,9-dien-28-oic acid, a novel and highly active inhibitor of nitric oxide production in mouse macrophages." Bioorg Med Chem Lett **8**(19): 2711-2714.

Hoppins, S., S. R. Collins, A. Cassidy-Stone, E. Hummel, R. M. Devay, L. L. Lackner, B. Westermann, M. Schuldiner, J. S. Weissman and J. Nunnari (2011). "A mitochondrial-focused genetic interaction map reveals a scaffold-like complex required for inner membrane organization in mitochondria." J Cell Biol **195**(2): 323-340.

Horibata, Y. and H. Sugimoto (2010). "StarD7 Mediates the Intracellular Trafficking of Phosphatidylcholine to Mitochondria." Journal of Biological Chemistry **285**(10): 7358-7365.

Hornig-Do, H. T., T. Tatsuta, A. Buckermann, M. Bust, G. Kollberg, A. Rotig, M. Hellmich, L. Nijtmans and R. J. Wiesner (2012). "Nonsense mutations in the COX1 subunit impair the stability of respiratory chain complexes rather than their assembly." EMBO J **31**(5): 1293-1307.

Hoskins, J. R., K. Yanagihara, K. Mizuuchi and S. Wickner (2002). "ClpAP and ClpXP degrade proteins with tags located in the interior of the primary sequence." Proc Natl Acad Sci U S A **99**(17): 11037-11042.

Houstek, J., U. Andersson, P. Tvrdik, J. Nedergaard and B. Cannon (1995). "The expression of subunit c correlates with and thus may limit the biosynthesis of the mitochondrial F0F1-ATPase in brown adipose tissue." J Biol Chem **270**(13): 7689-7694.

Houstek, J., P. Tvrdik, S. Pavelka and M. Baudysova (1991). "Low content of mitochondrial ATPase in brown adipose tissue is the result of post-transcriptional regulation." FEBS Lett **294**(3): 191-194.

Howard-Flanders, P., E. Simson and L. Theriot (1964). "A Locus That Controls Filament Formation and Sensitivity to Radiation in Escherichia Coli K-12." Genetics **49**: 237-246.

Chen, X., C. Van Valkenburgh, H. Fang and N. Green (1999). "Signal peptides having standard and nonstandard cleavage sites can be processed by Imp1p of the mitochondrial inner membrane protease." J Biol Chem **274**(53): 37750-37754.

Cheng, C. W., C. Y. Kuo, C. C. Fan, W. C. Fang, S. S. Jiang, Y. K. Lo, T. Y. Wang, M. C. Kao and A. Y. Lee (2013). "Overexpression of Lon contributes to survival and aggressive phenotype of cancer cells through mitochondrial complex I-mediated generation of reactive oxygen species." Cell Death Dis **4**: e681.

Chien, J., M. Campioni, V. Shridhar and A. Baldi (2009). "HtrA serine proteases as potential therapeutic targets in cancer." Curr Cancer Drug Targets **9**(4): 451-468.

Inoue, M., H. Kamada, Y. Abe, K. Higashisaka, K. Nagano, Y. Mukai, Y. Yoshioka, Y. Tsutsumi and S. Tsunoda (2015). "Aminopeptidase P3, a new member of the TNF-TNFR2 signaling complex, induces phosphorylation of JNK1 and JNK2." J Cell Sci **128**(4): 656-669.

Isaya, G., F. Kalousek and L. E. Rosenberg (1992). "Amino-terminal octapeptides function as recognition signals for the mitochondrial intermediate peptidase." J Biol Chem **267**(11): 7904-7910.

Isaya, G., F. Kalousek and L. E. Rosenberg (1992). "Sequence analysis of rat mitochondrial intermediate peptidase: similarity to zinc metallopeptidases and to a putative yeast homologue." Proc Natl Acad Sci U S A **89**(17): 8317-8321.

Isaya, G., W. R. Sakati, R. A. Rollins, G. P. Shen, L. C. Hanson, R. C. Ullrich and C. P. Novotny (1995). "Mammalian mitochondrial intermediate peptidase: structure/function analysis of a new homologue from Schizophyllum commune and relationship to thimet oligopeptidases." Genomics **28**(3): 450-461.

Ishihara, N., Y. Fujita, T. Oka and K. Mihara (2006). "Regulation of mitochondrial morphology through proteolytic cleavage of OPA1." EMBO J **25**(13): 2966-2977.

Ishihara, N. and K. Mihara (2017). "PARL paves the way to apoptosis." Nature Cell Biology **19**: 263.

Jan, P. S., K. Esser, E. Pratje and G. Michaelis (2000). "Som1, a third component of the yeast mitochondrial inner membrane peptidase complex that contains Imp1 and Imp2." Mol Gen Genet **263**(3): 483-491.

Jenkinson, E. M., A. U. Rehman, T. Walsh, J. Clayton-Smith, K. Lee, R. J. Morell, M. C. Drummond, S. N. Khan, M. A. Naeem, B. Rauf, N. Billington, J. M. Schultz, J. E. Urquhart, M. K. Lee, A. Berry, N. A. Hanley, S. Mehta, D. Cilliers, P. E. Clayton, H. Kingston, M. J. Smith, T. T. Warner, G. University of Washington Center for Mendelian, G. C. Black, D. Trump, J. R. Davis, W. Ahmad, S. M. Leal, S. Riazuddin, M. C. King, T. B. Friedman and W. G. Newman (2013). "Perrault syndrome is caused by recessive mutations in CLPP, encoding a mitochondrial ATP-dependent chambered protease." Am J Hum Genet **92**(4): 605-613.

Jiang, X., H. Jiang, Z. Shen and X. Wang (2014). "Activation of mitochondrial protease OMA1 by Bax and Bak promotes cytochrome c release during apoptosis." Proc Natl Acad Sci U S A **111**(41): 14782-14787.

Jin, S. M. and R. J. Youle (2013). "The accumulation of misfolded proteins in the mitochondrial matrix is sensed by PINK1 to induce PARK2/Parkin-mediated mitophagy of polarized mitochondria." Autophagy **9**(11): 1750-1757.

Jones, J. M., P. Datta, S. M. Srinivasula, W. Ji, S. Gupta, Z. Zhang, E. Davies, G. Hajnoczky, T. L. Saunders, M. L. Van Keuren, T. Fernandes-Alnemri, M. H. Meisler and E. S. Alnemri (2003). "Loss of Omi mitochondrial protease activity causes the neuromuscular disorder of mnd2 mutant mice." Nature **425**(6959): 721-727.

Kalousek, F., J. P. Hendrick and L. E. Rosenberg (1988). "Two mitochondrial matrix proteases act sequentially in the processing of mammalian matrix enzymes." Proc Natl Acad Sci U S A **85**(20): 7536-7540.

Kalousek, F., G. Isaya and L. E. Rosenberg (1992). "Rat liver mitochondrial intermediate peptidase (MIP): purification and initial characterization." EMBO J **11**(8): 2803-2809.

Kambacheld, M., S. Augustin, T. Tatsuta, S. Muller and T. Langer (2005). "Role of the novel metallopeptidase Mop112 and saccharolysin for the complete degradation of proteins residing in different subcompartments of mitochondria." J Biol Chem **280**(20): 20132-20139.

Kaneda, H., J. Hayashi, S. Takahama, C. Taya, K. F. Lindahl and H. Yonekawa (1995). "Elimination of paternal mitochondrial DNA in intraspecific crosses during early mouse embryogenesis." Proc Natl Acad Sci U S A **92**(10): 4542-4546.

Kang, S. G., M. N. Dimitrova, J. Ortega, A. Ginsburg and M. R. Maurizi (2005). "Human mitochondrial ClpP is a stable heptamer that assembles into a tetradecamer in the presence of ClpX." J Biol Chem **280**(42): 35424-35432.

Kang, S. G., M. R. Maurizi, M. Thompson, T. Mueser and B. Ahvazi (2004). "Crystallography and mutagenesis point to an essential role for the N-terminus of human mitochondrial ClpP." J Struct Biol **148**(3): 338-352.

Kao, T. Y., Y. C. Chiu, W. C. Fang, C. W. Cheng, C. Y. Kuo, H. F. Juan, S. H. Wu and A. Y. Lee (2015). "Mitochondrial Lon regulates apoptosis through the association with Hsp60-mtHsp70 complex." Cell Death Dis **6**: e1642.

Karata, K., T. Inagawa, A. J. Wilkinson, T. Tatsuta and T. Ogura (1999). "Dissecting the role of a conserved motif (the second region of homology) in the AAA family of ATPases. Site-directed mutagenesis of the ATP-dependent protease FtsH." J Biol Chem **274**(37): 26225-26232.

Karlberg, T., S. van den Berg, M. Hammarstrom, J. Sagemark, I. Johansson, L. Holmberg-Schiavone and H. Schuler (2009). "Crystal structure of the ATPase domain of the human AAA+ protein paraplegin/SPG7." PLoS One **4**(10): e6975.

Karube, K., M. Nakagawa, S. Tsuzuki, I. Takeuchi, K. Honma, Y. Nakashima, N. Shimizu, Y. H. Ko, Y. Morishima, K. Ohshima, S. Nakamura and M. Seto (2011). "Identification of FOXO3 and PRDM1 as tumor-suppressor gene candidates in NK-cell neoplasms by genomic and functional analyses." Blood **118**(12): 3195-3204.

Karzai, A. W., E. D. Roche and R. T. Sauer (2000). "The SsrA-SmpB system for protein tagging, directed degradation and ribosome rescue." Nat Struct Biol **7**(6): 449-455.

Kaser, M., M. Kambacheld, B. Kisters-Woike and T. Langer (2003). "Oma1, a novel membrane-bound metallopeptidase in mitochondria with activities overlapping with the m-AAA protease." J Biol Chem **278**(47): 46414-46423.

Katayama-Fujimura, Y., S. Gottesman and M. R. Maurizi (1987). "A multiple-component, ATP-dependent protease from Escherichia coli." J Biol Chem **262**(10): 4477-4485.

Kereiche, S., L. Kovacik, J. Bednar, V. Pevala, N. Kunova, G. Ondrovicova, J. Bauer, L. Ambro, J. Bellova, E. Kutejova and I. Raska (2016). "The N-terminal domain plays a crucial role in the structure of a full-length human mitochondrial Lon protease." Sci Rep **6**: 33631.

Khalimonchuk, O., A. Bird and D. R. Winge (2007). "Evidence for a pro-oxidant intermediate in the assembly of cytochrome oxidase." J Biol Chem **282**(24): 17442-17449.

Khalimonchuk, O., M. Y. Jeong, T. Watts, E. Ferris and D. R. Winge (2012). "Selective Oma1 protease-mediated proteolysis of Cox1 subunit of cytochrome oxidase in assembly mutants." J Biol Chem **287**(10): 7289-7300.

King, J. V., W. G. Liang, K. P. Scherpelz, A. B. Schilling, S. C. Meredith and W. J. Tang (2014). "Molecular basis of substrate recognition and degradation by human presequence protease." Structure **22**(7): 996-1007.

Kita, K., T. Suzuki and T. Ochi (2012). "Diphenylarsinic acid promotes degradation of glutaminase C by mitochondrial Lon protease." J Biol Chem **287**(22): 18163-18172.

Kitada, S., K. Shimokata, T. Niidome, T. Ogishima and A. Ito (1995). "A putative metal-binding site in the beta subunit of rat mitochondrial processing peptidase is essential for its catalytic activity." J Biochem **117**(6): 1148-1150.

Knight, C. G., P. M. Dando and A. J. Barrett (1995). "Thimet oligopeptidase specificity: evidence of preferential cleavage near the C-terminus and product inhibition from kinetic analysis of peptide hydrolysis." Biochem J **308 (Pt 1)**: 145-150.

Knight, J., N. S. Rochberg, S. F. Saccone, J. I. Nurnberger, Jr., N. G. I. B. D. Consortium and J. P. Rice (2010). "An investigation of candidate regions for association with bipolar disorder." Am J Med Genet B Neuropsychiatr Genet **153B**(7): 1292-1297.

Kobayashi, M., K. Takeda, T. Narita, K. Nagai, N. Okita, Y. Sudo, Y. Miura, H. Tsumoto, Y. Nakagawa, H. Shimano and Y. Higami (2017). "Mitochondrial intermediate peptidase is a novel regulator of sirtuin-3 activation by caloric restriction." FEBS Lett **591**(24): 4067-4073.

Koike, H., H. Seki, Z. Kouchi, M. Ito, T. Kinouchi, S. Tomioka, H. Sorimachi, T. C. Saido, K. Maruyama, K. Suzuki and S. Ishiura (1999). "Thimet oligopeptidase cleaves the full-length

Alzheimer amyloid precursor protein at a beta-secretase cleavage site in COS cells." J Biochem **126**(1): 235-242.

Kolmar, H., P. R. Waller and R. T. Sauer (1996). "The DegP and DegQ periplasmic endoproteases of Escherichia coli: specificity for cleavage sites and substrate conformation." J Bacteriol **178**(20): 5925-5929.

Kong, B., Q. Wang, E. Fung, K. Xue and B. K. Tsang (2014). "p53 is required for cisplatin-induced processing of the mitochondrial fusion protein L-Opa1 that is mediated by the mitochondrial metallopeptidase Oma1 in gynecologic cancers." J Biol Chem **289**(39): 27134-27145.

Konig, T., S. E. Troder, K. Bakka, A. Korwitz, R. Richter-Dennerlein, P. A. Lampe, M. Patron, M. Muhlmeister, S. Guerrero-Castillo, U. Brandt, T. Decker, I. Lauria, A. Paggio, R. Rizzuto, E. I. Rugarli, D. De Stefani and T. Langer (2016). "The m-AAA Protease Associated with Neurodegeneration Limits MCU Activity in Mitochondria." Mol Cell **64**(1): 148-162.

Koonin, E. V. and L. Aravind (2002). "Origin and evolution of eukaryotic apoptosis: the bacterial connection." Cell Death Differ **9**(4): 394-404.

Koppen, M., F. Bonn, S. Ehses and T. Langer (2009). "Autocatalytic processing of m-AAA protease subunits in mitochondria." Mol Biol Cell **20**(19): 4216-4224.

Koppen, M. and T. Langer (2007). "Protein degradation within mitochondria: versatile activities of AAA proteases and other peptidases." Crit Rev Biochem Mol Biol **42**(3): 221-242.

Koppen, M., M. D. Metodiev, G. Casari, E. I. Rugarli and T. Langer (2007). "Variable and tissue-specific subunit composition of mitochondrial m-AAA protease complexes linked to hereditary spastic paraplegia." Mol Cell Biol **27**(2): 758-767.

Korwitz, A., C. Merkwirth, R. Richter-Dennerlein, S. E. Troder, H. G. Sprenger, P. M. Quiros, C. Lopez-Otin, E. I. Rugarli and T. Langer (2016). "Loss of OMA1 delays neurodegeneration by preventing stress-induced OPA1 processing in mitochondria." J Cell Biol **212**(2): 157-166.

Koutnikova, H., V. Campuzano and M. Koenig (1998). "Maturation of wild-type and mutated frataxin by the mitochondrial processing peptidase." Hum Mol Genet **7**(9): 1485-1489.

Kruger, V., T. Becker, L. Becker, M. Montilla-Martinez, L. Ellenrieder, F. N. Vogtle, H. E. Meyer, M. T. Ryan, N. Wiedemann, B. Warscheid, N. Pfanner, R. Wagner and C. Meisinger (2017). "Identification of new channels by systematic analysis of the mitochondrial outer membrane." J Cell Biol **216**(11): 3485-3495.

Kumar, R., V. Kotapalli, A. Naz, S. Gowrishankar, S. Rao, J. R. Pollack and M. D. Bashyam (2018). "XPNPEP3 is a novel transcriptional target of canonical Wnt/beta-catenin signaling." Genes Chromosomes Cancer **57**(6): 304-310.

Kutik, S., D. Stojanovski, L. Becker, T. Becker, M. Meinecke, V. Kruger, C. Prinz, C. Meisinger, B. Guiard, R. Wagner, N. Pfanner and N. Wiedemann (2008). "Dissecting membrane insertion of mitochondrial beta-barrel proteins." Cell **132**(6): 1011-1024.

Lee, D. G., M. K. Kam, K. M. Kim, H. S. Kim, O. S. Kwon, H. S. Lee and D. S. Lee (2018). "Peroxiredoxin 5 prevents iron overload-induced neuronal death by inhibiting mitochondrial fragmentation and endoplasmic reticulum stress in mouse hippocampal HT-22 cells." Int J Biochem Cell Biol **102**: 10-19.

Lee, I. and C. K. Suzuki (2008). "Functional mechanics of the ATP-dependent Lon protease-lessons from endogenous protein and synthetic peptide substrates." Biochim Biophys Acta **1784**(5): 727-735.

Lee, S., S. Augustin, T. Tatsuta, F. Gerdes, T. Langer and F. T. Tsai (2011). "Electron cryomicroscopy structure of a membrane-anchored mitochondrial AAA protease." J Biol Chem **286**(6): 4404-4411.

Lee, Y. J. and R. B. Wickner (1992). "AFG1, a new member of the SEC18-NSF, PAS1, CDC48-VCP, TBP family of ATPases." Yeast **8**(9): 787-790.

Lemberg, M. K. and M. Freeman (2007). "Cutting proteins within lipid bilayers: rhomboid structure and mechanism." Mol Cell **28**(6): 930-940.

Lemberg, M. K., J. Menendez, A. Misik, M. Garcia, C. M. Koth and M. Freeman (2005). "Mechanism of intramembrane proteolysis investigated with purified rhomboid proteases." EMBO J **24**(3): 464-472.

Leonhard, K., A. Stiegler, W. Neupert and T. Langer (1999). "Chaperone-like activity of the AAA domain of the yeast Yme1 AAA protease." Nature **398**(6725): 348-351.

Levytskyy, R. M., E. M. Germany and O. Khalimonchuk (2016). "Mitochondrial Quality Control Proteases in Neuronal Welfare." J Neuroimmune Pharmacol **11**(4): 629-644.

Li, D. H., Y. S. Chung, M. Gloyd, E. Joseph, R. Ghirlando, G. D. Wright, Y. Q. Cheng, M. R. Maurizi, A. Guarne and J. Ortega (2010). "Acyldepsipeptide antibiotics induce the formation of a structured axial channel in ClpP: A model for the ClpX/ClpA-bound state of ClpP." Chem Biol **17**(9): 959-969.

Liu, T., B. Lu, I. Lee, G. Ondrovicova, E. Kutejova and C. K. Suzuki (2004). "DNA and RNA binding by the mitochondrial lon protease is regulated by nucleotide and protein substrate." J Biol Chem **279**(14): 13902-13910.

Liu, Y., L. Lan, K. Huang, R. Wang, C. Xu, Y. Shi, X. Wu, Z. Wu, J. Zhang, L. Chen, L. Wang, X. Yu, H. Zhu and B. Lu (2014). "Inhibition of Lon blocks cell proliferation, enhances chemosensitivity by promoting apoptosis and decreases cellular bioenergetics of bladder cancer: potential roles of Lon as a prognostic marker and therapeutic target in baldder cancer." Oncotarget **5**(22): 11209-11224.

Lo, S. C. and M. Hannink (2008). "PGAM5 tethers a ternary complex containing Keap1 and Nrf2 to mitochondria." Exp Cell Res **314**(8): 1789-1803.

Lodish, H., A. Berk, L. S. Zipursky, P. Matsudaira, D. Baltimore and J. Darnell (2000). Molecular Cell Biology, W. H. Freeman.

Logan, D. C. (2006). "The mitochondrial compartment." J Exp Bot **57**(6): 1225-1243.

Longen, S., M. Bien, K. Bihlmaier, C. Kloeppel, F. Kauff, M. Hammermeister, B. Westermann, J. M. Herrmann and J. Riemer (2009). "Systematic analysis of the twin cx(9)c protein family." J Mol Biol **393**(2): 356-368.

Lopez-Pelegrin, M., N. Cerda-Costa, F. Martinez-Jimenez, A. Cintas-Pedrola, A. Canals, J. R. Peinado, M. A. Marti-Renom, C. Lopez-Otin, J. L. Arolas and F. X. Gomis-Ruth (2013). "A novel family of soluble minimal scaffolds provides structural insight into the catalytic domains of integral membrane metallopeptidases." J Biol Chem **288**(29): 21279-21294.

Lu, B., J. Lee, X. Nie, M. Li, Y. I. Morozov, S. Venkatesh, D. F. Bogenhagen, D. Temiakov and C. K. Suzuki (2013). "Phosphorylation of human TFAM in mitochondria impairs DNA binding and promotes degradation by the AAA+ Lon protease." Mol Cell **49**(1): 121-132.

MacVicar, T. and T. Langer (2016). "OPA1 processing in cell death and disease - the long and short of it." Journal of Cell Science **129**(12): 2297-2306.

Madan, E., R. Gogna, P. Kuppusamy, M. Bhatt, A. A. Mahdi and U. Pati (2013). "SCO2 induces p53-mediated apoptosis by Thr845 phosphorylation of ASK-1 and dissociation of the ASK-1-Trx complex." Mol Cell Biol **33**(7): 1285-1302.

Mannella, C. A. (2006). "Structure and dynamics of the mitochondrial inner membrane cristae." Biochim Biophys Acta **1763**(5-6): 542-548.

Mannella, C. A. (2008). "Structural diversity of mitochondria: functional implications." Ann N Y Acad Sci **1147**: 171-179.

Mannella, C. A., M. Marko and K. Buttle (1997). "Reconsidering mitochondrial structure: new views of an old organelle." Trends Biochem Sci **22**(2): 37-38.

Mannella, C. A., M. Marko, P. Penczek, D. Barnard and J. Frank (1994). "The internal compartmentation of rat-liver mitochondria: tomographic study using the high-voltage transmission electron microscope." Microsc Res Tech **27**(4): 278-283.

Martin, A., T. A. Baker and R. T. Sauer (2008). "Diverse pore loops of the AAA+ ClpX machine mediate unassisted and adaptor-dependent recognition of ssrA-tagged substrates." Mol Cell **29**(4): 441-450.

Martins, L. M., I. Iaccarino, T. Tenev, S. Gschmeissner, N. F. Totty, N. R. Lemoine, J. Savopoulos, C. W. Gray, C. L. Creasy, C. Dingwall and J. Downward (2002). "The serine protease Omi/HtrA2 regulates apoptosis by binding XIAP through a reaper-like motif." J Biol Chem **277**(1): 439-444.

Martins, L. M., A. Morrison, K. Klupsch, V. Fedele, N. Moisoi, P. Teismann, A. Abuin, E. Grau, M. Geppert, G. P. Livi, C. L. Creasy, A. Martin, I. Hargreaves, S. J. Heales, H. Okada, S. Brandner, J. B. Schulz, T. Mak and J. Downward (2004). "Neuroprotective role of the Reaper-related serine protease HtrA2/Omi revealed by targeted deletion in mice." Mol Cell Biol **24**(22): 9848-9862.

Matoba, S., J. G. Kang, W. D. Patino, A. Wragg, M. Boehm, O. Gavrilova, P. J. Hurley, F. Bunz and P. M. Hwang (2006). "p53 regulates mitochondrial respiration." Science **312**(5780): 1650-1653.

Mayer, U. and C. Nusslein-Volhard (1988). "A group of genes required for pattern formation in the ventral ectoderm of the Drosophila embryo." Genes Dev **2**(11): 1496-1511.

McQuibban, G. A., S. Saurya and M. Freeman (2003). "Mitochondrial membrane remodelling regulated by a conserved rhomboid protease." Nature **423**(6939): 537-541.

Meisinger, C., A. Sickmann and N. Pfanner (2008). "The mitochondrial proteome: from inventory to function." Cell **134**(1): 22-24.

Mishra, P., V. Carelli, G. Manfredi and D. C. Chan (2014). "Proteolytic cleavage of Opa1 stimulates mitochondrial inner membrane fusion and couples fusion to oxidative phosphorylation." Cell Metab **19**(4): 630-641.

Mitchell, P. (1970). "Aspects of the chemiosmotic hypothesis." Biochem J **116**(4): 5P-6P.

Mitchell, P. and J. Moyle (1967). "Chemiosmotic hypothesis of oxidative phosphorylation." Nature **213**(5072): 137-139.

Miyata, N., N. Goda, K. Matsuo, T. Hoketsu and O. Kuge (2017). "Cooperative function of Fmp30, Mdm31, and Mdm32 in Ups1-independent cardiolipin accumulation in the yeast Saccharomyces cerevisiae." Sci Rep **7**(1): 16447.

Morais, V. A., D. Haddad, K. Craessaerts, P. J. De Bock, J. Swerts, S. Vilain, L. Aerts, L. Overbergh, A. Grunewald, P. Seibler, C. Klein, K. Gevaert, P. Verstreken and B. De Strooper (2014). "PINK1 loss-of-function mutations affect mitochondrial complex I activity via NdufA10 ubiquinone uncoupling." Science **344**(6180): 203-207.

Morgenstern, M., S. B. Stiller, P. Lubbert, C. D. Peikert, S. Dannenmaier, F. Drepper, U. Weill, P. Hoss, R. Feuerstein, M. Gebert, M. Bohnert, M. van der Laan, M. Schuldiner, C. Schutze, S. Oeljeklaus, N. Pfanner, N. Wiedemann and B. Warscheid (2017). "Definition of a High-Confidence Mitochondrial Proteome at Quantitative Scale." Cell Rep **19**(13): 2836-2852.

Mottis, A., V. Jovaisaite and J. Auwerx (2014). "The mitochondrial unfolded protein response in mammalian physiology." Mamm Genome **25**(9-10): 424-433.

Muffler, A., D. Fischer, S. Altuvia, G. Storz and R. Hengge-Aronis (1996). "The response regulator RssB controls stability of the sigma(S) subunit of RNA polymerase in Escherichia coli." EMBO J **15**(6): 1333-1339.

Mzhavia, N., Y. L. Berman, Y. Qian, L. Yan and L. A. Devi (1999). "Cloning, expression, and characterization of human metalloprotease 1: a novel member of the pitrilysin family of metalloendoproteases." DNA Cell Biol **18**(5): 369-380.

Naamati, A., N. Regev-Rudzki, S. Galperin, R. Lill and O. Pines (2009). "Dual targeting of Nfs1 and discovery of its novel processing enzyme, Icp55." J Biol Chem **284**(44): 30200-30208.

Nagy, M., H. C. Wu, Z. Liu, S. Kedzierska-Mieszkowska and M. Zolkiewski (2009). "Walker-A threonine couples nucleotide occupancy with the chaperone activity of the AAA+ ATPase ClpB." Protein Sci **18**(2): 287-293.

Nakai, T., T. Yasuhara, Y. Fujiki and A. Ohashi (1995). "Multiple genes, including a member of the AAA family, are essential for degradation of unassembled subunit 2 of cytochrome c oxidase in yeast mitochondria." Mol Cell Biol **15**(8): 4441-4452.

Narendra, D. P., S. M. Jin, A. Tanaka, D. F. Suen, C. A. Gautier, J. Shen, M. R. Cookson and R. J. Youle (2010). "PINK1 is selectively stabilized on impaired mitochondria to activate Parkin." PLoS Biol **8**(1): e1000298.

Narkiewicz, J., D. Klasa-Mazurkiewicz, D. Zurawa-Janicka, J. Skorko-Glonek, J. Emerich and B. Lipinska (2008). "Changes in mRNA and protein levels of human HtrA1, HtrA2 and HtrA3 in ovarian cancer." Clin Biochem **41**(7-8): 561-569.

Narkiewicz, J., S. Lapinska-Szumczyk, D. Zurawa-Janicka, J. Skorko-Glonek, J. Emerich and B. Lipinska (2009). "Expression of human HtrA1, HtrA2, HtrA3 and TGF-beta1 genes in primary endometrial cancer." Oncol Rep **21**(6): 1529-1537.

Nass, M. M. and S. Nass (1963). "Intramitochondrial Fibers with DNA Characteristics. I. Fixation and Electron Staining Reactions." J Cell Biol **19**: 593-611.

Nicolay, K., F. D. Laterveer and W. L. van Heerde (1994). "Effects of amphipathic peptides, including presequences, on the functional integrity of rat liver mitochondrial membranes." J Bioenerg Biomembr **26**(3): 327-334.

Nie, X., M. Li, B. Lu, Y. Zhang, L. Lan, L. Chen and J. Lu (2013). "Down-regulating overexpressed human Lon in cervical cancer suppresses cell proliferation and bioenergetics." PLoS One **8**(11): e81084.

Nicholls, D. (2013). Bioenergetics, Academic Press.

Nolden, M., S. Ehses, M. Koppen, A. Bernacchia, E. I. Rugarli and T. Langer (2005). "The m-AAA protease defective in hereditary spastic paraplegia controls ribosome assembly in mitochondria." Cell **123**(2): 277-289.

Nunnari, J., T. D. Fox and P. Walter (1993). "A mitochondrial protease with two catalytic subunits of nonoverlapping specificities." Science **262**(5142): 1997-2004.

Ogunbona, O. B., O. Onguka, E. Calzada and S. M. Claypool (2017). "Multitiered and Cooperative Surveillance of Mitochondrial Phosphatidylserine Decarboxylase 1." Mol Cell Biol **37**(17).

Olivares, A. O., T. A. Baker and R. T. Sauer (2018). "Mechanical Protein Unfolding and Degradation." Annu Rev Physiol **80**: 413-429.

Ondrovicova, G., T. Liu, K. Singh, B. Tian, H. Li, O. Gakh, D. Perecko, J. Janata, Z. Granot, J. Orly, E. Kutejova and C. K. Suzuki (2005). "Cleavage site selection within a folded substrate by the ATP-dependent lon protease." J Biol Chem **280**(26): 25103-25110.

Orlowski, M., C. Michaud and T. G. Chu (1983). "A soluble metalloendopeptidase from rat brain. Purification of the enzyme and determination of specificity with synthetic and natural peptides." Eur J Biochem **135**(1): 81-88.

Osman, C., M. Haag, C. Potting, J. Rodenfels, P. V. Dip, F. T. Wieland, B. Brugger, B. Westermann and T. Langer (2009). "The genetic interactome of prohibitins: coordinated control of cardiolipin and phosphatidylethanolamine by conserved regulators in mitochondria." J Cell Biol **184**(4): 583-596.

Osman, C., C. Wilmes, T. Tatsuta and T. Langer (2007). "Prohibitins interact genetically with Atp23, a novel processing peptidase and chaperone for the F1Fo-ATP synthase." Mol Biol Cell **18**(2): 627-635.

Palade, G. E. (1964). "The Organization of Living Matter." Proc Natl Acad Sci U S A **52**: 613-634.

Pallen, M. J. and B. W. Wren (1997). "The HtrA family of serine proteases." Mol Microbiol **26**(2): 209-221.

Passamonti, M. and F. Ghiselli (2009). "Doubly uniparental inheritance: two mitochondrial genomes, one precious model for organelle DNA inheritance and evolution." DNA Cell Biol **28**(2): 79-89.

Pawson, T. and J. Schlessingert (1993). "SH2 and SH3 domains." Curr Biol **3**(7): 434-442.

Payne, B. A., I. J. Wilson, P. Yu-Wai-Man, J. Coxhead, D. Deehan, R. Horvath, R. W. Taylor, D. C. Samuels, M. Santibanez-Koref and P. F. Chinnery (2013). "Universal heteroplasmy of human mitochondrial DNA." Hum Mol Genet **22**(2): 384-390.

Pellegrini, L., B. J. Passer, M. Canelles, I. Lefterov, J. K. Ganjei, B. J. Fowlkes, E. V. Koonin and L. D'Adamio (2001). "PAMP and PARL, two novel putative metalloproteases interacting with the COOH-terminus of Presenilin-1 and -2." J Alzheimers Dis **3**(2): 181-190.

Pereira, M. G., L. L. Souza, C. Becari, D. A. Duarte, F. R. Camacho, J. A. Oliveira, M. D. Gomes, E. B. Oliveira, M. C. Salgado, N. Garcia-Cairasco and C. M. Costa-Neto (2013). "Angiotensin II-independent angiotensin-(1-7) formation in rat hippocampus: involvement of thimet oligopeptidase." Hypertension **62**(5): 879-885.

Perkins, G., C. Renken, M. E. Martone, S. J. Young, M. Ellisman and T. Frey (1997). "Electron tomography of neuronal mitochondria: three-dimensional structure and organization of cristae and membrane contacts." J Struct Biol **119**(3): 260-272.

Perkins, G. A. and T. G. Frey (2000). "Recent structural insight into mitochondria gained by microscopy." Micron **31**(1): 97-111.

Petek, E., C. Windpassinger, J. B. Vincent, J. Cheung, A. P. Boright, S. W. Scherer, P. M. Kroisel and K. Wagner (2001). "Disruption of a novel gene (IMMP2L) by a breakpoint in 7q31 associated with Tourette syndrome." Am J Hum Genet **68**(4): 848-858.

Pierson, T. M., D. Adams, F. Bonn, P. Martinelli, P. F. Cherukuri, J. K. Teer, N. F. Hansen, P. Cruz, J. C. Mullikin For The Nisc Comparative Sequencing Program, R. W. Blakesley, G. Golas, J. Kwan, A. Sandler, K. Fuentes Fajardo, T. Markello, C. Tifft, C. Blackstone, E. I. Rugarli, T. Langer, W. A. Gahl and C. Toro (2011). "Whole-exome sequencing identifies homozygous AFG3L2 mutations in a spastic ataxia-neuropathy syndrome linked to mitochondrial m-AAA proteases." PLoS Genet **7**(10): e1002325.

Pinti, M., L. Gibellini, Y. Liu, S. Xu, B. Lu and A. Cossarizza (2015). "Mitochondrial Lon protease at the crossroads of oxidative stress, ageing and cancer." Cell Mol Life Sci **72**(24): 4807-4824.

Pinti, M., L. Gibellini, M. Nasi, S. De Biasi, C. A. Bortolotti, A. Iannone and A. Cossarizza (2016). "Emerging role of Lon protease as a master regulator of mitochondrial functions." Biochim Biophys Acta **1857**(8): 1300-1306.

Plun-Favreau, H., K. Klupsch, N. Moisoi, S. Gandhi, S. Kjaer, D. Frith, K. Harvey, E. Deas, R. J. Harvey, N. McDonald, N. W. Wood, L. M. Martins and J. Downward (2007). "The mitochondrial protease HtrA2 is regulated by Parkinson's disease-associated kinase PINK1." Nat Cell Biol **9**(11): 1243-1252.

Potting, C., C. Wilmes, T. Engmann, C. Osman and T. Langer (2010). "Regulation of mitochondrial phospholipids by Ups1/PRELI-like proteins depends on proteolysis and Mdm35." EMBO J **29**(17): 2888-2898.

Pratje, E. and B. Guiard (1986). "One nuclear gene controls the removal of transient pre-sequences from two yeast proteins: one encoded by the nuclear the other by the mitochondrial genome." EMBO J **5**(6): 1313-1317.

Pratje, E., G. Mannhaupt, G. Michaelis and K. Beyreuther (1983). "A nuclear mutation prevents processing of a mitochondrially encoded membrane protein in Saccharomyces cerevisiae." EMBO J **2**(7): 1049-1054.

Quiros, P. M., Y. Espanol, R. Acin-Perez, F. Rodriguez, C. Barcena, K. Watanabe, E. Calvo, M. Loureiro, M. S. Fernandez-Garcia, A. Fueyo, J. Vazquez, J. A. Enriquez and C. Lopez-Otin (2014). "ATP-dependent Lon protease controls tumor bioenergetics by reprogramming mitochondrial activity." Cell Rep **8**(2): 542-556.

Rainbolt, T. K., J. Lebeau, C. Puchades and R. L. Wiseman (2016). "Reciprocal Degradation of YME1L and OMA1 Adapts Mitochondrial Proteolytic Activity during Stress." Cell Rep **14**(9): 2041-2049.

Rainbolt, T. K., J. M. Saunders and R. L. Wiseman (2015). "YME1L degradation reduces mitochondrial proteolytic capacity during oxidative stress." EMBO Rep **16**(1): 97-106.

Rainey, R. N., J. D. Glavin, H. W. Chen, S. W. French, M. A. Teitell and C. M. Koehler (2006). "A new function in translocation for the mitochondrial i-AAA protease Yme1: import of polynucleotide phosphorylase into the intermembrane space." Mol Cell Biol **26**(22): 8488-8497.

Ramelot, T. A., Y. Yang, I. D. Sahu, H. W. Lee, R. Xiao, G. A. Lorigan, G. T. Montelione and M. A. Kennedy (2013). "NMR structure and MD simulations of the AAA protease intermembrane space domain indicates peripheral membrane localization within the hexaoligomer." FEBS Lett **587**(21): 3522-3528.

Rampello, A. J. and S. E. Glynn (2017). "Identification of a Degradation Signal Sequence within Substrates of the Mitochondrial i-AAA Protease." J Mol Biol **429**(6): 873-885.

Rampelt, H. and N. Pfanner (2016). "Coordination of Two Genomes by Mitochondrial Translational Plasticity." Cell **167**(2): 308-310.

Rao, S. T. and M. G. Rossmann (1973). "Comparison of super-secondary structures in proteins." J Mol Biol **76**(2): 241-256.

Redza-Dutordoir, M. and D. A. Averill-Bates (2016). "Activation of apoptosis signalling pathways by reactive oxygen species." Biochim Biophys Acta **1863**(12): 2977-2992.

Roise, D., S. J. Horvath, J. M. Tomich, J. H. Richards and G. Schatz (1986). "A chemically synthesized pre-sequence of an imported mitochondrial protein can form an amphiphilic helix and perturb natural and artificial phospholipid bilayers." EMBO J **5**(6): 1327-1334.

Rotanova, T. V., I. Botos, E. E. Melnikov, F. Rasulova, A. Gustchina, M. R. Maurizi and A. Wlodawer (2006). "Slicing a protease: structural features of the ATP-dependent Lon proteases gleaned from investigations of isolated domains." Protein Sci **15**(8): 1815-1828.

Ruan, Y., H. Li, K. Zhang, F. Jian, J. Tang and Z. Song (2013). "Loss of Yme1L perturbates mitochondrial dynamics." Cell Death Dis **4**: e896.

Russell, R. B., J. Breed and G. J. Barton (1992). "Conservation analysis and structure prediction of the SH2 family of phosphotyrosine binding domains." FEBS Lett **304**(1): 15-20.

Saita, S., H. Nolte, K. U. Fiedler, H. Kashkar, A. S. Venne, R. P. Zahedi, M. Kruger and T. Langer (2017). "PARL mediates Smac proteolytic maturation in mitochondria to promote apoptosis." Nat Cell Biol **19**(4): 318-328.

Saita, S., T. Tatsuta, P. A. Lampe, T. Konig, Y. Ohba and T. Langer (2018). "PARL partitions the lipid transfer protein STARD7 between the cytosol and mitochondria." EMBO J **37**(4).

Sancak, Y., A. L. Markhard, T. Kitami, E. Kovacs-Bogdan, K. J. Kamer, N. D. Udeshi, S. A. Carr, D. Chaudhuri, D. E. Clapham, A. A. Li, S. E. Calvo, O. Goldberger and V. K. Mootha (2013). "EMRE is an essential component of the mitochondrial calcium uniporter complex." Science **342**(6164): 1379-1382.

Sauer, R. T. and T. A. Baker (2011). "AAA+ proteases: ATP-fueled machines of protein destruction." Annu Rev Biochem **80**: 587-612.

Seo, J. H., D. B. Rivadeneira, M. C. Caino, Y. C. Chae, D. W. Speicher, H. Y. Tang, V. Vaira, S. Bosari, A. Palleschi, P. Rampini, A. V. Kossenkov, L. R. Languino and D. C. Altieri (2016). "The Mitochondrial Unfoldase-Peptidase Complex ClpXP Controls Bioenergetics Stress and Metastasis." PLoS Biol **14**(7): e1002507.

Sesaki, H., C. D. Dunn, M. Iijima, K. A. Shepard, M. P. Yaffe, C. E. Machamer and R. E. Jensen (2006). "Ups1p, a conserved intermembrane space protein, regulates mitochondrial shape and alternative topogenesis of Mgm1p." J Cell Biol **173**(5): 651-658.

Shah, Z. H., G. A. Hakkaart, B. Arku, L. de Jong, H. van der Spek, L. A. Grivell and H. T. Jacobs (2000). "The human homologue of the yeast mitochondrial AAA metalloprotease Yme1p complements a yeast yme1 disruptant." FEBS Lett **478**(3): 267-270.

Shi, H., A. J. Rampello and S. E. Glynn (2016). "Engineered AAA+ proteases reveal principles of proteolysis at the mitochondrial inner membrane." Nat Commun **7**: 13301.

Shi, T., F. Wang, E. Stieren and Q. Tong (2005). "SIRT3, a mitochondrial sirtuin deacetylase, regulates mitochondrial function and thermogenesis in brown adipocytes." J Biol Chem **280**(14): 13560-13567.

Shi, X., T. Wu, M. C. C, K. D. N and S. Joseph (2018). "Optimization of ClpXP activity and protein synthesis in an E. coli extract-based cell-free expression system." Sci Rep **8**(1): 3488.

Shimura, H., N. Hattori, S. Kubo, Y. Mizuno, S. Asakawa, S. Minoshima, N. Shimizu, K. Iwai, T. Chiba, K. Tanaka and T. Suzuki (2000). "Familial Parkinson disease gene product, parkin, is a ubiquitin-protein ligase." Nat Genet **25**(3): 302-305.

Schafer, A., M. Zick, J. Kief, M. Steger, H. Heide, S. Duvezin-Caubet, W. Neupert and A. S. Reichert (2010). "Intramembrane proteolysis of Mgm1 by the mitochondrial rhomboid protease is highly promiscuous regarding the sequence of the cleaved hydrophobic segment." J Mol Biol **401**(2): 182-193.

Schagger, H. and G. von Jagow (1991). "Blue native electrophoresis for isolation of membrane protein complexes in enzymatically active form." Anal Biochem **199**(2): 223-231.

Scharfenberg, F., J. Serek-Heuberger, M. Coles, M. D. Hartmann, M. Habeck, J. Martin, A. N. Lupas and V. Alva (2015). "Structure and evolution of N-domains in AAA metalloproteases." J Mol Biol **427**(4): 910-923.

Scherer, M. and G. Schmitz (2011). "Metabolism, function and mass spectrometric analysis of bis(monoacylglycero)phosphate and cardiolipin." Chem Phys Lipids **164**(6): 556-562.

Schirle, M., M. A. Heurtier and B. Kuster (2003). "Profiling core proteomes of human cell lines by one-dimensional PAGE and liquid chromatography-tandem mass spectrometry." Mol Cell Proteomics **2**(12): 1297-1305.

Schneider, A., W. Oppliger and P. Jeno (1994). "Purified inner membrane protease I of yeast mitochondria is a heterodimer." J Biol Chem **269**(12): 8635-8638.

Schneider, H., M. Arretz, E. Wachter and W. Neupert (1990). "Matrix processing peptidase of mitochondria. Structure-function relationships." J Biol Chem **265**(17): 9881-9887.

Schon, E. A., S. DiMauro and M. Hirano (2012). "Human mitochondrial DNA: roles of inherited and somatic mutations." Nat Rev Genet **13**(12): 878-890.

Schreiner, B., H. Westerburg, I. Forne, A. Imhof, W. Neupert and D. Mokranjac (2012). "Role of the AAA protease Yme1 in folding of proteins in the intermembrane space of mitochondria." Mol Biol Cell **23**(22): 4335-4346.

Schulte, U., M. Arretz, H. Schneider, M. Tropschug, E. Wachter, W. Neupert and H. Weiss (1989). "A family of mitochondrial proteins involved in bioenergetICS and biogenesis." Nature **339**(6220): 147-149.

Schwartz, M. and J. Vissing (2002). "Paternal inheritance of mitochondrial DNA." N Engl J Med **347**(8): 576-580.

Sica, V. and G. Kroemer (2018). "Author Correction: IMMP2L: a mitochondrial protease suppressing cellular senescence." Cell Res.

Sica, V. and G. Kroemer (2018). "IMMP2L: a mitochondrial protease suppressing cellular senescence." Cell Res **28**(6): 607-608.

Sickmann, A., J. Reinders, Y. Wagner, C. Joppich, R. Zahedi, H. E. Meyer, B. Schonfisch, I. Perschil, A. Chacinska, B. Guiard, P. Rehling, N. Pfanner and C. Meisinger (2003). "The proteome of Saccharomyces cerevisiae mitochondria." Proc Natl Acad Sci U S A **100**(23): 13207-13212.

Siddiqui, S. M., R. T. Sauer and T. A. Baker (2004). "Role of the processing pore of the ClpX AAA+ ATPase in the recognition and engagement of specific protein substrates." Genes Dev **18**(4): 369-374.

Sicheritz-Ponten, T., C. G. Kurland and S. G. Andersson (1998). "A phylogenetic analysis of the cytochrome b and cytochrome c oxidase I genes supports an origin of mitochondria from within the Rickettsiaceae." Biochim Biophys Acta **1365**(3): 545-551.

Simmen, T. and M. S. Herrera-Cruz (2018). "Plastic mitochondria-endoplasmic reticulum (ER) contacts use chaperones and tethers to mould their structure and signaling." Curr Opin Cell Biol **53**: 61-69.

Singh, R., S. N. Jamdar, V. D. Goyal, A. Kumar, B. Ghosh and R. D. Makde (2017). "Structure of the human aminopeptidase XPNPEP3 and comparison of its in vitro activity with Icp55 orthologs: Insights into diverse cellular processes." J Biol Chem **292**(24): 10035-10047.

Snider, J., G. Thibault and W. A. Houry (2008). "The AAA+ superfamily of functionally diverse proteins." Genome Biol **9**(4): 216.

Song, C., J. Zhao, B. Fu, D. Li, T. Mao, W. Peng, H. Wu and Y. Zhang (2017). "Melatonin-mediated upregulation of Sirt3 attenuates sodium fluoride-induced hepatotoxicity by activating the MT1-PI3K/AKT-PGC-1alpha signaling pathway." Free Radic Biol Med **112**: 616-630.

Song, J., Y. Tamura, T. Yoshihisa and T. Endo (2014). "A novel import route for an N-anchor mitochondrial outer membrane protein aided by the TIM23 complex." EMBO Rep **15**(6): 670-677.

Song, Z., H. Chen, M. Fiket, C. Alexander and D. C. Chan (2007). "OPA1 processing controls mitochondrial fusion and is regulated by mRNA splicing, membrane potential, and Yme1L." J Cell Biol **178**(5): 749-755.

Spiess, C., A. Beil and M. Ehrmann (1999). "A temperature-dependent switch from chaperone to protease in a widely conserved heat shock protein." Cell **97**(3): 339-347.

Spinazzi, M. and B. De Strooper (2016). "PARL: The mitochondrial rhomboid protease." Semin Cell Dev Biol **60**: 19-28.

Stahl, A., P. Moberg, J. Ytterberg, O. Panfilov, H. Brockenhuus Von Lowenhielm, F. Nilsson and E. Glaser (2002). "Isolation and identification of a novel mitochondrial metalloprotease (PreP) that degrades targeting presequences in plants." J Biol Chem **277**(44): 41931-41939.

Stames, E. M. and J. F. O'Toole (2013). "Mitochondrial aminopeptidase deletion increases chronological lifespan and oxidative stress resistance while decreasing respiratory metabolism in S. cerevisiae." PLoS One **8**(10): e77234.

Stiburek, L., J. Cesnekova, O. Kostkova, D. Fornuskova, K. Vinsova, L. Wenchich, J. Houstek and J. Zeman (2012). "YME1L controls the accumulation of respiratory chain subunits and is required for apoptotic resistance, cristae morphogenesis, and cell proliferation." Mol Biol Cell **23**(6): 1010-1023.

Stiburek, L., D. Fornuskova, L. Wenchich, M. Pejznochova, H. Hansikova and J. Zeman (2007). "Knockdown of human Oxa1l impairs the biogenesis of F1Fo-ATP synthase and NADH:ubiquinone oxidoreductase." J Mol Biol **374**(2): 506-516.

Stojanovski, D., M. Bohnert, N. Pfanner and M. van der Laan (2012). "Mechanisms of protein sorting in mitochondria." Cold Spring Harb Perspect Biol **4**(10).

Strauss, K. M., L. M. Martins, H. Plun-Favreau, F. P. Marx, S. Kautzmann, D. Berg, T. Gasser, Z. Wszolek, T. Muller, A. Bornemann, H. Wolburg, J. Downward, O. Riess, J. B. Schulz and R. Kruger (2005). "Loss of function mutations in the gene encoding Omi/HtrA2 in Parkinson's disease." Hum Mol Genet **14**(15): 2099-2111.

Strisovsky, K., H. J. Sharpe and M. Freeman (2009). "Sequence-specific intramembrane proteolysis: identification of a recognition motif in rhomboid substrates." Mol Cell **36**(6): 1048-1059.

Sutovsky, P. (2003). "Ubiquitin-dependent proteolysis in mammalian spermatogenesis, fertilization, and sperm quality control: killing three birds with one stone." Microsc Res Tech **61**(1): 88-102.

Suzuki, C. K., K. Suda, N. Wang and G. Schatz (1994). "Requirement for the yeast gene LON in intramitochondrial proteolysis and maintenance of respiration." Science **264**(5161): 891.

Szabadkai, G., K. Bianchi, P. Varnai, D. De Stefani, M. R. Wieckowski, D. Cavagna, A. I. Nagy, T. Balla and R. Rizzuto (2006). "Chaperone-mediated coupling of endoplasmic reticulum and mitochondrial Ca2+ channels." J Cell Biol **175**(6): 901-911.

Tamura, Y., T. Endo, M. Iijima and H. Sesaki (2009). "Ups1p and Ups2p antagonistically regulate cardiolipin metabolism in mitochondria." J Cell Biol **185**(6): 1029-1045.

Tamura, Y., O. Onguka, A. E. Hobbs, R. E. Jensen, M. Iijima, S. M. Claypool and H. Sesaki (2012). "Role for two conserved intermembrane space proteins, Ups1p and Ups2p, [corrected] in intra-mitochondrial phospholipid trafficking." J Biol Chem **287**(19): 15205-15218.

Tatsuta, T., S. Augustin, M. Nolden, B. Friedrichs and T. Langer (2007). "m-AAA protease-driven membrane dislocation allows intramembrane cleavage by rhomboid in mitochondria." EMBO J **26**(2): 325-335.

Taylor, A. B., B. S. Smith, S. Kitada, K. Kojima, H. Miyaura, Z. Otwinowski, A. Ito and J. Deisenhofer (2001). "Crystal structures of mitochondrial processing peptidase reveal the mode for specific cleavage of import signal sequences." Structure **9**(7): 615-625.

Teixeira, P. F. and E. Glaser (2013). "Processing peptidases in mitochondria and chloroplasts." Biochim Biophys Acta **1833**(2): 360-370.

Temperley, R., R. Richter, S. Dennerlein, R. N. Lightowlers and Z. M. Chrzanowska-Lightowlers (2010). "Hungry codons promote frameshifting in human mitochondrial ribosomes." Science **327**(5963): 301.

Thompson, M. W., S. K. Singh and M. R. Maurizi (1994). "Processive degradation of proteins by the ATP-dependent Clp protease from Escherichia coli. Requirement for the multiple array of active sites in ClpP but not ATP hydrolysis." J Biol Chem **269**(27): 18209-18215.

Tian, Q., T. Li, W. Hou, J. Zheng, L. W. Schrum and H. L. Bonkovsky (2011). "Lon peptidase 1 (LONP1)-dependent breakdown of mitochondrial 5-aminolevulinic acid synthase protein by heme in human liver cells." J Biol Chem **286**(30): 26424-26430.

Trinh, D. L., A. N. Elwi and S. W. Kim (2010). "Direct interaction between p53 and Tid1 proteins affects p53 mitochondrial localization and apoptosis." Oncotarget **1**(6): 396-404.

Tuppen, H. A., E. L. Blakely, D. M. Turnbull and R. W. Taylor (2010). "Mitochondrial DNA mutations and human disease." Biochim Biophys Acta **1797**(2): 113-128.

Twig, G., A. Elorza, A. J. Molina, H. Mohamed, J. D. Wikstrom, G. Walzer, L. Stiles, S. E. Haigh, S. Katz, G. Las, J. Alroy, M. Wu, B. F. Py, J. Yuan, J. T. Deeney, B. E. Corkey and O. S. Shirihai (2008). "Fission and selective fusion govern mitochondrial segregation and elimination by autophagy." EMBO J **27**(2): 433-446.

Urban, S. (2006). "Rhomboid proteins: conserved membrane proteases with divergent biological functions." Genes Dev **20**(22): 3054-3068.

Urban, S., J. R. Lee and M. Freeman (2001). "Drosophila rhomboid-1 defines a family of putative intramembrane serine proteases." Cell **107**(2): 173-182.

Urban, S. and M. S. Wolfe (2005). "Reconstitution of intramembrane proteolysis in vitro reveals that pure rhomboid is sufficient for catalysis and specificity." Proc Natl Acad Sci U S A **102**(6): 1883-1888.

Valente, E. M., P. M. Abou-Sleiman, V. Caputo, M. M. Muqit, K. Harvey, S. Gispert, Z. Ali, D. Del Turco, A. R. Bentivoglio, D. G. Healy, A. Albanese, R. Nussbaum, R. Gonzalez-Maldonado, T. Deller, S. Salvi, P. Cortelli, W. P. Gilks, D. S. Latchman, R. J. Harvey, B. Dallapiccola, G. Auburger and N. W. Wood (2004). "Hereditary early-onset Parkinson's disease caused by mutations in PINK1." Science **304**(5674): 1158-1160.

Van Dyck, L., D. A. Pearce and F. Sherman (1994). "PIM1 encodes a mitochondrial ATP-dependent protease that is required for mitochondrial function in the yeast Saccharomyces cerevisiae." J Biol Chem **269**(1): 238-242.

Vande Walle, L., M. Lamkanfi and P. Vandenabeele (2008). "The mitochondrial serine protease HtrA2/Omi: an overview." Cell Death Differ **15**(3): 453-460.

Varshavsky, A. (2011). "The N-end rule pathway and regulation by proteolysis." Protein Sci **20**(8): 1298-1345.

Venkatesh, S., J. Lee, K. Singh, I. Lee and C. K. Suzuki (2012). "Multitasking in the mitochondrion by the ATP-dependent Lon protease." Biochim Biophys Acta **1823**(1): 56-66.

Verhagen, A. M., J. Silke, P. G. Ekert, M. Pakusch, H. Kaufmann, L. M. Connolly, C. L. Day, A. Tikoo, R. Burke, C. Wrobel, R. L. Moritz, R. J. Simpson and D. L. Vaux (2002). "HtrA2 promotes cell death through its serine protease activity and its ability to antagonize inhibitor of apoptosis proteins." J Biol Chem **277**(1): 445-454.

Voet, D., Voet, J.G. (2010). Biochemistry.

Vogtle, F. N., J. M. Burkhart, H. Gonczarowska-Jorge, C. Kucukkose, A. A. Taskin, D. Kopczynski, R. Ahrends, D. Mossmann, A. Sickmann, R. P. Zahedi and C. Meisinger (2017). "Landscape of submitochondrial protein distribution." Nat Commun **8**(1): 290.

Vogtle, F. N., C. Prinz, J. Kellermann, F. Lottspeich, N. Pfanner and C. Meisinger (2011). "Mitochondrial protein turnover: role of the precursor intermediate peptidase Oct1 in protein stabilization." Mol Biol Cell **22**(13): 2135-2143.

Vogtle, F. N., S. Wortelkamp, R. P. Zahedi, D. Becker, C. Leidhold, K. Gevaert, J. Kellermann, W. Voos, A. Sickmann, N. Pfanner and C. Meisinger (2009). "Global analysis of the mitochondrial N-proteome identifies a processing peptidase critical for protein stability." Cell **139**(2): 428-439.

Wagner, I., L. van Dyck, A. S. Savel'ev, W. Neupert and T. Langer (1997). "Autocatalytic processing of the ATP-dependent PIM1 protease: crucial function of a pro-region for sorting to mitochondria." EMBO J **16**(24): 7317-7325.

Wai, T., J. Garcia-Prieto, M. J. Baker, C. Merkwirth, P. Benit, P. Rustin, F. J. Ruperez, C. Barbas, B. Ibanez and T. Langer (2015). "Imbalanced OPA1 processing and mitochondrial fragmentation cause heart failure in mice." Science **350**(6265): aad0116.

Walder, K., L. Kerr-Bayles, A. Civitarese, J. Jowett, J. Curran, K. Elliott, J. Trevaskis, N. Bishara, P. Zimmet, L. Mandarino, E. Ravussin, J. Blangero, A. Kissebah and G. R. Collier (2005). "The mitochondrial rhomboid protease PSARL is a new candidate gene for type 2 diabetes." Diabetologia **48**(3): 459-468.

Walker, J. E., M. Saraste, M. J. Runswick and N. J. Gay (1982). "Distantly related sequences in the alpha- and beta-subunits of ATP synthase, myosin, kinases and other ATP-requiring enzymes and a common nucleotide binding fold." EMBO J **1**(8): 945-951.

Wallace, D. C. (2005). "A mitochondrial paradigm of metabolic and degenerative diseases, aging, and cancer: a dawn for evolutionary medicine." Annu Rev Genet **39**: 359-407.

Waltner, M. and H. Weiner (1995). "Conversion of a nonprocessed mitochondrial precursor protein into one that is processed by the mitochondrial processing peptidase." J Biol Chem **270**(44): 26311-26317.

Wang, J., J. A. Hartling and J. M. Flanagan (1997). "The structure of ClpP at 2.3 A resolution suggests a model for ATP-dependent proteolysis." Cell **91**(4): 447-456.

Wang, N., S. Gottesman, M. C. Willingham, M. M. Gottesman and M. R. Maurizi (1993). "A human mitochondrial ATP-dependent protease that is highly homologous to bacterial Lon protease." Proc Natl Acad Sci U S A **90**(23): 11247-11251.

Wang, N., M. R. Maurizi, L. Emmert-Buck and M. M. Gottesman (1994). "Synthesis, processing, and localization of human Lon protease." J Biol Chem **269**(46): 29308-29313.

Wang, Y., Y. Zhang and Y. Ha (2006). "Crystal structure of a rhomboid family intramembrane protease." Nature **444**(7116): 179-180.

Wang, Y. Y., Y. X. Yang, H. Zhe, Z. X. He and S. F. Zhou (2014). "Bardoxolone methyl (CDDO-Me) as a therapeutic agent: an update on its pharmacokinetic and pharmacodynamic properties." Drug Des Devel Ther **8**: 2075-2088.

Weber, E. R., T. Hanekamp and P. E. Thorsness (1996). "Biochemical and functional analysis of the YME1 gene product, an ATP and zinc-dependent mitochondrial protease from S. cerevisiae." Mol Biol Cell **7**(2): 307-317.

Whitman, J. C., B. H. Paw and J. Chung (2018). "The role of ClpX in erythropoietic protoporphyria." Hematol Transfus Cell Ther **40**(2): 182-188.

Wojtyra, U. A., G. Thibault, A. Tuite and W. A. Houry (2003). "The N-terminal zinc binding domain of ClpX is a dimerization domain that modulates the chaperone function." J Biol Chem **278**(49): 48981-48990.

Wolfe, M. S., W. Xia, B. L. Ostaszewski, T. S. Diehl, W. T. Kimberly and D. J. Selkoe (1999). "Two transmembrane aspartates in presenilin-1 required for presenilin endoproteolysis and gamma-secretase activity." Nature **398**(6727): 513-517.

Wu, X., L. Li and H. Jiang (2018). "Mitochondrial inner-membrane protease Yme1 degrades outer-membrane proteins Tom22 and Om45." J Cell Biol **217**(1): 139-149.

Wu, Z., N. Yan, L. Feng, A. Oberstein, H. Yan, R. P. Baker, L. Gu, P. D. Jeffrey, S. Urban and Y. Shi (2006). "Structural analysis of a rhomboid family intramembrane protease reveals a gating mechanism for substrate entry." Nat Struct Mol Biol **13**(12): 1084-1091.

Yamano, K., Y. Yatsukawa, M. Esaki, A. E. Hobbs, R. E. Jensen and T. Endo (2008). "Tom20 and Tom22 share the common signal recognition pathway in mitochondrial protein import." J Biol Chem **283**(7): 3799-3807.

Yien, Y. Y., S. Ducamp, L. N. van der Vorm, J. R. Kardon, H. Manceau, C. Kannengiesser, H. A. Bergonia, M. D. Kafina, Z. Karim, L. Gouya, T. A. Baker, H. Puy, J. D. Phillips, G. Nicolas and B. H. Paw (2017). "Mutation in human CLPX elevates levels of delta-aminolevulinate synthase and protoporphyrin IX to promote erythropoietic protoporphyria." Proc Natl Acad Sci U S A **114**(38): E8045-E8052.

Young, L., K. Leonhard, T. Tatsuta, J. Trowsdale and T. Langer (2001). "Role of the ABC transporter Mdl1 in peptide export from mitochondria." Science **291**(5511): 2135-2138.

Yu, J. N., B. J. Kim, C. Kim, J. H. Yeo and S. Kim (2017). "The complete mitochondrial genome of the black star fat minnow (Rhynchocypris semotilus), an endemic and endangered fish of Korea." Mitochondrial DNA A DNA Mapp Seq Anal **28**(1): 114-115.

Yuan, L., L. Zhai, L. Qian, Huang, Y. Ding, H. Xiang, X. Liu, J. W. Thompson, J. Liu, Y. H. He, X. Q. Chen, J. Hu, Q. P. Kong, M. Tan and X. F. Wang (2018). "Switching off IMMP2L signaling drives senescence via simultaneous metabolic alteration and blockage of cell death." Cell Res **28**(6): 625-643.

Zeng, X., W. Neupert and A. Tzagoloff (2007). "The metalloprotease encoded by ATP23 has a dual function in processing and assembly of subunit 6 of mitochondrial ATPase." Mol Biol Cell **18**(2): 617-626.

Zhang, H., D. Ryu, Y. Wu, K. Gariani, X. Wang, P. Luan, D. D'Amico, E. R. Ropelle, M. P. Lutolf, R. Aebersold, K. Schoonjans, K. J. Menzies and J. Auwerx (2016). "NAD(+) repletion improves mitochondrial and stem cell function and enhances life span in mice." Science **352**(6292): 1436-1443.

Zhang, J., A. Lin, J. Powers, M. P. Lam, C. Lotz, D. Liem, E. Lau, D. Wang, N. Deng, P. Korge, N. C. Zong, H. Cai, J. Weiss and P. Ping (2012). "Perspectives on: SGP symposium on mitochondrial physiology and medicine: mitochondrial proteome design: from molecular identity to pathophysiological regulation." J Gen Physiol **139**(6): 395-406.

Zhang, K., H. Li and Z. Song (2014). "Membrane depolarization activates the mitochondrial protease OMA1 by stimulating self-cleavage." EMBO Rep **15**(5): 576-585.

Zhang, X. P., S. Sjoling, M. Tanudji, L. Somogyi, D. Andreu, L. E. Eriksson, A. Graslund, J. Whelan and E. Glaser (2001). "Mutagenesis and computer modelling approach to study determinants for recognition of signal peptides by the mitochondrial processing peptidase." Plant J **27**(5): 427-438.

Zhbanko, M., V. Zinchenko, M. Gutensohn, A. Schierhorn and R. B. Klosgen (2005). "Inactivation of a predicted leader peptidase prevents photoautotrophic growth of Synechocystis sp. strain PCC 6803." J Bacteriol **187**(9): 3071-3078.

Zhuang, J., P. Y. Wang, X. Huang, X. Chen, J. G. Kang and P. M. Hwang (2013). "Mitochondrial disulfide relay mediates translocation of p53 and partitions its subcellular activity." Proc Natl Acad Sci U S A **110**(43): 17356-17361.

Zick, M., S. Duvezin-Caubet, A. Schafer, F. Vogel, W. Neupert and A. S. Reichert (2009). "Distinct roles of the two isoforms of the dynamin-like GTPase Mgm1 in mitochondrial fusion." FEBS Lett **583**(13): 2237-2243.

Zuhlke, C., B. Mikat, D. Timmann, D. Wieczorek, G. Gillessen-Kaesbach and K. Burk (2015). "Spinocerebellar ataxia 28: a novel AFG3L2 mutation in a German family with young onset, slow progression and saccadic slowing." Cerebellum Ataxias **2**: 19.

7. LIST OF ORIGINAL ARTICLES (in chronological order)

Cesnekova J, Rodinova M, Hansikova H, Houstek J, Zeman J, Stiburek L. The mammalian homologue of yeast Afg1 ATPase (lactation elevated 1) mediates degradation of nuclear-encoded complex IV subunits. Biochem J (IF 4.396), 2016 Mar 15; 473(6); 797-804

Cesnekova J, Spacilova J, Hansikova H, Houstek J, Zeman J, Stiburek L. LACE1 interacts with p53 and mediates its mitochondrial translocation and apoptosis. Oncotarget (IF 6.359) 2016 Jul 26;7(30):47687-47698

Cesnekova J, Rodinova M, Hansikova H, Zeman J, Stiburek L. Loss of both AFG3L2 and YME1L leads to respiratory chain deficiency and impaired mitochondrial dynamics and ultrastructure, submitted to AM J PHYSIOL-CELL PH (IF 3.454)

Univerzita Karlova v Praze, 1. lékařská fakulta

Kateřinská 32, Praha 2

Prohlášení zájemce o nahlédnutí
do závěrečné práce absolventa studijního programu
uskutečňovaného na 1. lékařské fakultě Univerzity Karlovy v Praze

Jsem si vědom/a, že závěrečná práce je autorským dílem a že informace získané nahlédnutím do zpřístupněné závěrečné práce nemohou být použity k výdělečným účelům, ani nemohou být vydávány za studijní, vědeckou nebo jinou tvůrčí činnost jiné osoby než autora.

Byl/a jsem seznámen/a se skutečností, že si mohu pořizovat výpisy, opisy nebo kopie závěrečné práce, jsem však povinen/a s nimi nakládat jako s autorským dílem a zachovávat pravidla uvedená v předchozím odstavci.

Příjmení, jméno (hůlkovým písmem)	**Číslo dokladu totožnosti vypůjčitele (např. OP, cestovní pas)**	**Signatura závěrečné práce**	**Datum**	**Podpis**